MEDIUM ACCESS CONTROL LAYER PERFORMANCE ISSUES IN WIRELESS SENSOR NETWORKS

by

Ilker Seyfettin Demirkol

B.S, Computer Engineering, Boğaziçi University, 1998

M.S, Computer Engineering, Boğaziçi University, 2002

Submitted to the Institute for Graduate Studies in
Science and Engineering in partial fulfillment of
the requirements for the degree of
Doctor of Philosophy

Graduate Program in
Boğaziçi University
2008

ACKNOWLEDGEMENTS

The most enjoyable job in the world is to be a PhD student, if you have an advisor like *Prof. Cem Ersoy*, a mother like *Müzeyyen Demirkol*, a father like *İlhan Demirkol*, a girlfriend like *Yeliz*, a lot of sincere friends like *Atay Özgövde, Rabun Koşar, Burak Gürdağ, Itır Karaç, Ertan Onur, İsmail Arı, Oya Aran, Aydın Ulaş, Onur Dikmen, Albert Ali Salah, Fatih Köksal, Mehmet Gönen, Abuzer Yakarylmaz, Onur Büyükceran, Birkan Yılmaz, Evren Önem, Reyhan Aydoğan, Gül Çalıklı, Suzan Bayhan, Koray Balcı, Berk Gökberk* and the all adorable CMPE people, *Yıldız Yanmaz, Seda Akbalık, Lalender Demir, Ersin Başruh, M. Emin Eroğlu* and my other Elan colleagues, if you dance, if you work with people like *H. Levent Akın, Ali Vahit Şahiner, Cem Ersoy, Suzan Üsküdarlı, M. Ufuk Çağlayan, Tuna Tuğcu and Jacop Peled*, if you are optimist, if you do not smoke, if you join the activities organized by *Lale Akarun and Cem Ersoy*, if you do sports regularly, if you have a brother like *Aykut Soner Demirkol* and a sister like *Z. Meltem Demirkol*, if you laugh frequently, if you have a chance to do research with people like *Assoc. Prof. Fatih Alagöz and Prof. Hakan Deliç*, if your research group has members like *Can Komar, Yunus Dönmez, Sinan Işık, Yunus Durmuş, Tolga Önel, Özgür Akduran*, and *Aykut Yiğitel*. All these reasons enabled me to write this thesis.

I would like to give my grateful and sincere thanks to Prof. Cem Ersoy for his guidance, patience, and support during my graduate studies. I am inspired by not only his research capability but also his humanity and friendship.

I would also like to thank Prof. Sema Oktuğ for her valuable feedback to this thesis.

The OPNET models of the VSN protocols evaluated in this thesis are developed in collaboration with Atay Ozgovde, Department of Computer Engineering, Boğaziçi University.

This work has been supported by the State Planning Organization of Turkey under the grant number 03K120250, and by TUBITAK under the grant number 106E082.

ABSTRACT

MEDIUM ACCESS CONTROL LAYER PERFORMANCE ISSUES IN WIRELESS SENSOR NETWORKS

Wireless sensor networks (WSNs) present a promising technology for many applications, providing an intelligent and remote observation of a destination. Among the various potential applications, there are health monitoring, disaster monitoring, habitat monitoring, precision agriculture, and surveillance systems. With the ongoing research both on new sensor types and on the hardware for improved computation, communication and power capacities, the emergence of novel application areas are expected.

Due to the limited power sources of the sensor nodes which are generally irreplaceable, the WSN research is focused on the energy-efficient network operation. This energy concern requires new studies at each networking layer, including the medium access control (MAC) layer. In this thesis, we investigate a number of MAC layer performance issues for WSN by first presenting a comparative survey of different MAC protocol schemes proposed in the literature. For the correct performance evaluation of the protocols, one needs to utilize a realistic packet traffic model that reflects the specific features of the WSN application represented. We derive an analytical packet traffic model for Surveillance WSN where sensor nodes inform the sink for detected intrusion events. The sensor detection model used is probabilistic and parametric, which enables the adaptation of the packet traffic model to the sensor types deployed.

One important contribution of this thesis is the optimization of the MAC layer contentions for minimization of the energy consumption or the delay incurred in contention slotted medium access protocols. This is achieved by by analyzing the energy consumption and the contention delay and, then, extracting the contention window

size that optimizes the corresponding performance metric. For its practical implementation in the distributed environment of WSNs, a method is proposed which achieves near-optimal performance values.

To investigate the effect of the contention optimization on the the overall network performance, video sensor networks (VSNs) are studied. VSNs are a special type of WSNs where the sensor nodes are equipped with cameras and send image or video of a target area based on the specifications of the application. First, the network performance of the VSNs are investigated via simulations for the currently available hardware technology. Then, by applying the contention optimization proposed in this thesis, we show how the capacity of VSNs can be improved with intelligent contention window size setting.

ÖZET

TELSİZ ALGILAYICI AĞLARDA ORTAM ERİŞİMİ KONTROL KATMANI BAŞARIM KONULARI

Telsiz algılayıcı ağlar (TAA), belli bir hedef alanın akıllı ve uzaktan erişimli gözlemlenmesini sağladıklarından, birçok uygulama için gelecek vaadeden bir teknoloji alternatifi oluşturmaktadırlar. Çeşitli potansiyel uygulama alanlarından bazıları sağlıksal takip, olağanüstü durum gözlemleme, doğa gözlemleme, hassas tarım ve sızma sezme sistemleridir. Ayrıca, yeni algılayıcı türleri ve gelişmiş hesaplama, haberleşme ve güç kapasiteleri için yapılan donanım çalışmaları, yeni uygulama alanlarının ortaya çıkmasını sağlayacaktır.

Algılayıcı düğümlerdeki genellikle değiştirilemeyen, limitli güç kaynakları nedeniyle TAA çalışmaları enerji-verimli ağ çalışması üzerine yoğunlaşmıştır. Bu enerji-verimli çalışma hedefi, ortam erişim kontrol (OEK) katmanı dahil her ağ katmanı için yeni çalışmaların yapılmasını gerektirmektedir. Bu tezde, TAA'lardaki OEK katmanı ile ilgili çeşitli başarım konuları incelenmiştir. İlk olarak, literatürde bulunan değişik OEK protokol yöntemlerini içeren karşılaştırmalı bir özet sunulmuştur. Protokollerin doğru başarım değerlendirmeleri için hedef TAA uygulamasının özelliklerini temsil edebilen gerçekçi bir paket trafik modeline ihtiyaç vardır. Bu ihtiyaç doğrultusunda, telsiz gözetim algılayıcı ağları için analitik bir paket trafik modeli önermekteyiz. Telsiz gözetim algılayıcı ağlarda, algılayıcı düğümler bir sızma sezdiklerinde toplayıcı düğümü haberdar etmekle görevlidirler. Kullanılan algılayıcı tiplerine uyarlanabilirlik özelliği sağlamak için olasılıksal ve parametrik bir sızma sezme modeli temel alınmıştır.

Bu tezin bir diğer önemli katkısı da, OEK katmanı çekişmelerinin enerji ve gecikme kriterleri için eniyilenebilmesini sağlayacak çalışmalardır. Bu çalışmalar, belirtilen iki ayrı kriter için matematiksel formüllerin geliştirilmesi ve bu formüller ışığında

çekişme penceresi boyutunun eniyilemesi ile başarılmıştır. Bu eniyilemelerin TAA'ların dağıtık yapısında kullanımını sağlayacak, en iyi sonuca yakın başarım değerleri sergilediğini gösterdiğimiz bir yöntem de bu tezde önerilmiştir.

Bu çekişme eniyilemesi çalışmalarının genel ağ başarımına etkisini incelemek için de video algılayıcı ağları (VAA) üzerine çalışmalar yapılmıştır. VAA, düğümlerin kameralarla donatılmış olduğu ve uygulamanın istekleri doğrultusunda hedef bölgenin görüntülerini toplayıcı düğüme yollayan özel bir TAA türüdür. İlk olarak VAA'ların günümüz donanım teknolojilerinin özellikleri ile elde edebilecekleri ağ başarımı benzetim yoluyla çıkarılmıştır. Daha sonra, bu tezde önerilen çekişme eniyilemesi, bu VAA'lara uygulanmış ve akıllı çekişme penceresi boyutu tanımlamanın VAA'ların kapasitelerini nasıl arttırdığı gösterilmiştir.

TABLE OF CONTENTS

LIST OF FIGURES

LIST OF TABLES

LIST OF SYMBOLS

$\mathcal{C}_i$	Location of target at instance i
c_i	Coverage degree at point $\mathcal{C}_i$
$c_{x,y}$	Coverage degree at point (x, y), i.e., the number of sensor nodes that have positive detection probability for a target at (x, y)
$\mathcal{D}_i$	Disk whose center is at $\mathcal{C}_i$ and whose radius is d_u, i.e., the coverage area of a the sensor at location $\mathcal{C}_i$
d_c	Detection range
d_u	Sensing range
$\hat{E}_{coll}$	Expected energy consumed at one collision till its retrial
$\dot{E}_{coll}$	The total energy consumed for unsuccessful communication till a successful medium access
E_{coll}	The total energy consumed for the communications of the colliding packets and their retrials
E_{rx}	The energy consumed for reception per unit time
E_{ssa}	Total energy consumed for the carrier sensing in the successful slot assignments
E_{total}	The energy consumed for resolution of all contentions
E_{tx}	The energy consumed for transmission per unit time
$\mathcal{F}$	Random variable that represents the number of first occupied slot given that it is selected by only one node
H	Border width
$\mathcal{K}_i$	Random variable that represents the detection degree of the event point $\mathcal{C}_i$
k_i	Detection degree at point $\mathcal{C}_i$
$k_{x,y}$	Detection degree at point (x, y), i.e., the number of sensor nodes that detects the target at (x, y)
L	Border length
$\mathcal{M}$	Number of contending nodes
N	Number of sensors

p	Probability that a deployed node is within the d_u-distance of the target point
r	Radial coordinate of the sensor when the pole is set to the target location
s_i	The slot chosen by node i
t_{ACK}	Time needed for the transmission of an ACK packet
t_c	The duration after the collision till the new contention begins, i.e., collision timeout
t_{coll}	Time spent for the collided packets' transmissions
t_{CTS}	Time needed for the transmission of a CTS packet
t_{CW}	Time spent for waiting the first occupied contention slot
t_{DATA}	Time needed for the transmission of a $DATA$ packet
t_{listen}	Listen period in seconds
t_{RTS}	Time needed for the transmission of an RTS packet
t_s	Sensing interval
t_{slot}	Slot duration
t_{stx}	Time required for a successful packet transmission
v_T	Target velocity
W	Contention window size
W_t^*	Delay optimizing contention window size
$\mathcal{X}_i$	Number of sensor nodes that have non-zero detection probability, i.e., the sensor nodes that resides within the d_u-distance of the event point $\mathcal{C}_i$
$\mathcal{Y}_i$	Number of nodes that reside in $\mathcal{A}_i$
$\mathcal{Z}$	Number of contention slots in a contention window
z	Number of successive collisions
α	Elfes detection parameter
β	Elfes detection parameter
γ	Probability of detection for any one sensor within the d_u-distance of the target
Γ	Expected carrier sense duration within this successful contention

ζ	Probability of packet collision in a contention period
θ	Angular coordinate of the sensor when the pole is set to the target location
$\theta(\psi, n, m)$	Total energy consumed for one retrial if the first selected slot is ψ and m nodes out of n select that slot
Λ	Expected time spent for collisions and retrials till the beginning of the collisionless slot selection
ξ	Probability that a slot assignment results in a collisionless transmission
ρ_{max}	Maximum stable throughput
τ	Expected number of contention retrials
Υ	Random variable indicating whether the slot selection is successful
$\varphi(d)$	Probability of detection of a target at distance d
Ψ	Random variable of the slot number of the first occupied slot
Ω	Expected contention delay

LIST OF ABBREVIATIONS

ACK	Acknowledgement
BEB	Binary Exponential Backoff
CDMA	Code Division Multiple Access
CSMA	Carrier Sense Multiple Access
CTS	Clear-to-Send
CW	Contention Window
ENCO	Estimated Number of Contenders Method
FDMA	Frequency Division Multiple Access
i.i.d.	Independent and identically-distributed
MAC	Medium Access Control
PMF	Probability Mass Function
PTM	Packet Traffic Model
RFID	Radio-frequency identification
RTS	Request-to-Send
S-MAC	Sensor MAC
SPTM	Packet Traffic Model for Surveillance WSN
SWSN	Surveillance Wireless Sensor Networks
TDMA	Time Division Multiple Access
VSN	Video Sensor Networks
WBAN	Wireless Body Area Networks
WSN	Wireless Sensor Networks

1. INTRODUCTION

The evolution of communication technology is observed to be from wired communication to wireless communication, from circuit switching to packet switching, from centralized devices to distributed/ubiquitous devices and from infrastructured communications to infrastructureless communication. The wireless sensor networks (WSNs) is a part of this evolution that relays a *processed* observation of a remote target area to a desired location. Paul Saffo had stated that "Sensors will be to this decade what microprocessors were to the 1980s and the Internet to the 1990s"[1] in 1997. Recent advances in sensor hardware and wide range of WSN application areas, including environmental monitoring, disaster monitoring, precision agriculture, surveillance and tactical systems, show that his statement is becoming true. As the digital technology is embedded to our daily life, new application areas are realized such as the ones resulting from the cooperation of Wireless Body Area networks (WBANs) and WSNs [2, 3, 4, 5, 6] or the implementations of radio-frequency identification (RFID) systems with WSNs [7, 8, 9]. As the variety of these application areas increase, we will be using WSNs in many part of our lives to *observe the world*. According to Boone, "How *browsing stored information* has become the primary use of the Internet, the killer application for wireless sensor networks will be *browsing the reality*"[10].

WSNs are a special type of wireless networks where the nodes are static, have limited computation and battery capacities and have limited transmission ranges. Unlike other wireless networks, in a WSN, the wireless nodes have a common task to accomplish which puts the fairness issues as a secondary objective. However, due to the battery constraints, the primary objective is to operate the network in an energy-efficient manner. From the communication point of view, this efficiency must be achieved in all layers of the network stack or if possible, to develop cross-layer protocols that achieves the same task with less energy consumption. Although there are various communication protocols proposed for sensor networks, there is no protocol accepted as a standard. One of the reasons behind this is the protocol choice will, in general, be application-dependent, which means that there will not be one standard protocol for

sensor networks. Another reason is the lack of standardization at the physical layer and the sensor hardware.

In this thesis, we investigated the Medium Access Control (MAC) layer of WSN which is subject to a number of challenges due to the limited communication capabilities and the energy efficiency requirement of WSN. The Wireless World Research Forum (WWRF) projects that in 2017, there will be seven trillion electronic devices serving seven billion people [11]. Assuming that WSNs will compose an important part of the future technology and there will be a shared communication medium for interoperability, the importance of MAC layer for WSNs can be observed easily. There are numerous MAC protocols proposed for WSN. Therefore, instead of developing a new MAC alternative from scratch, we investigated methods to help the performance analysis of MAC protocols as well as methods to increase the performance of a certain type of MAC protocols.

1.1. MAC Layer in Wireless Sensor Networks

Improvements in hardware technology have resulted in low-cost sensor nodes which are composed of a single chip with embedded memory, processor, and transceiver. Low power capacities lead to limited coverage and communication range for sensor nodes compared to other mobile devices. Hence, for example in target tracking and border surveillance applications, sensor networks must include a large number of nodes to cover the target area successfully.

Unlike other wireless networks, it is generally hard (or impractical) to charge/replace exhausted batteries. That is why, the primary objective in wireless sensor networks design is maximizing node/network lifetime, leaving the other performance metrics as secondary objectives. Since the communication of sensor nodes will be more energy consuming than their computation, it is a primary concern to minimize communication while achieving the desired network operation.

However, the medium access decision within a dense network composed of nodes with low duty-cycles is a hard problem that must be solved in an energy-efficient manner. Having these in mind, Section 1.1.1 emphasizes the peculiar features of sensor networks including reasons of potential energy waste at medium access communication.

1.1.1. MAC Layer Related Sensor Network Properties

Maximizing the network lifetime is a common objective of sensor network research, since sensor nodes are assumed to be dead when they are out of battery. Under these circumstances, the proposed MAC protocol must be energy-efficient by reducing the potential energy waste presented in Section 1.1.1.1. Types of communication patterns that are observed in sensor network applications should be investigated since these patterns determine the behavior of the sensor network traffic that has to be handled by a given MAC protocol. Categorization of the possible communication patterns is outlined in Section 1.1.1.2. Afterwards, the properties that must be possessed by a MAC protocol to suit a sensor network environment are presented in Section 1.1.1.3.

1.1.1.1. Reasons of Energy Waste. When a node receives more than one packet at the same time, these packets are called collided even when they coincide only partially. All packets that cause the *collision* have to be discarded and the re-transmissions of these packets are required which increase the energy consumption. Although some packets could be recovered by a *capture* effect, a number of requirements have to be achieved for successful recovery. The second reason of energy waste is *overhearing*, meaning that a node receives packets that are destined to other nodes. The third energy waste occurs as a result of *control packet overhead*. Minimal number of control packets should be used to achieve data transmission. One of the major sources of energy waste is *idle listening*, i.e., listening to an idle channel to receive possible traffic. The last reason for energy waste is *overemitting*, which is caused by the transmission of a message when the destination node is not ready. Given the facts above, a correctly-designed MAC protocol should prevent these types of energy waste.

1.1.1.2. Communication Patterns. Kulkarni define three types of communication patterns in wireless sensor networks [12]: *broadcast, convergecast*, and *local gossip*. Broadcast is generally used by a base station (sink) to transmit some information to all sensor nodes of the network. Broadcasted information may include queries of sensor query-processing architectures, program updates for sensor nodes, or control packets for the whole system. The broadcast communication pattern should not be confused with broadcast packets. For the former, all nodes of the network are intended receivers whereas for the latter the intended receivers are the nodes within the communication range of the transmitting node.

In some scenarios, the sensors that detect an event communicate with each other locally. This kind of communication pattern is called local gossip, where a sensor sends a message to its neighboring nodes within a range. The sensors that detect the event, then, need to send what they perceive to the information center. That communication pattern is called convergecast, where a group of sensors communicate to a specific sensor. The destination node could be a clusterhead, a data fusion center, or a base station.

In protocols that include clustering, clusterheads communicate with their members and thus the intended receivers may not be all neighbors of the clusterhead, but just a subset of the neighbors. To serve such scenarios, we define a fourth type of communication pattern, multicast, where a sensor sends a message to a specific subset of sensors. Among all four patterns, the pattern that occurs most is the convergecast. Since, the destination of the packets is a sink nodes most of the time.

1.1.1.3. Properties of a Well-defined MAC Protocol. To design a good MAC protocol for wireless sensor networks, the following attributes must be considered [13]. The first attribute is energy efficiency. We have to define energy-efficient protocols in order to prolong the network lifetime. Other important attributes are scalability and adaptability to changes. Changes in network size, node density and topology should be handled rapidly and effectively for a successful adaptation. Some of the reasons be-

hind these network property changes are limited node lifetime, addition of new nodes to the network and varying interference which may alter the connectivity and hence the network topology. A good MAC protocol should gracefully accommodate such network changes. Other usually important attributes such as latency, throughput and bandwidth utilization may be secondary in sensor networks. Contrary to other wireless networks, fairness among sensor nodes is not usually a design goal, since all sensor nodes share a common task.

1.2. Addressed Problems and Contributions

To investigate MAC layer properties for WSN along with the alternative medium access methods proposed and the challenges encountered in development of MAC layer protocols, a detailed survey is conducted [14]. The MAC layer protocols in this survey are representative protocols for different medium access schemes. The working principles and the advantages/disadvantages of these methods are presented in Chapter 2.

For performance evaluation of communication protocols, the packet traffic model is crucial. In telecommunications systems, Poisson arrivals are assumed based on the fact that there are a high number of users but their probability of call generation is low. However, in WSN, the packet generation model is heavily dependent on the WSN application. For instance, in environmental monitoring or structural monitoring applications, a periodic data traffic is possible. However, for event-driven WSN applications such as target tracking and disaster monitoring applications, the generated traffic is shaped by the event generation rates which results in a bursty packet traffic that cannot be modeled by a periodic or Possion traffic.

Based on this realization, we developed an analytical packet traffic model (PTM) for Surveillance Wireless Sensor Networks (SWSN) assuming a binary sensor detection model [15]. In SWSN, a target area is controlled for possible intrusions. If an intrusion is detected by a sensor, a data packet is generated by the server to provide specific information about the intrusion. An important observation is that the sensor nodes that

are triggered in consecutive times are not independent which results in a dependency of the consecutive number of detecting nodes, i.e., consecutive number of data packets generated. This dependency affects the packet traffic generated, hence considered in the PTM proposed. Furthermore, the model is extended to achieve a more generic packet traffic model, namely SPTM [16], where a probabilistic and parametric sensor detection model is employed instead of the binary detection model. By adjusting the parameters of the detection model, different sensor types can be represented by SPTM. An analytical framework is defined to develop SPTM which is described thoroughly in Chapter 3. The resulting PTM can be used to observe the load created in the network by the application layer and can be extended to include the different layers' packet overhead.

The impact of having a realistic PTM is also shown in Chapter 3 by simulating three different PTMs and comparing their effect on the performance results of a well-known WSN MAC protocol. Simulation results indicate that evaluating a communication protocol with a packet traffic model other than SPTM may give misleading results for the surveillance wireless sensor networks.

Another topic investigated in this thesis is the contention window (CW) size optimization for the slotted-CSMA based MAC protocols. The CW size setting brings an important trade-off between high collision probability and high idle listening durations. By realizing its importance, there are various CW size adjustment studies for other type of wireless networks, however no study exist for CW size optimization for WSN. Since the performance objectives in WSN is specific and the back-off mechanism preferred in WSN is different than the other network types, a specific CW size optimization work is needed for WSN. By presenting the effect of CW size on the two WSN objectives separately, the energy-optimizing and the delay-optimizing CW size formulas are derived analytically [17]. However, these optimizations use the knowledge of number of contending nodes which cannot be readily available in a distributed environment. Hence, a method is proposed for the practical implementation of the CW size optimizations for event-driven WSNs that leads to near-optimal results. The optimized contention for WSN studies are presented in Chapter 4.

Moreover, although nearly all slotted medium access methods employ the uniformly random slot selection method, an interesting work in the literature propose a collision-minimizing slot selection algorithm, namely p^* method. It is analytically proven that the method p^* method minimizes the collision probabilities, however neither in that work nor in any other work, its effect on an overall performance metric is not investigated. In Chapter 4, we also present the effect of p^* method on the contention delay. Our observations are interesting: If uniformly random slot selection method is used with our CW size optimization, it gives better results than the p^* method [18].

Video sensor networks (VSNs) are a special type of WSNs where sensor nodes equipped with video cameras send the captured video according to the requirements of the VSN application implemented. VSNs provide a promising alternative for applications such as border surveillance, target tracking and elderly monitoring. Since compared to the traditional WSN, the network bandwidth requirements and computational requirements are different, separate studies are needed for VSNs. In Chapter 5, we first investigate the overall network performance of intrusion-detecting VSN that can be achieved with limitations of current hardware technologies and currently feasible encoding settings [19, 20]. An important finding is that increasing the quality of the video stream of the camera does not necessarily increase the video quality (frame rate) received at the sink even for low frame rates.

Moreover, along with the proposed contention window size optimization work, ENCO method is employed to improve the overall VSN performance. The network performance results of VSN with the ENCO method is presented in Chapter 5 which shows that ENCO method can extend the capabilities of VSN by both decreasing the end-to-end delay and increasing the average number of frames received at sink, i.e., the system throughput [21].

2. LITERATURE SURVEY OF KEY MAC LAYER PROTOCOLS

In this chapter, a subset of MAC protocols defined for sensor networks that employ alternative access schemes are described briefly by stating the essential behavior of the protocols wherever possible. Moreover, the advantages and disadvantages of these protocols are presented.

2.1. Sensor-MAC (S-MAC)

Locally managed synchronizations and periodic sleep-listen schedules based on these synchronizations form the basic idea behind the Sensor-MAC (S-MAC) protocol [13]. Neighboring nodes form virtual clusters to set up a common sleep schedule. If two neighboring nodes reside in two different virtual clusters, they wake up at listen periods of both clusters. A drawback of S-MAC algorithm is this possibility of following two different schedules, which results in more energy consumption via idle listening and overhearing. Schedule exchanges are accomplished by periodic SYNC packet broadcasts to immediate neighbors. The period for each node to send a SYNC packet is called the synchronization period. Figure 2.1 represents a sample sender-receiver communication. Collision avoidance is achieved by a carrier sense, which is represented as CS in the figure. Furthermore, RTS/CTS packet exchanges are used for unicast type data packets.

S-MAC also includes the concept of message-passing where long messages are divided into frames and sent in a burst. With this technique, one may achieve energy saving by minimizing the communication overhead at the expense of unfairness in the medium access. Periodic sleeping may result in high latency especially for multi-hop routing algorithms, since all intermediate nodes have their own sleep schedules. The latency caused by periodic sleeping is called *the sleep delay* [13]. The adaptive listening technique is proposed to improve the sleep delay and thus the overall latency. In that

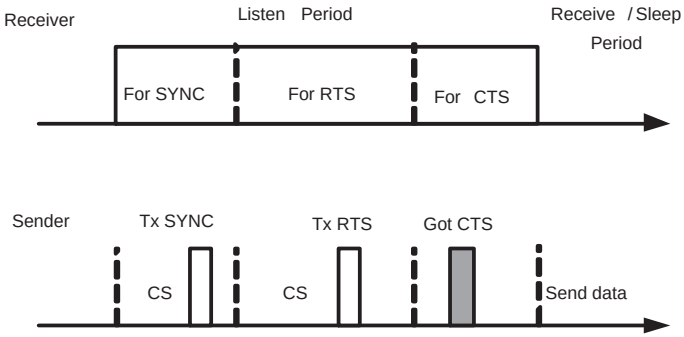

Figure 2.1. S-MAC Messaging Scenario [13]

technique, the node who overhears its neighbor's transmissions wakes up for a short time at the end of the transmission. Hence, if the node is the next-hop node, its neighbor could pass data immediately. The end of the transmissions is known by the duration field of RTS/CTS packets.

Advantages: The energy waste caused by idle listening is reduced by sleep schedules. In addition to its implementation simplicity, time synchronization overhead may be prevented by sleep schedule announcements.

Disadvantages: Broadcast data packets do not use RTS/CTS which increase the collision probability. Adaptive listening incurs overhearing or idle listening if the packet is not destined to the listening node. Sleep and listen periods are predefined and constant, which decreases the efficiency of the algorithm under variable traffic load.

2.2. WiseMAC

Hoiydi proposed "Spatial TDMA and CSMA with Preamble Sampling" protocol where all sensor nodes are defined to have two communication channels [22]. The data channel is accessed using TDMA, whereas the control channel is accessed by CSMA. WiseMAC [23] protocol is similar to Hoiydi's work [22], but requires only a single-channel. WiseMAC protocol uses non-persistent CSMA (np-CSMA) with preamble sampling as in [22] to decrease idle listening. In the preamble sampling technique, a preamble precedes each data packet for alerting the receiving node. All nodes in a

network sample the medium with a common period, but their relative schedule offsets are independent. If a node finds the medium busy after it wakes up and samples the medium, it continues to listen until it receives a data packet or the medium becomes idle again. The size of the preamble is initially set to be equal to the sampling period. However, the receiver may not be ready at the end of the preamble, due to reasons like interference, which causes the possibility of overemitting type energy waste. Moreover, overemitting is increased with the length of the preamble and the data packet, since no handshake is done with the intended receiver.

To reduce the power consumption incurred by the pre-determined fixed-length preamble, WiseMAC offers a method to dynamically determine the length of the preamble. That method uses the knowledge of the sleep schedules of the transmitter node's direct neighbors. The nodes learn and refresh their neighbor's sleep schedule during every data exchange as part of the acknowledgement message. In that way, every node keeps a table of sleep schedules of its neighbors. Based on neighbors' sleep schedule tables, WiseMAC schedules transmissions so that the destination node's sampling time corresponds to the middle of the sender's preamble. To decrease the possibility of collisions caused by that specific start time of wake-up preamble, a random wake-up preamble is advised. Another parameter affecting the choice of the wake-up preamble length is the potential clock drift between the source and the destination. A lower bound for the preamble length is calculated as the minimum of destination's sampling period, T_w, and the potential clock drift with the destination which is a multiple of the time since the last ACK packet arrived. Considering this lower bound, a preamble length (T_p) is chosen randomly. Figure 2.2 presents the WiseMAC concept.

Advantages: The simulation results show that WiseMAC performs better than one of the S-MAC variants [23]. Besides, its dynamic preamble length adjustment results in better performance under variable traffic conditions. In addition, clock drifts are handled in the protocol definition which mitigates the external time synchronization requirement.

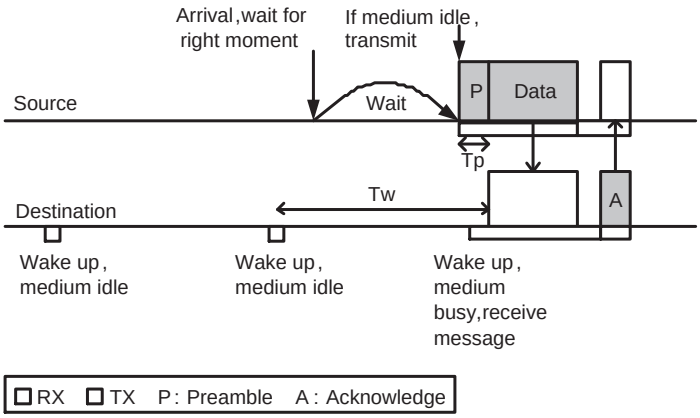

Figure 2.2. WiseMAC Concept [23]

Disadvantages: Main drawback of WiseMAC is that decentralized sleep-listen scheduling results in different sleep and wake-up times for each neighbor of a node. This is especially an important problem for broadcast type of communication, since broadcasted packet will be buffered for neighbors in sleep mode and delivered many times as each neighbor wakes up. However, this redundant transmission will result in higher latency and power consumption. In addition, the hidden terminal problem comes along with the WiseMAC model as in the Spatial TDMA and CSMA with Preamble Sampling algorithm. That is because WiseMAC is also based on non-persistent CSMA. This problem will result in collisions when one node starts to transmit the preamble to a node that is already receiving another node's transmission where the preamble sender is not within the range.

2.3. Traffic-Adaptive MAC Protocol (TRAMA)

TRAMA [24] is a TDMA-based algorithm and proposed to increase the utilization of classical TDMA in an energy-efficient manner. It is similar to Node Activation Multiple Access (NAMA) [25], where for each time slot a distributed election algorithm is used to select one transmitter within each two-hop neighborhood. This kind of election eliminates the hidden terminal problem and hence ensures that all nodes in the one-hop neighborhood of the transmitter will receive data without any collision. However, NAMA is not energy-efficient and incurs overhearing.

Time is divided into random-access and scheduled-access (transmission) periods. The random-access period is used to establish two-hop topology information and the channel access is contention-based within that period. A basic assumption is that, using the information passed by the application layer, the MAC layer can calculate the transmission duration needed which is denoted as *SCHEDULE_INTERVAL*. Then, at time t, the node calculates the number of slots for which it will have the highest priority among two-hop neighbors within the period $[t, t + SCHEDULE\_INTERVAL]$. The node announces the slots it will use as well as the intended receivers for these slots with a schedule packet. Additionally, the node announces the slots for which it has the highest priority but will not be used. The schedule packet indicates the intended receivers using a bitmap whose length is equal to the number of its neighbors. Bits correspond to one-hop neighbors ordered by their identities. Since the receivers of those messages have the exact list and identities of the one-hop neighbors, they find out the intended receiver. When the vacant slots are announced, potential senders are evaluated for re-use of those slots. Priority of a node on a slot is calculated with a hash function of node's and slot's identities. Analytical models for the delay performances of TRAMA and NAMA protocols are also presented and supported by simulations [24]. Delays are found to be higher compared to contention-based protocols due to higher percentage of sleep times.

Advantages: Higher percentage of sleep time and less collision probability is achieved compared to CSMA based protocols. Since intended receivers are indicated with a bitmap, less communication is performed for multicast and broadcast type of communication patterns compared other protocols.

Disadvantages: Transmission slots are set to be seven times longer than the random access period [24]. However, all nodes are defined to be either in receive or transmit states during the random access period for schedule exchanges. This means that without considering the transmissions and receptions, the duty cycle is at least 12.5 per cent, which is a considerably high value. For a time slot, every node calculates each of its two-hop neighbors' priorities on that slot. In addition, this calculation is repeated for each time slot, since the parameters of the calculation change with time.

2.4. Sift

Sift [26] is a MAC protocol proposed for event-driven sensor network environments. The motivation behind Sift is that when an event is sensed, the first R of N potential reports are the most crucial part of messaging and have to be relayed with low latency where R is a system parameter. Jamieson *et al.* use a non-uniform probability distribution function of picking a slot within the slotted contention window. If no node starts to transmit in the first slot of the window, then each node increases its transmission probability exponentially for the next slot assuming that the number of competing nodes is small.

In [26], Sift is compared with the 802.11 MAC protocol and it is showed that Sift decreases latency considerably when there are many nodes trying to send a report. Since Sift is a contention slot assignment algorithm, it is proposed to co-exist with other MAC protocols like S-MAC. Based on the same idea, CSMA/p^* [27] is proposed where p^* is a non-uniform probability distribution that optimally minimizes latency. However, Tay *et al.* state that the achieved probability distribution function for slot selection by Sift method is approximate to that of CSMA/p^*.

Advantages: Very low latency is achieved for many traffic sources. Energy consumption is traded off for latency as indicated below. However, when the latency is an important parameter of the system, slightly increased energy consumption must be accepted. Sift algorithm could be tuned to incur less energy consumption. The high energy consumption is a result of the arguments indicated below.

Disadvantages: One of the main drawbacks is increased idle listening caused by listening to all slots before sending. The second drawback is the increased overhearing. When there is an ongoing transmission, nodes must listen till the end in order to contend for the next transmission which causes overhearing.

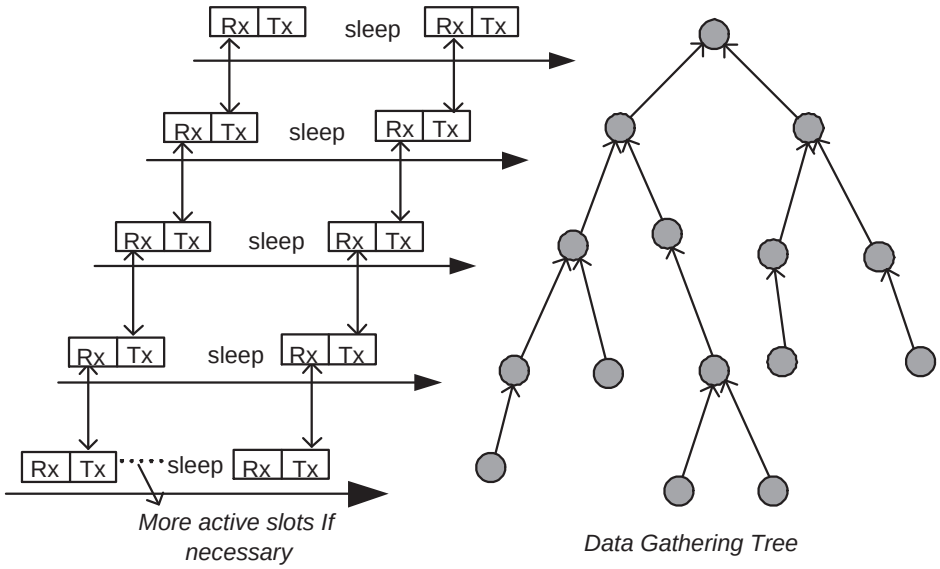

Figure 2.3. A data gathering tree and its DMAC implementation [28]

2.5. DMAC

Convergecast is the most frequent communication pattern observed within sensor networks. Unidirectional paths from possible sources to the sink could be represented as data gathering trees. The principal aim of DMAC [28] is to achieve very low latency for convergecast communications, but still to be energy-efficient. DMAC could be summarized as an improved Slotted Aloha algorithm where slots are assigned to the sets of nodes based on a data gathering tree as shown in Figure 2.3. Hence, during the receive period of a node, all of its child nodes have transmit periods and contend for the medium. Low latency is achieved by assigning subsequent slots to the nodes that are successive in the data transmission path.

Advantages: DMAC achieves very good latency compared to other sleep/listen period assignment methods. The latency of the network is crucial for certain scenarios, in which DMAC could be a strong candidate.

Disadvantages: Collision avoidance methods are not utilized, hence when a number of nodes that have the same schedule (same level in the tree) try to send to the same node, collisions will occur. This is a possible scenario in event-triggered sensor

networks. Besides, the data transmission paths may not be known in advance, which precludes the formation of the data gathering tree.

2.6. Timeout-MAC (T-MAC) / Dynamic Sensor-MAC (DSMAC)

Static sleep-listen periods of S-MAC result in high latency and lower throughput as indicated earlier. Timeout-MAC (T-MAC) [29, 30] is proposed to enhance the poor results of S-MAC protocol under variable traffic load. In T-MAC, listen period ends when no activation event has occurred for a time threshold TA. The decision for TA is presented along with some solutions to the early sleeping problem defined in [30]. Variable load in sensor networks are expected, since the nodes that are closer to the sink must relay more traffic and since traffic may change over time. Although T-MAC gives better results under these variable loads, the synchronization of the listen periods within virtual clusters is broken. This is one of the reasons for the early sleeping problem.

Dynamic Sensor-MAC (DSMAC) [31] adds a dynamic duty cycle feature to S-MAC. The aim is to decrease the latency for delay-sensitive applications. Within the SYNC period, all nodes share their one-hop latency values (time between the reception of a packet into the queue and its transmission). All nodes start with the same duty cycle. Figure 2.4 conceptually depicts DSMAC duty cycle doubling. When a receiver node notices that average one-hop latency value is high, it decides to shorten its sleep time and announces it within SYNC period. Accordingly, after a sender node receives this sleep period decrement signal, it checks its queue for packets destined to that receiver node. If there is one, it decides to double its duty cycle when its battery level is above a specified threshold.

The duty cycle is doubled so that the schedules of the neighbors will not be affected. The latency observed with DSMAC is better than the one observed with S-MAC. Moreover, it is also shown to have better average power consumption per packet.

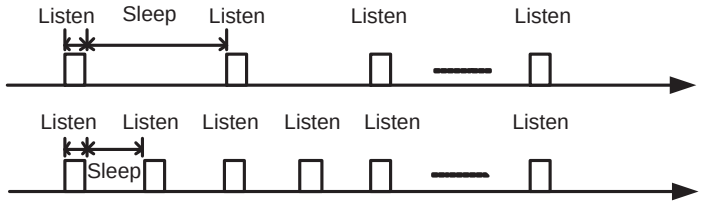

Figure 2.4. DSMAC duty cycle doubling [31]

2.7. Integration of MAC with Other Layers

Limited research has been carried out on integrating different network layers into one layer or to benefit from cross-layer interactions between routing and MAC layers for sensor networks. For instance, Safwat *et al.* proposed two routing algorithms that favor the information about successful/unsuccessful CTS or ACK reception [32].

Cui *et al.* looked at MAC/Physical layer integration and Routing/MAC/Physical layer integration [33]. They propose a variable length TDMA scheme where the slot length is assigned according to some criteria for the optimum energy consumption in the network. Among these criteria, the most crucial ones are information about the traffic generated by each node and distances between each node pair. Based on these values, they formulate a Linear Programming (LP) problem where the decision variables are normalized time slot lengths between nodes. They solve this LP problem using an LP solver which returns the optimum number of time slots for each node pair as well as the related routing decisions for the system.

The proposed solution could be beneficial for scenarios where the required data could be prepared. However, it is generally hard to have the node distance information and the traffic generated by the nodes. Besides, the LP solver could only be run on a powerful node. The dynamic behavior of sensor networks will require online decisions which are very costly to calculate and hard to adapt to an existing system.

Multihop Infrastructure Network Architecture (MINA) is another work for integrating MAC and routing protocols [34]. Ding *et al.* propose a layered multi-hop

network architecture where the network nodes with the same hop-count to the base station are grouped into the same layer. Channel access is a TDMA-based MAC protocol combined with CDMA or FDMA. The super-frame is composed of a control packet, a beacon frame and a data transmission frame. Beacon and data frames are time slotted. In the clustered network architecture, all members of a cluster submit their transmission requests in beacon slots. Accordingly, the cluster-head announces the schedule of the data frame.

The routing protocol is a simple multi-hop protocol where each node has a forwarder node at one nearer layer to the base station. The forwarding node is chosen from candidates based on the residual energies. Ding *et al.* then formulate the channel allocation problem as an NP-complete problem and propose a sub-optimal solution. Moreover, the transmission range of sensor nodes is a decision variable, since it affects the layering of the network (hop-counts change). Simulations are run to find a good range of values for a specific scenario.

The proposed system in [34] is a well-defined MAC/Routing system. However, the tuning of the range parameter is an important task which should be done at the system initialization. In addition, all node-to-sink paths are defined at the startup and are defined to be static, since channel frequency assignments of nodes are done at the startup accordingly. This makes the system intolerant to failures.

Geographic Random Forwarding (GeRaF) is actually proposed as a routing protocol, but the underlying MAC algorithm is also defined in the work which is based on CSMA/CA [35]. That gives us not an integrated but a complete solution for a sensor network's communication layers. The difficulty of the system proposed is its need for additional radio, which is used for busy tone announcement. Rugin *et al.* [36] and Zorzi [37] improved GeRaF reducing it to a one-channel system. However, sensor nodes' and their neighbors' location information are needed for those protocols. Besides, the forwarding node is chosen among nodes that are awake at the time of the transmission request. That may result in more power consuming routing and an increase in latency.

Table 2.1. Comparison of MAC protocols

Protocol	Time Synch. Needed	Comm.Pattern Support	Type	Adaptivity to Changes
S-MAC	No	All	CSMA	Good
WiseMAC	No	All	np-CSMA	Good
TRAMA	Yes	All	TDMA / CSMA	Good
SIFT	No	All	CSMA/CA	Good
DMAC	Yes	Convergecast	TDMA /Slotted Aloha	Weak

2.8. Open Issues and Conclusions for Literature Survey

Table 2.1 represents a comparison of MAC protocols investigated. *Time Synchronization Needed* column indicates whether the protocol assumes that the time synchronization is achieved externally. *Adaptivity to Changes* means ability to handle topology changes. The two S-MAC variants, namely, T-MAC and DSMAC, have the same features as S-MAC given in Table 2.1. The cross-layer protocols include additional layers other than the MAC layer and are not considered in this comparison.

TDMA has a natural advantage of collision-free medium access. However, it includes clock drift problems and decreased throughput at low traffic loads due to idle slots. The difficulty with TDMA systems are the synchronization of the nodes and adaptation to topology changes where these changes are caused by insertion of new nodes, exhaustion of battery capacities, broken links because of interference, sleep schedules of relay nodes, scheduling caused by clustering algorithms. The slot assignments, therefore, should be done regarding such possibilities. However, it is not easy to change the slot assignment within a decentralized environment for traditional TDMA, since all nodes must agree on the slot assignments. In accordance with the common networking lore, CSMA methods have a lower delay and promising throughput potential at lower traffic loads, which generally happens to be the case in wireless sensor networks. However, additional collision avoidance or collision detection methods should be employed.

FDMA is another scheme that offers a collision-free medium, but it requires an additional circuitry to dynamically communicate with different radio channels. This increases the cost of the sensor nodes, which is contrary to the objective of the sensor network systems.

CDMA also offers collision-free medium, but its high computational requirement is a major obstacle for less energy consumption objective of the sensor networks. Moreover, due to the sleep schedules, a signal synchronization method is also needed. In pursuit of low computational cost of wireless CDMA sensor networks, there has been limited effort to investigate source and modulation schemes, particular signature waveforms, designing simple receiver models, and other signal synchronization problems. If it is shown that the high computational complexity of CDMA could be traded off against its collision avoidance feature, CDMA protocols could also be considered as candidate solutions for sensor networks. Lack of comparison of TDMA, CSMA or other medium access protocols in a common framework is a crucial deficiency of the literature.

Common wireless networking experience also suggests that link-level performance alone may provide misleading conclusions about the system performance. Similar conclusion can be drawn for upper layers as well. Hence, the more layers contributing to the decision, the more efficient the system can be. For instance, the routing path could be chosen depending on the collision information from the medium access layer. Moreover, layering of the network protocols creates overheads for each layer which causes more energy consumption for each packet. Therefore, integration of the layers is also a promising research area which has to be studied more extensively.

3. PACKET TRAFFIC MODELING FOR SURVEILLANCE WIRELESS SENSOR NETWORKS

3.1. Introduction and Motivation

Sensor nodes are power-limited, and research has focused on designing energy-efficient algorithms. However, the potential application areas of wireless sensor networks show contrasting properties which prevent the development of universal algorithms that serve for all purposes. Military applications may require very fast response time, whereas in agriculture, delay sensitivity may be traded with energy conservation. Likewise, a communication protocol may perform in a very energy-efficient manner when used for one application, and it may perform quite poorly in another. One application-dependent characteristic of a WSN is the type of data traffic generated by the nodes. The model that represents the aggregate packet traffic in the network or a cluster of the network can be used to determine the maximum stable throughput, expected delay and the packet loss statistics. Furthermore, the effects of parameters such as node density and target velocity can be investigated in depth once an appropriate data traffic model is available.

When communication protocols are developed without taking into account the properties of the data traffic, they may behave inefficiently. For instance, in the WSN literature, the performance evaluation of the protocols are generally carried out with periodic data traffic as in [38, 39, 40], or using common data traffic models such as Poisson point processes [41, 42, 43, 44]. However, event-driven applications such as target detection and tracking produce bursty traffic which cannot be modeled as either periodic or Poisson. Although there are packet traffic models available for legacy communication networks, the unique features and requirements of WSNs call for the design and development of dedicated models. One such characteristic is the limited battery capacity, which results in the use of sleep-listen periods and sensing intervals to extend the lifetime of the network.

In this chapter, we investigate the importance of using a realistic packet traffic model by deriving a specific packet traffic model for Surveillance WSN (SPTM) and comparing the performance of a WSN medium-access control protocol for two traditional and one proposed packet traffic models. We show that the underlying packet traffic can result in dissimilar performance results for the same average packet traffic loads. This observation is significant since the improper packet traffic models may not correctly represent the realistic traffic characteristics, and lead to inefficient protocol design and implementation.

In the WSN literature, the application-specific packet traffic models are not studied extensively. A packet traffic model for intrusion detecting WSN is investigated in [15] in which binary sensor detection model is assumed. However, the binary detection is an idealized model in which the detection probability is defined with only a single parameter. To achieve a more realistic and accurate packet traffic, a probabilistic detection model employed in this work which includes a set of parameters to define the range-based detection probabilities. These detection parameters can be set according to the physical properties of the sensors deployed and of the potential targets. Based on this probabilistic detection model, we introduce a framework for the SPTM and derive the analytical formula for its components. The derived SPTM model is used to corroborate how a realistic packet traffic modeling makes a difference.

In Section 3.2, we describe the packet traffic framework that is used for the SPTM and present an analytical model for the framework proposed. Then, in Section 3.3, we verify the introduced analytical model with simulations. In Section 3.4, packet traffic generation algorithms are presented based on the proposed analytical model. The performance evaluation results of the well-known S-MAC protocol [13] are compared for SPTM, as well as the periodic and the binomial packet traffic models in Section 3.5. Finally, Section 3.6 includes the analytical derivations of the maximum stable throughput to verify the simulation results.

3.2. Surveillance Wireless Sensor Networks Packet Traffic Model (SPTM)

Surveillance Wireless Sensor Networks (SWSN) represent the WSN applications in which the deployed sensor nodes monitor an area such as a border for potential intruder entrance. When an intrusion is detected, the detecting sensors send data packets to the sink so that the necessary actions can be taken. Such a network can be employed for security applications, habitat monitoring, or disaster management applications. Because of the distinctive properties of these applications, the generated data are bursty and require a specific packet traffic model.

3.2.1. SWSN Packet Traffic Model (SPTM) Framework

Packet traffic models can be represented by a Markov process where the *state* $\tilde{s}$ corresponds to the event that s data packets are generated at a given time. Moreover, the state transition probability from *state* $\tilde{a}$ to *state* $\tilde{b}$ indicates the probability of generating b data packets with the knowledge of a data packets generated at the previous event detection. If there exists a correlation between successive data generation rates, this Markov process is said to have memory and the packet traffic model should also encapsulate this dependency.

The order of the Markov process represents the dependency of the successive data generation rates. The order is zero for memoryless packet traffic models such as Poisson and periodic data traffic, i.e., the probability of a transition to *state* $\tilde{b}$ is independent from the current state. However, for SPTM, the order is a positive value depending on the properties of the intruder movements and sensor node attributes which is formulated in [15]. The dependency in the subsequent number of detections is represented in Figure 3.1. The cross shaded sensors in Figure 3.1 detect the target in the two consecutive sampling instances, and hence, generate data packets in both sampling instances. The subsequent set of detecting sensors is determined by the target velocity and the sensing interval of the sensors.

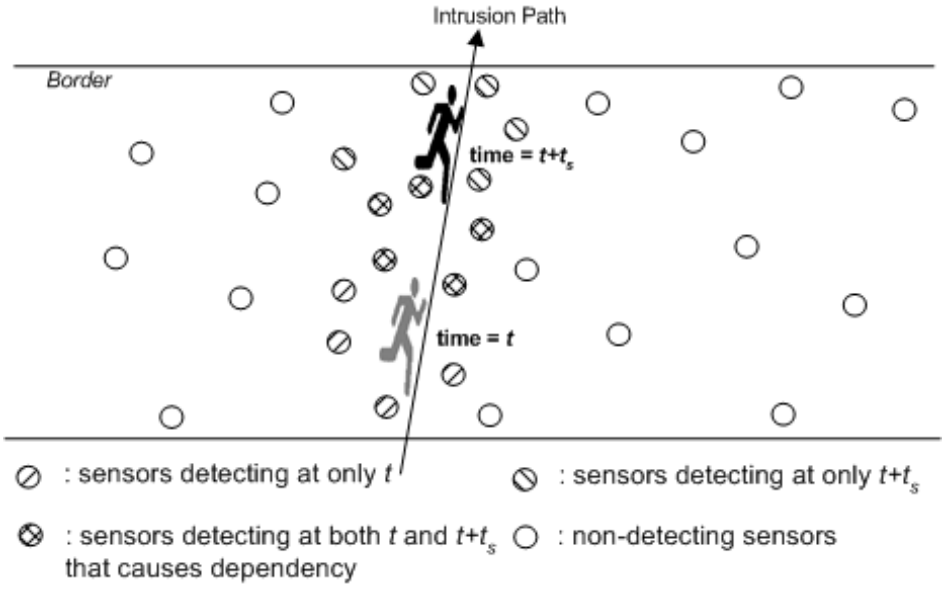

Figure 3.1. Illustration of the dependency between subsequent number of detections where t_s is the sensor sampling period

Since radio communication and sensing are two separate power consuming operations for sensors[1] , each have its own duty cycle. The duty cycles can be static or can be increased dynamically in case of event presence. For either case, assume that the sensing duty cycle interval is t_s in the presence of a target, which means that each node senses the environment once in t_s seconds. Hence, after the target is detected by a sensor at location (x, y) at time t, it will possibly be detected by the same node again at location (x', y') at time $t + t_s$, where the Euclidian distance between (x, y) and (x', y') is $v_T t_s$, with v_T being the velocity of the target within the $(t, t + t_s)$ period as illustrated in Figure 3.1. When one data packet is created at each target detection, assuming that the sensing offset of all sensors are the same, the number of data packets generated at point (x, y) is equal to the *detection degree* of that location, $k_{x,y}$, which is defined as the number of sensor nodes that actually detect the event[2] . Hence, a realistic packet traffic model for an SWSN application should provide the probability mass function (PMF) of detection degrees regarding the dependency of the consecutive detection degrees.

[1]As a numerical example, Crossbow motes require 5 mA for the sensor board operations whereas 8 mA and 12 mA are required by the radio board for reception and transmission, respectively. However, when both boards are in sleep mode, they require only a few μA's [45].

[2]Since *intrusion detection* is investigated as the event-driven application, the terms *target detection* and *event* are used interchangeably.

In the literature, the intruder detection probabilities of individual sensor nodes are modeled in several ways which are called *sensor detection models*. There are several sensor detection models proposed for wireless sensor nodes [46]. The detection probability of an event by a sensor node is a function of the sensor-to-event distance, in general. According to *the binary detection model*, an event occurring within a specific range of a sensor node is detected by that node with probability one, and it is not detected, otherwise. In other words, for the binary detection model, the probability of the target detection by a sensor is

$$\varphi(d) = \begin{cases} 1 & \text{if } d \leq d_c, \\ 0 & \text{if } d_c < d, \end{cases} \tag{3.1}$$

where d is the distance between the target and the sensor node and d_c is the threshold distance for detection which is also called the sensing range. The binary detection model is the most widely utilized sensor detection model whereas it is not realistic since it does not consider any type of failure or miss probability in detection.

Zou *et al.* [47] proposed a more general and probabilistic sensor detection model based on the Elfes' work [48]. Here, the dependency is parametric enabling the representation of different sensor types. Specifically, in the *Elfes sensor detection model*, the probability that a sensor detects an event at distance d is

$$\varphi(d) = \begin{cases} 1 & \text{if } d \leq d_c, \\ e^{-\alpha(d-d_c)^\beta} & \text{if } d_c < d < d_u, \\ 0 & \text{if } d_u \leq d, \end{cases} \tag{3.2}$$

where d_c, d_u define the certainty and uncertainty boundaries in detection, respectively. To clarify the term *sensing range*, d_c can be called the detection range and d_u can be called the sensing range, for the Elfes case. Hence, the target is detected with probability 1, if the target is within the detection range and it is detected with an exponential probability, if it is outside of the detection range but still within the sensing range. No detection occurs by the sensors that are further than the sensing range. The

parameters α and β, as well as d_u, d_c, reflect the physical properties of the sensors. In particular, α and β determine the rate and region of decay in $\varphi(d)$. An alternative detection model that incorporates the false alarm rate and additive white Gaussian noise is the Neyman-Pearson detector [49]. However, the Elfes model can accommodate the Neyman-Pearson detector through proper parameter matching as indicated in [50].

Calculation of the total number of detecting sensor nodes requires the knowledge of the number of sensor nodes that have positive detection probability, which is called the coverage degree and represented as $c_{x,y}$ for the detection point (x, y). For the Elfes model, the sensor nodes that have positive detection probability are the sensor nodes within d_u distance of the event point and for the binary detection model, they are the nodes within d_c distance. In addition, with the Elfes model, the locations of the sensor nodes determine the probabilities of the number of detections, since the per-sensor detection probability is a function of the target-sensor distance. Note that:

1. The number of detecting sensor nodes (detection degree) is always less than or equal to the number of sensor nodes that have a positive detection probability (coverage degree), i.e., $k_{x,y} \leq c_{x,y}$.
2. For the binary detection model, the detection degree is always equal to the coverage degree, i.e., $k_{x,y} = c_{x,y}$.
3. The Elfes model reduces to the binary detection model, if $d_u = d_c$.

Hence, the Elfes detection model incorporates binary detection and as a result enables more general and flexible sensor detection modeling.

The framework for SPTM is shown schematically in Figure 3.2 and described as follows. As the target crosses the border, it can be detected by the sensor nodes deployed to the border which sample the environment periodically, i.e., once in t_s seconds. Hence, to find the number of data packets generated because of the target detections at the location (x, y), we first need to know the coverage degree of that location, $c_{x,y}$. Once we have the coverage degree, we then need to calculate the detection degree, $k_{x,y}$, based on $c_{x,y}$. Hence, for the consecutive number of detections, we have

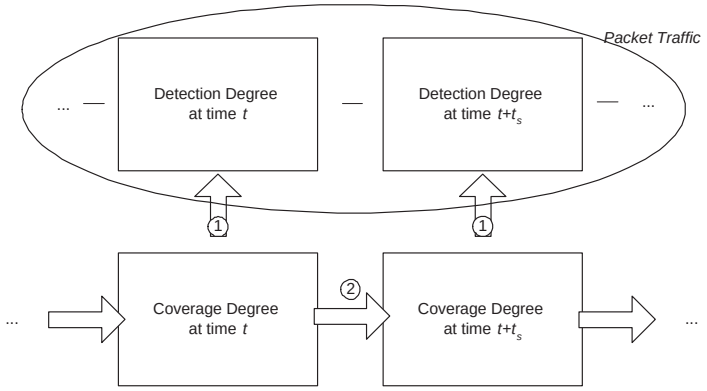

Figure 3.2. SWSN packet traffic model (SPTM) framework

to know the correlation between the coverage degrees of the target locations at the consecutive sampling times. The main components of the framework are i) the coverage degree, ii) the detection degree, iii) relation between the detection degree and the coverage degree (arrow 1), and iv) the correlation of successive coverage degrees (arrow 2). The analytical derivations of these components and correlations are given in Section 3.2.2.

3.2.2. Analytical Model of the SPTM Framework

In the WSN literature, two types of deployment are assumed in general: random deployment (e.g. [51], [52]) and grid deployment (e.g. [53], [54]). In *grid deployment*, nodes are placed deterministically along grid points, while in *random deployment* they are placed randomly in the application area. In this work, we assume uniformly random deployment. However, we use the probabilities of the number of sensor nodes deployed within a specific area instead of setting the individual locations randomly. That enables the calculation of the coverage degree of the event locations without generating the whole deployment map.

Since $c_{x,y}$ is defined as the number of sensor nodes that has a positive probability to detect the target at (x, y), PMF of $c_{x,y}$ is determined by the probability of the total number of sensors within the distance d_u of (x, y). However, as the target area is known and all sensors are deployed within its borders, for each sensor node deployment,

the event that the deployed node is within the d_u-distance of the target point is a Bernoulli trial with the probability of success $p = \pi {d_u}^2/LH$, where (L,H) is the length and width of the borders of the surveillance area. Hence, the total number of sensor nodes within distance d_u of a point forms a Binomial distribution. Moreover, for large N and small p, which is generally the case in intrusion detection applications, this Binomial distribution can be approximated by a Poisson distribution. The mean of the equivalent Poisson distribution is

$$\lambda = Np = \frac{N\pi {d_u}^2}{LH}. \tag{3.3}$$

The coverage degree probabilities of area points, hence, form a Poisson PMF. However, as illustrated in Figure 3.1, because the number of sensor nodes within the sensing ranges will be similar, the coverage degree probabilities of two nearby surveillance area points are not independent of each other. If we are given the coverage degree of the target location at time t, we cannot use the Poisson distribution with the mean value given in Equation 3.3 to estimate the coverage degree of the target location at time $t + t_s$, which will be the next detection point. Here, the locations that the target resides at sampling times are named *detection point* or *event point*, even if the detection degree is zero for the sake of readability.

Figure 3.3 shows the reason for the degree-dependency between the successive points. Let $\mathcal{C}_1$ and $\mathcal{C}_2$ denote locations of the target at times t and $t + t_s$, respectively. If the target velocity at time t is v_T, then the distance between $\mathcal{C}_1$ and $\mathcal{C}_2$ is equal to $v_T t_s$. In addition, the coverage degree of point $\mathcal{C}_1$ ($\mathcal{C}_2$) equals to the number of sensor nodes residing on $\mathcal{D}_1$ ($\mathcal{D}_2$), where $\mathcal{D}_i$ is the disk whose center is at $\mathcal{C}_i$ and whose radius is d_u. The dependency of the coverage degrees of points $\mathcal{C}_1$ and $\mathcal{C}_2$ is represented by the intersection of the two disks.

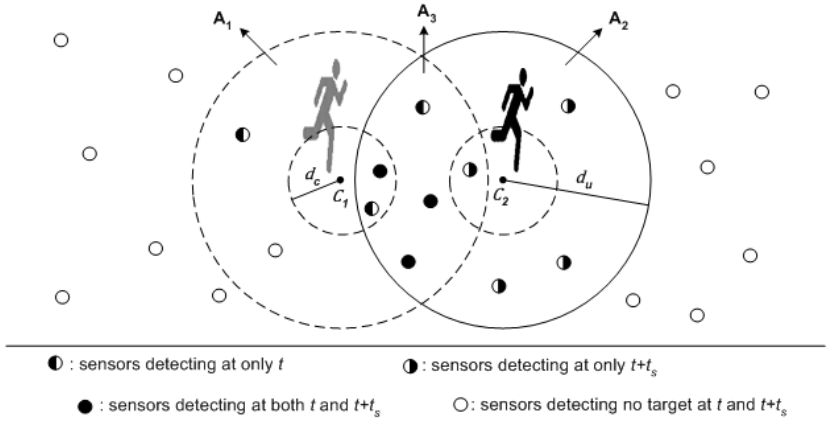

Figure 3.3. Geometric representation of successive target detection locations

To investigate the dependency of the coverage degrees, we have to first look into the deployment probabilities of the crescent areas $\mathcal{A}_1$ and $\mathcal{A}_2$, and the intersection area $\mathcal{A}_3$ which are defined as

$$\mathcal{A}_3 = \mathcal{D}_1 \cap \mathcal{D}_2, \quad \mathcal{A}_i = \mathcal{D}_i - \mathcal{A}_3, \quad i = 1, 2. \tag{3.4}$$

Let the random variable $\mathcal{Y}_i$ denote the number of nodes that reside in $\mathcal{A}_i$. Then,

$$P(\mathcal{Y}_i + \mathcal{Y}_3 = n) = P(\mathcal{X}_i = n), \quad i = 1, 2, \tag{3.5}$$

where the random variable $\mathcal{X}_i$ denotes the number of sensor nodes that have non-zero detection probability, i.e., the sensor nodes that resides within the d_u-distance of the event point $\mathcal{C}_i$. Given that point $\mathcal{C}_1$ has coverage degree c_1, the probability that point $\mathcal{C}_2$ has coverage degree c_2 is found as follows. Define $c_{\min} = \min(c_1, c_2)$. Then,

$$P(\mathcal{X}_2 = c_2 | \mathcal{X}_1 = c_1) = \sum_{i=0}^{c_{\min}} P(\mathcal{X}_2 = c_2 | \mathcal{Y}_3 = i) P(\mathcal{Y}_3 = i | \mathcal{X}_1 = c_1). \tag{3.6}$$

If it is known that there exist c_1 sensors on the first disk, then the probability of having i of them inside $\mathcal{A}_3$ possesses the Binomial distribution, where the probability

of success is $\mathcal{A}_3/\pi {d_u}^2$. Hence,

$$P(\mathcal{Y}_3 = i|\mathcal{X}_1 = c_1) = \binom{c_1}{i} \left(\frac{\mathcal{A}_3}{\pi {d_u}^2}\right)^i \left(1 - \frac{\mathcal{A}_3}{\pi {d_u}^2}\right)^{c_1 - i}. \tag{3.7}$$

The probability of having $c_2 - i$ sensors within $\mathcal{A}_2$ again possesses the Binomial distribution. However, c_1 sensors are known to be out of that area. Hence, we are left with $N - c_1$ sensors to be deployed in the entire surveillance area minus $\mathcal{D}_1$. As a result,

$$P(\mathcal{X}_2 = c_2|\mathcal{Y}_3 = i) = P(\mathcal{Y}_2 = c_2 - i) = \binom{N - c_1}{c_2 - i} \times \left(\frac{\mathcal{A}_2}{LH - \pi {d_u}^2}\right)^{c_2 - i} \left(1 - \frac{\mathcal{A}_2}{LH - \pi {d_u}^2}\right)^{N - c_1 - (c_2 - i)}. \tag{3.8}$$

Therefore, given c_1, probability of having a coverage degree of c_2 in the next detection point can be calculated by using Equation 3.6 - Equation 3.8. However, according to Equation 3.2, even if the coverage degree of a detection point is known, the number of target detections, and hence, the number of data packets generated are probabilistic. To calculate the detection degree of an event point, we first have to find the probability of event detection, $\varphi(d)$, per sensor node within the sensing range d_u. Then, a PMF for the number of detecting nodes can be generated which is a function of coverage degree $c_{x,y}$. For that, we utilize the *circle area element* definition which is illustrated in Figure 3.4. The circle area element is defined as

$$dA = r\, dr\, d\theta. \tag{3.9}$$

Assume that a sensor node resides within the sensing range of the event location. Then, the probability of detection equals to the probability that the sensor resides in any specific circle area element and detects the target from that distance. Then,

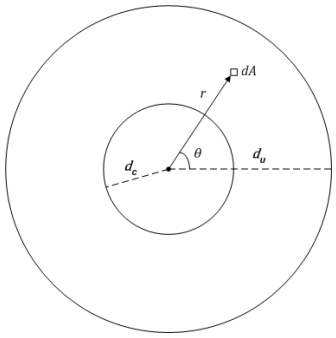

Figure 3.4. Circle area element at distance r and with angle θ

probability of detection for any one sensor within the d_u-distance of the target is

$$\gamma = \int_0^{2\pi}\int_0^{d_u} \frac{dA}{\pi {d_u}^2}\varphi(r) = \int_0^{2\pi}\int_0^{d_u} \frac{r\,dr\,d\theta}{\pi {d_u}^2}\varphi(r). \tag{3.10}$$

However, $\varphi(r)$ is a piecewise function and therefore the integral in Equation 3.10 can be divided into appropriate intervals as in

$$\gamma = \int_0^{2\pi}\int_{d_c}^{d_u} \frac{r\,dr\,d\theta}{\pi {d_u}^2}e^{-\alpha(r-d_c)^\beta} + \int_0^{2\pi}\int_0^{d_c} \frac{r\,dr\,d\theta}{\pi {d_u}^2}. \tag{3.11}$$

Equation 3.11 can be integrated according to the Elfes parameter values used. For $\beta = 1$, the probability of detection is found to be

$$\gamma = \frac{{d_c}^2}{{d_u}^2} + \frac{2}{\alpha^2 {d_u}^2}[1 + \alpha d_c - e^{\alpha(d_c - d_u)}(1 + \alpha d_u)]. \tag{3.12}$$

When all sensors are identical, which implies the same γ, and because sensor nodes are distributed uniformly, the PMF of the detection degree of the event point is Binomial with the probability of success, γ.

If we define $\mathcal{K}_i$ to be the random variable that represents the detection degree of the event point $\mathcal{C}_i$, then

$$P(\mathcal{K}_i = k_i | \mathcal{X}_i = c_i) = \binom{c_i}{k_i}\gamma^{k_i}(1-\gamma)^{c_i - k_i}. \tag{3.13}$$

The probabilities of possible detection degrees of a point, hence, can be calculated if the coverage degree of that point is known. However, as Equation 3.6 indicates, the coverage degrees of successive detection points are not i.i.d., which means that the numbers of successive data packet generations are dependent. Given that $\mathcal{C}_j$ is the subsequent point of detection point that comes right after $\mathcal{C}_i$, and k_j is the detection degree of the detection point $\mathcal{C}_j$, this dependency can be formulated as

$$P(\mathcal{K}_j = k_j | \mathcal{X}_i = c_i) = \sum_{c_j=0}^{N-c_i} P(\mathcal{K}_j = k_j | \mathcal{X}_j = c_j) P(\mathcal{X}_j = c_j | \mathcal{X}_i = c_i). \tag{3.14}$$

The correctness of the analytical formulation derived for the components of SPTM framework is verified in Section 3.3. Moreover, the packet traffic generation using these formula is presented in Section 3.4.

3.3. Validation of SWSN Packet Traffic Model (SPTM) Framework

As a reference scenario, we set the system parameter values as specified in Table 3.1, and investigate the coverage and the detection degrees of the area points under uniformly distributed random deployment. The value for the parameter *Number of Sensors* is selected so that if regular grid deployment is employed, that many nodes are required for a minimum coverage of 99 per cent of the surveillance area.

For evaluating the case with the Elfes detection model, 10000 simulation runs are performed. At each run, N sensors are randomly deployed to a rectangle surveillance area that has length L and width H with uniform distribution. Then, one target crosses the area with the velocity v_T. While the target crosses the area, at each t_s seconds, the coverage degree of the target location and the number of target detections generated are logged with the corresponding time values to be able to extract the dependency of successive target locations.

Table 3.1. SWSN reference scenario parameters for SPTM simulations

Parameter	Notation	Value
Border length	L	10000 m
Border width	H	1000 m
Number of sensors	N	10000
Sensing range	d_u	20 m
Certain Detection range	d_c	0 m
Sensing parameter	α	0.1
Sensing parameter	β	1
Target velocity	v_T	10 m/sec
Sensing interval	t_s	1 sec

Detection of the target by the surrounding sensor nodes are determined probabilistically based on the sensor-target distance. The target uses the shortest crossing path[3] . As a result, at each simulation run, $\lfloor H/v_T t_s \rfloor = 100$ samples are taken in which the target is possibly detected. At each sampling, the coverage and detection degree values of the target locations are logged.

After all simulations are completed, the probability mass functions are constructed based on the following histograms of the logged data:

- Histogram of the detection degrees observed, k_i, for the target detection points with coverage degree c_i, which is denoted as $Hist(k_i|\mathcal{X}_i = c_i)$,
- Histogram of the coverage degrees of the successor target detection points for the locations with coverage degree c_i, which is denoted as $Hist(c_{i+1}|\mathcal{X}_i = c_i)$.

Figure 3.5 depicts $P(\mathcal{K}_i = k|\mathcal{X}_i = 5)$, which is the detection degree PMF for the points with coverage degree of five. As seen in the figure, the simulation results verify the analytical work presented for the probabilities of the number of sensors detecting an event, given the number of sensors within the sensing range. However, if the binary

[3]As will be described in Section 3.4, any target trajectory with varying direction and speed can be used as an input to generate successive coverage and detection degrees, analytically.

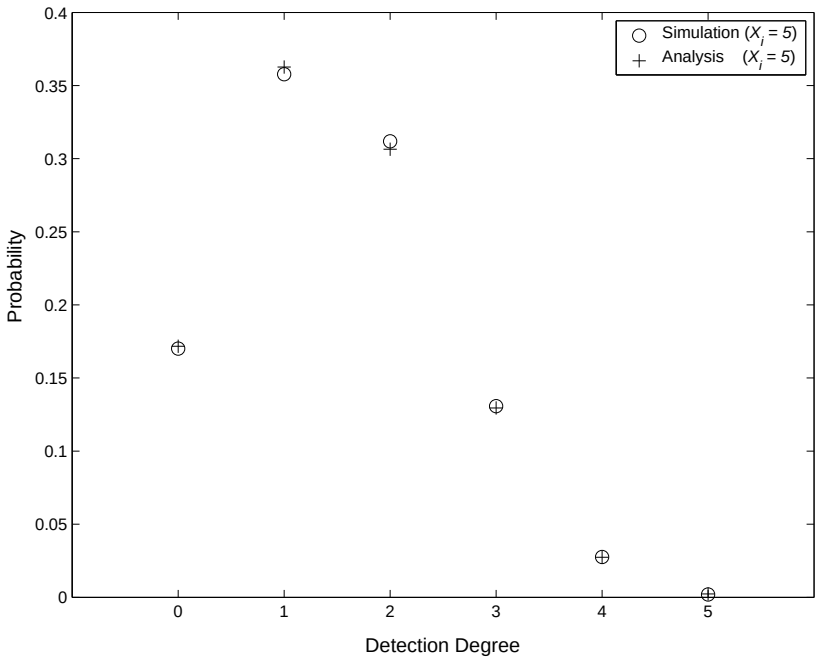

Figure 3.5. The detection degree PMF for points with coverage degree five

sensor detection model was used instead, the resulting PMF would give the probabilities of

$$P(\mathcal{K}_i = k|\mathcal{X}_i = 5) = \begin{cases} 1 & \text{if } k = 5, \\ 0 & \text{otherwise,} \end{cases} \tag{3.15}$$

which have very diverse values since it discards the effect of the sensor-target distance on the target detection probability. To show that the detection degree PMF of an event point is determined by its coverage degree regardless of the history of coverage degrees, $P\left(\mathcal{K}_i = k|\mathcal{X}_i = 4\right)$ is compared to $P(\mathcal{K}_i = k|(\mathcal{X}_i = 4)(\mathcal{X}_{i-1} = j))$ in Figure 3.6. As Figure 3.5 and Figure 3.6 show, the packet traffic model presented in Section 3.2 provides a mathematical framework for the packet traffic incurred by the SWSN.

To obtain an accurate packet traffic model, Elfes parameters should be set according to the detection characteristics of the sensors deployed. Note that, the binary detection model is achieved for the special case where the detection range parameter, d_c is equal to the sensing range parameter, d_u. To show how the binary detection model gives different results compared to those of the Elfes model, Figure 3.7 depicts

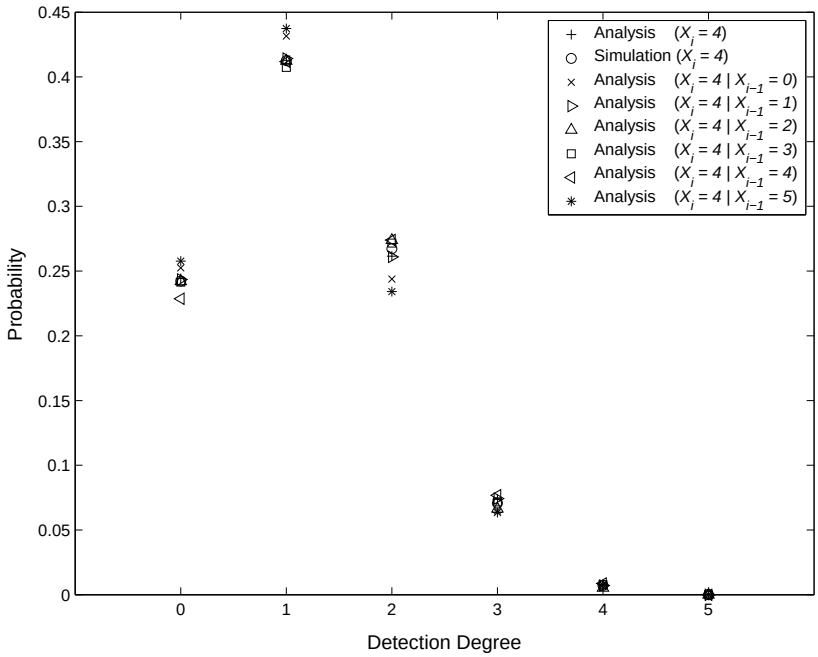

Figure 3.6. The detection degree PMF for points with coverage degree four

the effect of different detection ranges on the number of detections. As seen in Figure 3.7, the packet traffic based on the parametric detection model will be very different than the one based on the idealized binary detection model.

Moreover, the significance of setting the Elfes parameters accurately is also seen in Figure 3.8 where the detection degrees for different values of the Elfes detection parameter α is shown. As the figure depicts, given a point with a specific coverage degree value, the detection degree probabilities varies considerably depending on the detection parameter value used. Hence, in addition to the use of a parametric detection model, the use of sensor-specific parameter values is also very crucial.

3.4. Packet Traffic Generation Using Analytical SPTM Model

Based on the presented analytical work for the coverage and the detection degree models, synthetic packet traffic for an intrusion detection scenario can be generated as follows.

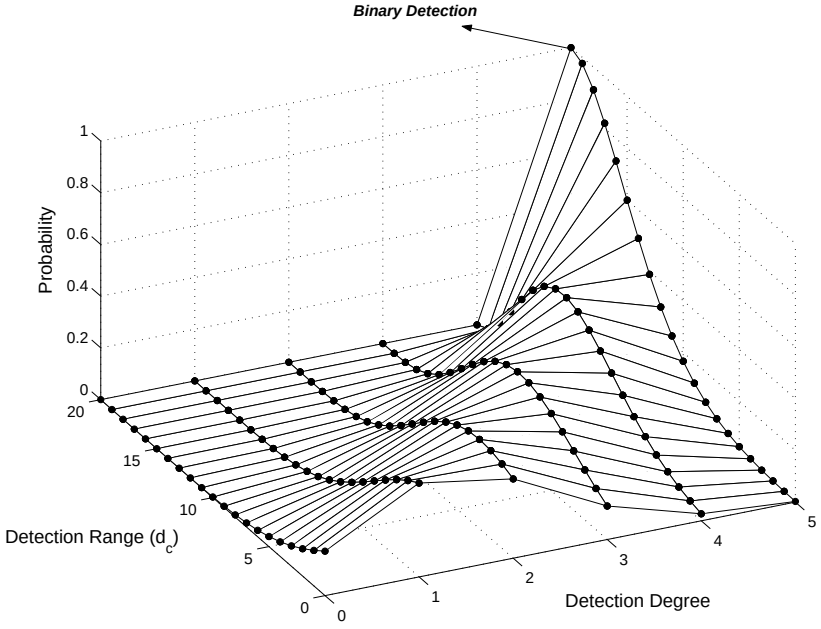

Figure 3.7. The effect of the detection range parameter, d_c, on the detection degree probabilities for coverage degree of five

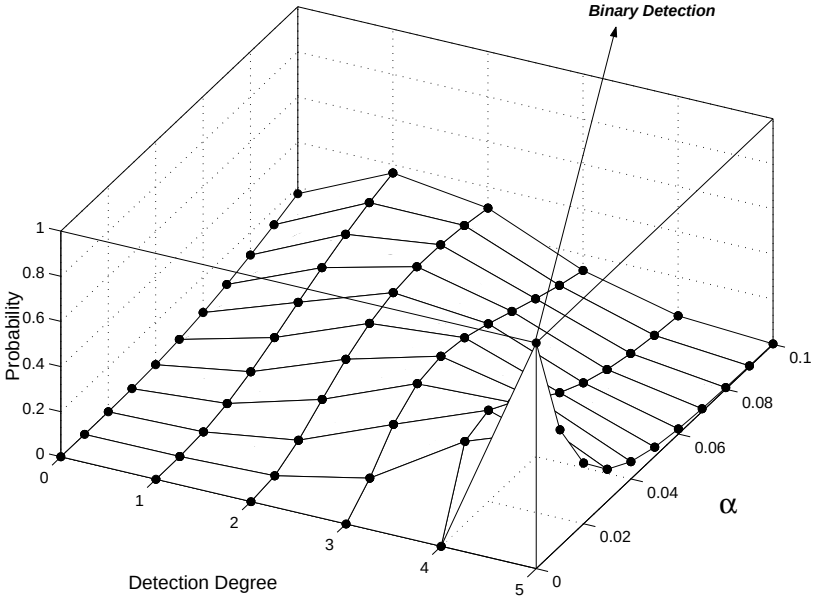

Figure 3.8. The effect of the detection parameter α on the detection degree probabilities for coverage degree of five

1: Set c_0 to be a random value chosen from the Poisson distribution with mean given in Equation 3.3 {*entrance point cov. deg.*}
2: Calculate $\mathcal{A}_s$ based on the v_T, t_s and d_u.
3: Calculate k_0 based on the probabilities found in Equation 3.12 and Equation 3.13 {*entrance point detection deg.*}
4: **for** $t = 1$ to $\lfloor \frac{H}{v_T t_s} \rfloor$ {*assuming a shortest crossing path*} **do**
5: Choose a value for c_t randomly, based on the probabilities found in Equation 3.6 - Equation 3.8.
6: Calculate k_t based on the probabilities found in Equation 3.12 and Equation 3.13.
7: **end for**

Figure 3.9. Packet traffic generation algorithm for the Elfes model

3.4.1. SPTM Packet Traffic Generation Algorithm

Packet traffic starts with the entrance of the target to the surveillance area. Since there is no coverage degree history at that time, the initial coverage degree is generated according to the Poisson distribution with mean given in Equation 3.3. Based on the detection degree PMF for the generated coverage degree value, a detection degree value is produced. Then, with the dependencies described in Section 3.2, subsequent coverage degrees and the corresponding detection degree values are generated. The algorithm presented in Figure 3.9 presents the steps to create sample packet traffic streams considering the Elfes detection model for $\beta = 1$ case.

Although algorithm in Figure 3.9 assumes a shortest crossing path for the target, any path with constant target speed can be evaluated by changing the second term in Step 4 with $\lfloor \ell / v_T t_s \rfloor$, where ℓ represents the length of the target crossing path. That is because all analytical work presented is still applicable by dividing the path into piecewise linear paths. In addition, if a target with varying speed and/or varying direction is to be simulated, the target trajectory can be used to generate the corre-

1: Set c_0 to be a random value chosen from the Poisson distribution with mean given in Equation 3.3 {*entrance point cov. deg.*}
2: Calculate $\mathcal{A}_s$ based on the v_T, t_s and d_u.
3: Calculate k_0 based on the probabilities found in Equation 3.12 and Equation 3.13 {*entrance point detection deg.*}
4: **for** $t = 1$ to η {*assuming a given target trajectory*} **do**
5: Choose a value for c_t randomly, based on the probabilities found in Equation 3.6 - Equation 3.8 where $v_T t_s$ is replaced by the Euclidean distance between $\mathcal{C}_t$ and $\mathcal{C}_{t+1}$ in the area calculations.
6: Calculate k_t based on the probabilities found in Equation 3.12 and Equation 3.13.
7: **end for**

Figure 3.10. Packet traffic generation algorithm for the Elfes model using a target trajectory

sponding packet traffic as follows: Assume that the target trajectory is given as the vector $\mathbf{C} = [\mathcal{C}_1 \ \ \mathcal{C}_2 \ \ \cdots \ \ \mathcal{C}_\eta]^T$ where $\mathcal{C}_i$ stores the location of the target at ith sampling and η here represents the last sampling number before the target leaves the surveillance area. The modified algorithm that utilizes the target trajectory is given in Figure 3.10.

3.4.2. Traffic Characteristics

Data traffic streams generated with the algorithm presented in Figure 3.9 are illustrated in Figure 3.11 for varying number of sensor deployments, in other terms for varying sensor densities. If the target uses the shortest crossing path, then the path takes $\lfloor H/v_T \rfloor = 100$ seconds and the target is sensed for $\lfloor H/v_T t_s \rfloor = 100$ times by the sensors if $t_s = 1$ seconds. Figure 3.11 depicts that the probability of target detection, and hence the data traffic rate increases as the sensor density increases as expected.

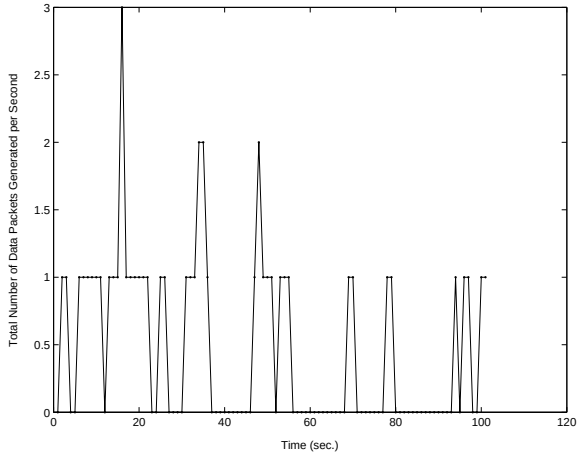

(a)

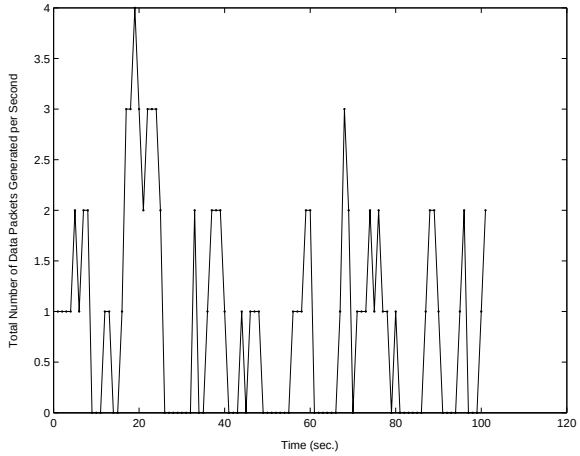

(b)

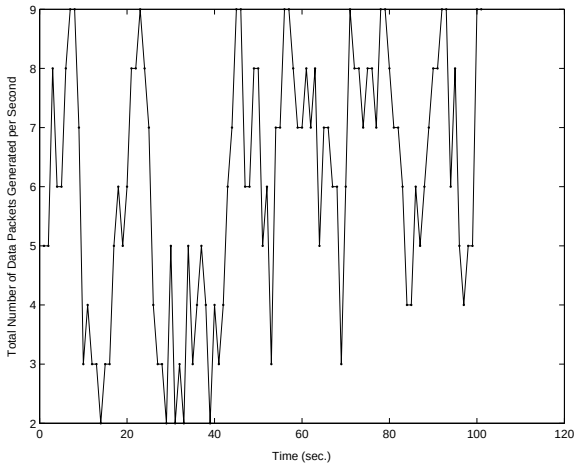

(c)

Figure 3.11. Effect of node density on data traffic for (a) $N = 5000$, (b) $N = 10000$, and (c) $N = 50000$

The effect of the target velocity is investigated in Figure 3.12. As the target velocity decreases, the dependency between the successive number of data packet generations increases and the probability that similar number of data packets are generated at consecutive detections increases. However, as the target velocity increases, PMF of the number of data packets generated approaches to the *memoryless* Poisson distribution with the mean given in Equation 3.3 which results in sharper changes in the number of data packets generated at consecutive detections. Hence, the packet traffic model proposed enables the generation of sample data traffic streams or investigation of the effect of system parameter settings as illustrated in Figure 3.11 and Figure 3.12. Next, we will investigate why one should use a separate packet traffic model for SWSN instead of using simpler models such as periodic or binomial models.

3.5. Impact of a Realistic Packet Traffic Model

To investigate the effect of the underlying packet traffic model, we conduct various simulations with three different types of packet traffic generation: i) periodic data generation, ii) binomial data generation achieved by Bernoulli trials of the individual nodes, iii) data generation by SPTM which corresponds to the realistic packet traffic for SWSN. We study the impact by examining the performance results for the Sensor-MAC (S-MAC) protocol [13]. S-MAC is a CSMA/CA-based MAC protocol that divides the network into virtual clusters, where the cluster members have the same sleep-listen schedules and the members at the intersection of different clusters also wake up at listen periods' of their neighboring clusters. Although there are a number of improvements on S-MAC such as Timeout-MAC (T-MAC) [29] and Dynamic Sensor-MAC (DSMAC) [31], because our goal is to show that using a realistic traffic model makes a difference, we will focus on the basic S-MAC protocol.

The performance of S-MAC is evaluated with the three different packet traffic models based on two performance criteria. The first one is the *average packet delay* as used in [55, 56] which is a crucial performance metric for time-critical applications such as disaster monitoring and target tracking. For MAC protocols, packet delay is defined as the time passed from the data packet's reception by the sender's MAC layer

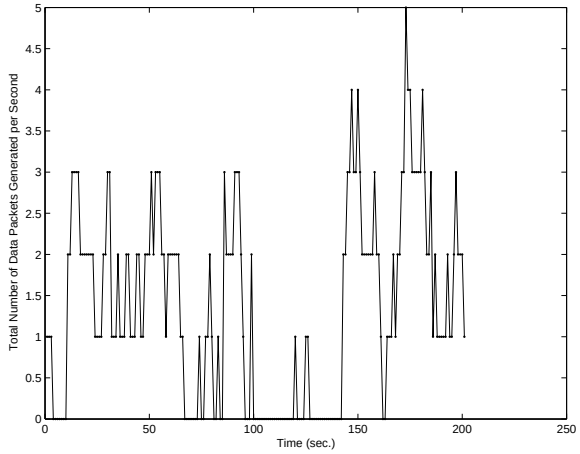

(a)

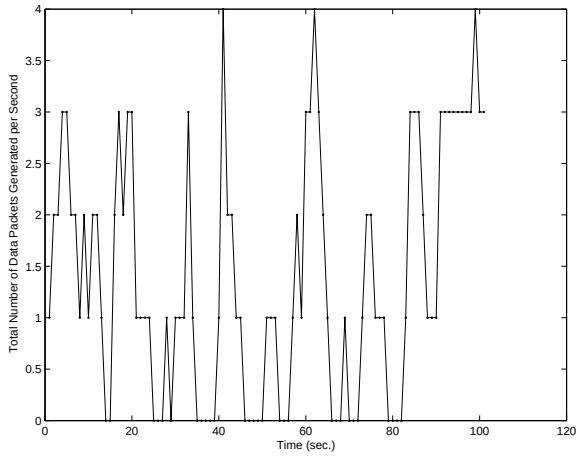

(b)

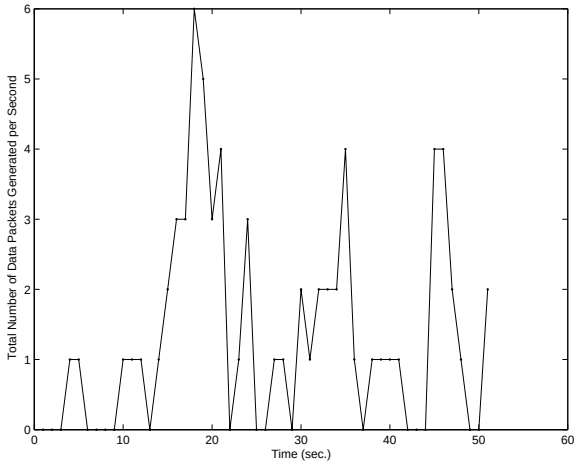

(c)

Figure 3.12. Effect of target velocity on data traffic for (a) $v_T = 5\,m/s$, (b) $v_T = 10\,m/s$, and (c) $v_T = 30\,m/s$

to its arrival to the destination node's MAC layer which includes the delays incurred by queueing, collisions and transmission. Selecting the average delay as a performance metric also enables the investigation of the maximum stable throughput of a system by inspecting the traffic load that results in infinite or unacceptable average delay.

The second performance criterion inspected is the packet drop rate as in [57, 58], which is described as the rate of the packets dropped due to the limited buffer, or some other system or environment effects such as protocol time-outs. The packet drop rate is critical if the redundancy of the information sent is low, in other words, if the information within each data packet is crucial for the application.

We consider one of the virtual clusters formed in the network separately to investigate the performance of the S-MAC protocol without the influence of the overlaying protocols such as the routing protocol. Within a virtual cluster, all members that have a data packet to send contend for the medium. S-MAC allocates contention slots for election of the node that will be given access to the medium. At the beginning of the contention slot period, all pending nodes pick a slot randomly. If a node did not receive start of any transmission before its slot's time arrives, it starts to transmit a Ready-To-Send (RTS) packet. Once the transmitted packet arrives at the destination node successfully, the destination node replies with a Clear-To-Send (CTS) packet. On the other hand, if the first occupied slot is actually selected by two or more nodes, then these nodes start transmitting their RTS packets at the same time, which results in a collision. These sender nodes realize the collision when no CTS packet is returned by the destination node within a specified time. Once the CTS packet is transmitted or the CTS time-out triggers, the contention slot procedure is started again. S-MAC simulation parameters and their values are listed in Table 3.2. Section 3.5.1 describes the three packet traffic patterns used in the simulations. Then, Section 3.5.2 presents the comparison results.

Table 3.2. Scenario parameters for simulations of packet traffic model impact

Parameter	Value
Number of contending sensors	20
Bandwidth	20 Kbps
Data packet size	128 bit
RTS/CTS/ACK packet size	26 bit
Listen period	0.1 sec
SYNC+Sleep period	0.9 sec

3.5.1. Packet Traffic Patterns

To evaluate the impact of the SPTM traffic pattern, two other data traffic patterns with different data traffic loads are used for comparison. The traffic load is defined as the number of new packet arrivals to a system, i.e., the total number of data packets created per unit time for WSN applications[4] . The periodic data traffic is achieved when each sensor node generates data with a specific time interval. A common interval is used by all sensors; however, they are allowed to choose a random offset. As a result, a periodically repeating packet traffic occurs. In this traffic model, average packet traffic load can be varied by changing the data generation interval defined in the system. To have a simplistic and non-periodic packet traffic, probabilistic data generation is used where the sensor nodes generate data packet at each unit time based on a specific probability. Consequently, the individual data traffic is a Bernoulli process and the aggregate data traffic becomes a Binomial traffic. Here, the traffic load is determined by the probability value assigned to all sensor nodes for data generation. Both periodic data traffic and Binomial packet traffic have the common property of being independent of external events such as target detection. Moreover, in both types of traffic, individual sensor data generation times are independent of the other sensors' data generations.

[4]Two types of traffic loads are defined in the literature, namely, the *offered* and the *carried* traffic loads. In this work, we study the changes in the system performance according to the number of data packets generated. Hence, we use the term *traffic load* to represent the *offered traffic load*.

Table 3.3. Parameters of the packet traffic patterns

Traffic Type	Parameter	Value Range
Periodic	Data generation interval	2.25-20 sec
Binomial	Data generation probability	0.05-0.4
SPTM	Sensing range	15-40 m
SPTM	Target speed	1 m/sec
SPTM	Pause time	0 sec
SPTM	Area length	100 m
SPTM	Area width	100 m

The SPTM traffic is composed of data packets generated by the sensor nodes at target detections. Hence, there is a dependency between data generations of the neighboring sensors which results in a bursty packet traffic. SPTM packet traffic scenario is generated as follows. Within the cluster area in which sensor nodes are deployed uniformly random, one target is assumed to move according to the random waypoint mobility model, which is commonly adopted in ad hoc networking research community [59, 60]. In this model, the mobile is assigned a destination point ("waypoint") within the rectangular area defined and a speed uniformly in a given interval. When it reaches the destination, it remains static for a predefined pause time and then starts moving again according to the same rule. With SPTM, different packet traffic loads are achieved by altering the value of the sensing range parameter of the detection degree model. The crucial parameters of the packet traffic scenarios and their value ranges used for the simulations are listed in Table 3.3.

Since we investigate the performance of the S-MAC and try to isolate it from the other communication layers, instead of simulating the whole border, we simulate just one part of it in which all nodes are one-hop away and are able to contend for the medium. Thus, we set a square shaped area in which all nodes can hear each other.

3.5.2. Packet Traffic Model Simulation Results

S-MAC is implemented in OPNET Modeler simulator [61] based on its ns-2 implementation [62]. Results presented in this section include the average delay and the packet drop rate of the S-MAC protocol for the three different packet traffic patterns under various average traffic loads. Each simulation run with a different seed generated a slightly different average aggregate load. Therefore, each simulation run is presented as a separate data point in the figures. The simulated network execution durations are limited to 12 hours, which is sufficient for the convergence of the performance values and to have realistic performance results. For instance, within that duration, each sensor node generates approximately 2000 packets when periodic data traffic is selected with the packet interval parameter equal to 20 seconds.

3.5.2.1. Unlimited Buffer Case. The S-MAC performance results of one-hop delay averages are shown in Figure 3.13 for different packet traffic patterns. As seen in the figure, except for very low data loads where no contention occurs and for very high data loads where the system is overloaded, SPTM results in much higher delays than the binomial and periodic data traffic. The reason is that although the amount of data packets generated are close, the packet traffic generated by SPTM is bursty, which results in more contention compared to the other traffic types. Note that these delays are only one-hop link delays, and they must be accumulated until the data packet reaches the sink node for the calculation of the end-to-end delay. Hence, other traffic models overestimate the performance results of the S-MAC protocol for the SWSN applications, which may result in an inefficient system design.

In addition to the average packet delays, we also explore the variance of the packet delays which can be important for the implemented WSN application. We choose sample runs from each type of packet traffic pattern that has similar average traffic loads. Figure 3.14 shows the delay histogram for the sample runs with the average data traffic load around five packets per second. The system is found to be

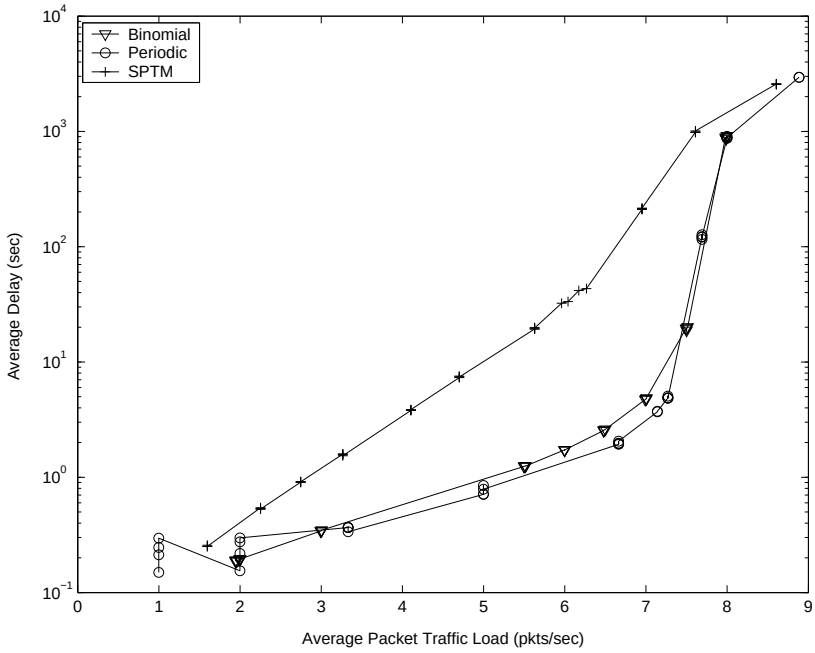

Figure 3.13. Average delay vs. average load for the S-MAC protocol under different packet traffic patterns (*log*)

stable in all of the traffic patterns under this average load. However, as seen in Figure 3.14, for similar average traffic loads, the packets arrive with larger delays when the SPTM pattern is used.

The SPTM scenario parameter settings also shape the MAC performance as shown in Figure 3.15, where the average delay results for two different target velocities are shown. Hence, to have a realistic model, appropriate values of the system parameters should also be determined.

3.5.2.2. Limited Buffer Case. An important limitation in sensor nodes that should be considered is the limited memory capacity. That is why, in the real life scenarios, certain protocol limits are defined for the number of data packets to be buffered. In addition, if the delay of the packets in the queue reaches to a certain level, packet content can be useless for an application in which case the packet should be dropped. If a new data packet arrives from the application layer when the data buffer is full, either this packet can be merged to the previous packets by data aggregation, or one

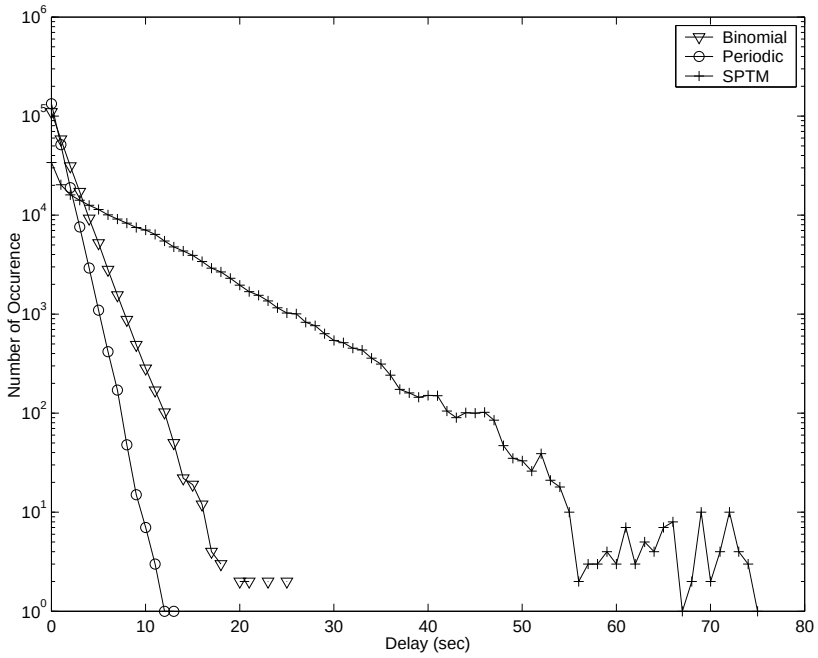

Figure 3.14. Delay histogram of sample runs with similar average traffic loads

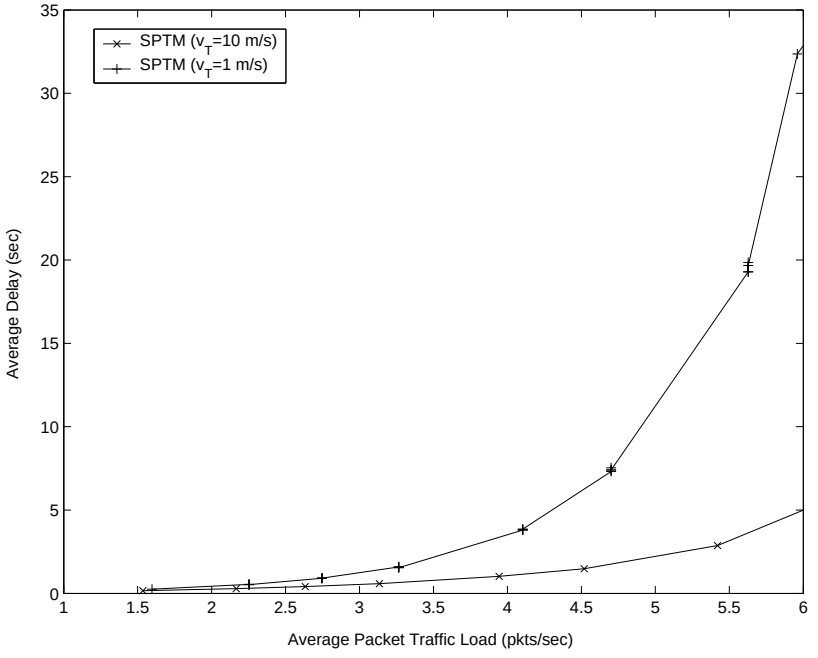

Figure 3.15. Average delay vs. average load for the S-MAC protocol with different system parameter values

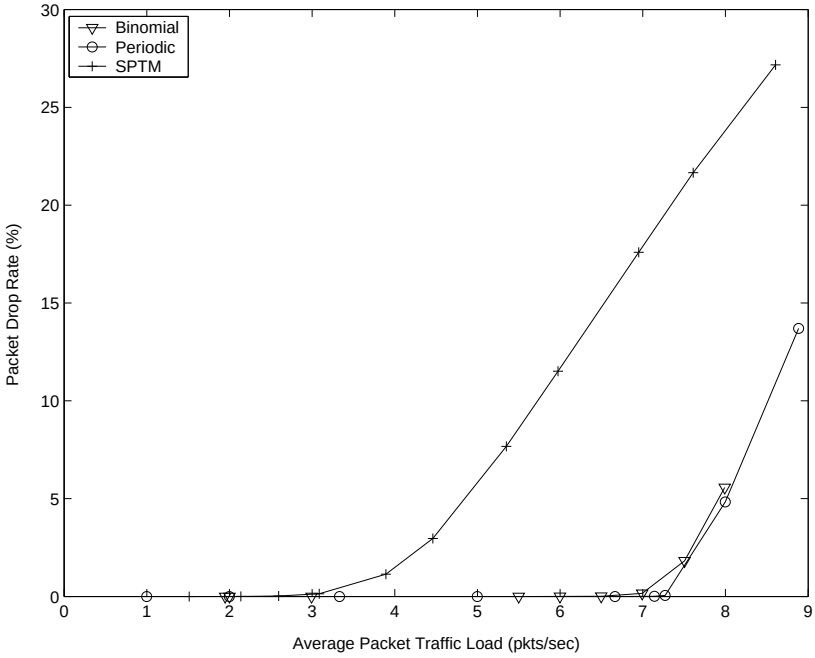

Figure 3.16. Packet drop rate vs. average load for the S-MAC protocol with the buffer size of 10 packets

of the old packets or the new packet may be dropped. Since the packet drop rate is an important indicator for the MAC protocol performance, we study the limited buffer systems for this criterion, setting the data packet buffer limit to be 10 or 50 packets.

The packet drop percentages for different packet traffic patterns are shown in Figure 3.16 and Figure 3.17 for the buffer size of 10 and 50 packets, respectively. The SPTM resulted in much higher packet drop rates for the traffic loads higher than three and five packets per second, respectively. This is also an indication of burstiness of the packet traffic generated by the SPTM, since similar traffic loads always result in more packet drops for SPTM. Moreover, for the range of $3-7$ packets per second, although there is no packet drops in the other traffic types, SPTM packet traffic results in non-negligible packet drop rates.

Assuming that packet drop rates are allowed up to a certain threshold, we investigate the average delay results for the three packet traffic patterns for the case where the newly created packets are dropped when the buffer is full. Assigning a packet drop rate threshold of 10 per cent, Figure 3.18 and Figure 3.19 show the average packet

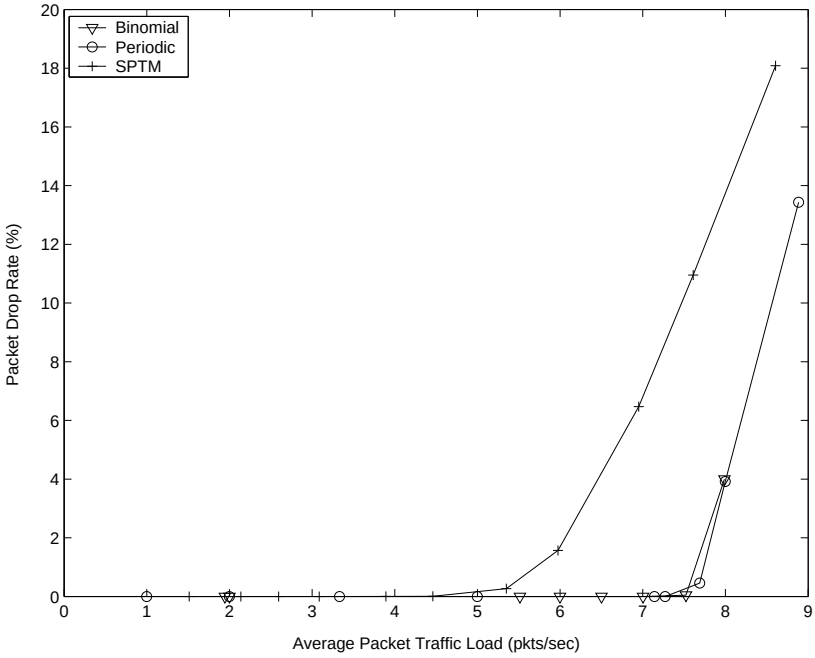

Figure 3.17. Packet drop rate vs. average load for the S-MAC protocol with the buffer size of 50 packets

delays encountered for the buffer size of 10 and 50 packets, respectively. The SPTM packet traffic still creates much higher average delays compared to the two other packet traffic patterns.

3.6. Analytical Verification of the Maximum Throughput found by the SPTM Packet Traffic

The figures presented in Section 3.5 includes the performance results of the S-MAC communication protocol achieved by simulation for the three different packet traffic models. To verify these results in part, we investigate the maximum stable throughput by analytical derivations and compare the outcome with the simulation results presented in Section 3.5.

In a multiple access system, offered load can be increased up to a certain point after which the system will be unstable, i.e., the expected delay will be unacceptable. This value will result in the maximum stable throughput. As the system approaches to an unstable point, every node will have data packets to send, and hence if there are

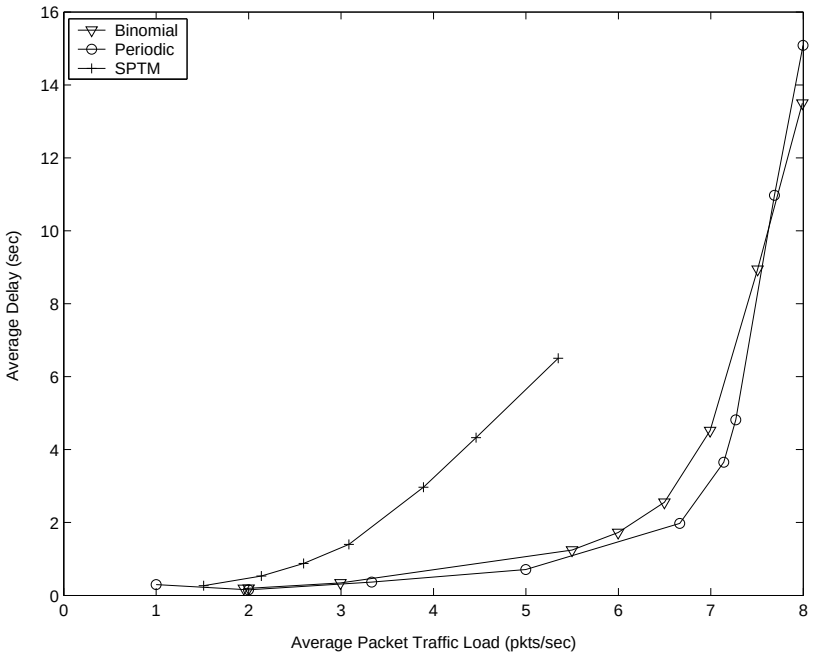

Figure 3.18. Average delay vs. average load for the S-MAC protocol with allowable drop rates for the buffer size of 10 packets

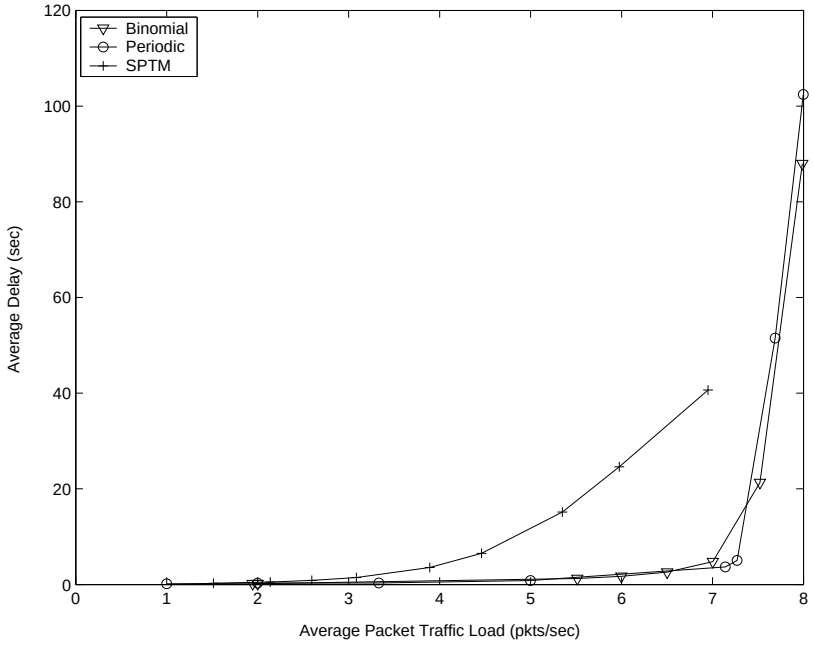

Figure 3.19. Average delay vs. average load for the S-MAC protocol with allowable drop rates for the buffer size of 50 packets

$\mathcal{M}$ nodes within the investigated cluster, all $\mathcal{M}$ nodes will contend for the medium. However, for a MAC protocol, the maximum stable throughput is the maximum number of data packets that can be sent successfully per unit time in the steady state. Then for S-MAC, the maximum stable throughput, ρ_{max} is calculated as

$$\rho_{max} = \frac{t_{listen}}{E[t_{stx}]}, \tag{3.16}$$

where t_{listen} is the listen period in seconds and t_{stx} is the time required for a successful packet transmission including the time lost with packet collisions and the duration of wait timers. Note that ρ_{max} has the unit *packets per listen-sleep period*. In Equation 3.16, the expected value of the successful packet transmission time is used instead of the shortest feasible transmission time, since the steady state is considered when the maximum throughput is investigated.

Because S-MAC utilizes contention slots and the RTS/CTS mechanism, the expected duration of a successful packet transmission is calculated as

$$E[t_{stx}] = E[t_{coll}] + E[t_{CW}] + t_{RTS} + t_{CTS} + t_{DATA} + t_{ACK}, \tag{3.17}$$

where t_{coll} represents the time spent for the collided packets' transmissions, t_{CW} represents the time spent for waiting the first occupied contention slot and all other t_X represent the time needed for the transmission of a packet of type X.

Since S-MAC is 1-persistent CSMA and collision is understood by the CTS timeout triggered when no CTS packet is received after t_{CTS}, the expected time spent for collisions is calculated as

$$E[t_{coll}] = \sum_{z=0}^{\infty} z \left(E[t_{CW}] + t_{RTS} + t_{CTS}\right) \zeta^z, \tag{3.18}$$

where z is the number of successive collisions and ζ is the probability of packet collision in a contention period. However, in a protocol with contention slots, a collision occurs when the first occupied slot is selected by two or more nodes. Therefore, the probability

that a slot assignment results in a collisionless transmission is

$$\xi = (1 - \zeta) = \sum_{f=1}^{\mathcal{Z}-1} P(\mathcal{F} = f \mid \mathcal{Z}, \mathcal{M}), \tag{3.19}$$

where $P(\mathcal{F} = f \mid \mathcal{Z}, \mathcal{M})$ represents the probability that f is the first occupied slot and it is selected by only one node given that the contention window consists of $\mathcal{Z}$ contention slots and there are $\mathcal{M}$ contending nodes. Thus,

$$P(\mathcal{F} = f \mid \mathcal{Z}, \mathcal{M}) = \frac{\mathcal{M}(\mathcal{Z} - f)^{\mathcal{M}-1}}{\mathcal{Z}^{\mathcal{M}}}, \tag{3.20}$$

because there are $\mathcal{Z}^{\mathcal{M}}$ different slot assignment possibilities among which the following assignments results in collisionless transmission: f is chosen by any of $\mathcal{M}$ nodes and the slots $f+1$ to $\mathcal{Z}$, i.e., $\mathcal{Z} - f$ slots, are chosen randomly by $\mathcal{M} - 1$ nodes. Incorporating Equation 3.20 into Equation 3.21 yields

$$\xi = \sum_{f=1}^{\mathcal{Z}-1} P(\mathcal{F} = f \mid \mathcal{Z}, \mathcal{M}) = \mathcal{M} \frac{(1^{\mathcal{M}-1} + \ldots + (\mathcal{Z} - 1)^{\mathcal{M}-1})}{\mathcal{Z}^{\mathcal{M}}}. \tag{3.21}$$

The expected waiting time till the first occupied contention slot is

$$E[t_{CW}] = \sum_{\psi=1}^{\mathcal{Z}} (\psi - 1) P(\Psi = \psi) t_{slot}, \tag{3.22}$$

where t_{slot} is one slot duration and Ψ represents the random variable of the slot number of the first occupied slot. Therefore, $P(\Psi = \psi)$ gives the probability that the ψth slot is the first occupied slot which can be defined as

$$P(\Psi = \psi) = P\left((s_i \geq \psi, \quad \forall i = 1..\mathcal{M}) \wedge (s_i = \psi, \quad \exists i = 1..\mathcal{M})\right), \tag{3.23}$$

where s_i represents the slot chosen by node i. Consequently,

$$P(\Psi = \psi) = (\frac{\mathcal{Z} - \psi + 1}{\mathcal{Z}})^{\mathcal{M}} - (\frac{\mathcal{Z} - \psi}{\mathcal{Z}})^{\mathcal{M}}. \tag{3.24}$$

Table 3.4. Simulation parameters used for maximum throughput formula verification of SPTM

Parameter	Value
Number of contention slots	63
Number of contending nodes	20
Slot time	0.001 sec
Sleep period	0.9 sec
Listen period	0.1 sec
Bandwidth	20 Kbps
Data packet size	128 bits
RTS/CTS/ACK packet size	26 bits

Table 3.5. Numerical results found by the SPTM maximum throughput analysis

Parameter	Calculated Value
ξ	0.8492
ζ	0.1508
$E[t_{CW}]$	0.0025 sec
$E[t_{coll}]$	0.0011 sec
$E[t_{stx}]$	0.0139 sec

The maximum stable throughput of S-MAC under SPTM packet traffic can be calculated analytically once the system parameter values are given. To compare the maximum stable throughput achieved at simulation results with the analytically found throughput, the simulation parameters values given in Table 3.4 are applied to Equation 3.16 - Equation 3.24, and the maximum stable throughput formula components are calculated to be as tabulated in Table 3.5. According to these values, the maximum stable throughput is found to be 7.195 packets per second. The traffic load that results in instability in Figure 3.13 matches the analytical maximum stable throughput result. Although the simulation results conforms to the analytical results at the maximum stable throughput, the verification of the intermediate throughput-delay values remains as an open issue. Note that these calculations require the exact average delay deriva-

tions for the given average traffic loads which must consider the randomly deployed node locations, randomly moving target's trajectory, MAC collision probabilities that depend on the number of data packets of the nodes and individual packet delays that depend on the packet queue size of the sensor nodes.

3.7. SPTM Conclusions and Future Work

In this chapter, a new packet traffic model framework is devised for intrusion detection applications using the Elfes sensor detection model. The system design parameters considered in this framework are the number of sensors deployed, the area size of the border, the detection distance thresholds, the target velocity, the sampling interval and the Elfes detection model parameters. Simulation results support the analytical work presented for the packet traffic model under this probabilistic detection model.

To show the importance of using a realistic packet traffic model for evaluating WSN communication protocols, we investigate the performance of S-MAC for different packet traffic models. Simulation results indicate that evaluating S-MAC with a packet traffic model other than the one proposed may give misleading results for the intrusion-detection applications. The reason is revealed to be the bursty nature of the SPTM packet traffic which is proven analytically. Although, the effect of using a realistic packet traffic model is demonstrated for a MAC protocol, it can also be emphasized for other layers such as routing protocols. Moreover, the proposed model can be a baseline to have separate analytical studies for event-based WSN.

As a future work, the presented packet traffic model can be extended to include multiple target trajectories. In addition, different sensor node deployment strategies can be considered which may change the dependency relation of the consecutive coverage and detection degrees. Hence, a variation of the packet traffic model can be obtained by considering these new dependencies. Moreover, the analytical traffic model can be updated by considering the relayed packets as part of the routing activity.

4. ENERGY AND DELAY OPTIMIZED CONTENTION FOR WIRELESS SENSOR NETWORKS

4.1. Introduction and Motivation

The limited battery capacities of the sensor nodes require energy-efficient operation of the wireless sensor networks (WSNs). As a result, WSN research is concentrated on communication protocols that reduce the redundant communication either by developing WSN-specific protocols obeying the layered approach or developing cross-layer protocols that exploit the layer-interactions for efficiency. The utilized medium access scheme should also be optimized considering the energy efficiency. WSN designers prefer contention-based medium access schemes such as those used in Xbow sensors [63]. The reason for that unlike TDMA-based access schemes, the contention-based protocols do not need precise time synchronization and do not need extra circuitry as required by FDMA-based systems. Moreover, the computational complexity added by the CDMA-based schemes results in higher energy consumptions.

Contention-based protocols commonly use slotted medium access via contention windows [13, 64, 65, 66]. A contention window (CW) consists of a specific number of contention slots which is started before each contention. All contending nodes select a slot from the contention window uniformly randomly. Each contending node, then, listens to the medium till its slot time arrives or receives the transmission of another node before its slot time. As a result, the contending node that selects the slot with the lowest index acquire the medium. All other nodes receives this transmission and performs a back-off till the next contention window. Figure 4.1 illustrates a contention-window-based medium access with four contending nodes. Since Node 3 selects the slot with the lowest index, it starts the packet transmission at its slot time. All the other nodes receives this transmission and performs a back-off till the next contention window.

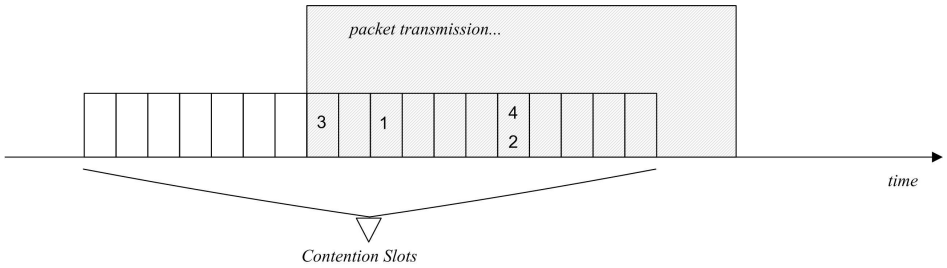

Figure 4.1. A contention window based medium access with collisionless slot selection

Idle listening and collisions are two kinds of energy waste in contention based channel access systems. Idle listening occurs if a node listens to the medium when there is no transmission whereas a collision occurs when a node receives multiple transmissions at the same time. An efficient communication protocol should reduce both kinds of energy waste. In contention-based medium access, all contending nodes have to do carrier sensing till the first occupied slot which results in idle listening type of energy waste. However, if the first occupied slot is actually selected by two or more nodes, packet transmissions of these nodes start at the same slot which results in a collision. When the destination nodes of the transmitting nodes are not the same and are not within the transmission range of multiple transmitting nodes, still collisions occur since the *interference range* of the contending nodes includes the *transmission range* of each other as observed in the measurements given in [67].

In contention-based schemes, the contention window size creates a trade-off between carrier sense duration and collision probability since a larger contention window results in higher expected carrier sense time and a smaller contention window increases the probability of collisions and hence energy waste due to retrials. To set the contention window size carefully is therefore very crucial for better performance. As a numerical example, S-MAC [13] defines 63 contention slots where one slot time is set to be the time to transmit 20 bits. Consequently, if a node contends for the medium alone, the expected carrier sense time is $63/2 = 31.5$ slots which corresponds to the transmission duration of 630 bits. However, the size of one data packet is generally small in WSN applications, for instance 400 bits in S-MAC defaults which results in more time for contention than for the actual data transmission. As a result, the contention based communication is not efficient when the contention window size, which

actually requires an engineering optimization, is set independently from the network properties.

Energy consumption caused by the contention-based medium access is affected significantly by the CW size. In this work, we show that the energy consumed for contentions can be reduced significantly by setting the contention window size to its energy optimizing value. We derive an analytical formula for the energy consumption for the overall contentions of the nodes as a function of *the contention window size* and *the number of contending nodes*. Another possible objective in WSN is minimizing the latency, i.e., the delay between the event and the notification of the sink. This objective is especially crucial for time-critical applications such as intrusion detection and tactical systems. To decrease the latency observed, the contention delay, i.e., the time till the successful medium access occurs has to be minimized. The successful medium access time is also formulated as a function of *the contention window size* and *the number of contending nodes* which is used to find the delay optimizing CW size.

The energy optimizing and the delay optimizing CW sizes can be found using the derived equations. However, the knowledge of the number of contending nodes used in the equations may not be readily available at individual sensors. Hence, in practice, each node should have a method to approximate that information for distributed implementation. In this work, we propose the *Estimated Number of Contenders (ENCO)* method for the event-driven WSN based on the mean coverage degree idea [15]. We demonstrate in Section 4.6 that the ENCO method can give close results to the theoretical best performance which could be reached by using a centralized CW size setting algorithm.

The rest of the chapter is organized as follows. A brief overview of the contention window size related studies are presented in Section 4.2. The relation between the contention window size and the contention delay is investigated analytically, in Section 4.3. The energy consumption for the resolution of all contending packets requires a separate analysis which is presented in Section 4.4. Then, the derived analytical formulas are verified with simulations in Section 4.5. The ENCO method is presented for

distributed implementation and its effectiveness is demonstrated with the simulations of two different types of wireless sensor network applications in Section 4.6. An alternative slot selection method is investigated in Section 4.7 which is shown to minimize the collision probability. Its effect on the contention delay is simulated and compared to the contention delay performance of uniformly random slot selection method where the contention window size is set to its delay-optimizing value. Finally, Section 4.8 concludes the chapter.

4.2. Related Work

Since the sensor nodes do not transmit and receive at the same time, a collision is recognized by the sender nodes with the lack of ACK or CTS reply depending on whether CSMA or CSMA/CA is implemented. In the case of collisions, IEEE 802.11 and IEEE 802.15.4 standards use binary exponential backoff (BEB) which requires doubling the CW size at each collision. However, since BEB results in exponential increase of window size on collisions and hence long carrier sense times [26, 68], instead of the exponential backoff method, the *uniform backoff*[5] method is preferred in WSN as used in S-MAC [13], SCP-MAC [69], Z-MAC [70] and Sift [26]. A contention scenario that results in collisions after which uniform backoff is performed is illustrated in Figure 4.2. Four sensor nodes contend for the medium and in the first contention window, the first occupied slot is actually occupied by the nodes 2 and 3. Both nodes start the packet transmission at their slot time resulting in a collision which is detected by observing that no reply is sent by the destination nodes. After not receiving any reply for collision timeout duration, t_c, all the contending nodes start a new contention window for the retrial. The time passed till the start of the successful contention is denoted as the collision and the retrial duration. After the collision and the retrial duration, the successful contention occurs where carrier sensing is done till the first occupied slot of the successful slot assignment. Total contention duration, Ω, is dependent on the collision and the retrial duration, Λ and the carrier sensing duration in the successful slot assignment, Γ.

[5]The non-exponential backoff method that does not alter the CW size is referred as *uniform backoff* in this work.

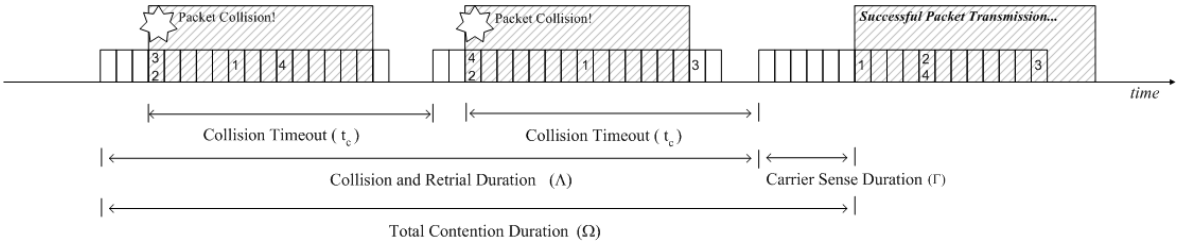

Figure 4.2. A contention window-based medium access with collisions

The impact of the CW size on the network performance has been studied previously especially for IEEE 802.11 and IEEE 802.15.4 networks. Although these IEEE 802 protocols do not employ uniform backoff, it is still worthwhile to summarize the previous research on CW size setting for these protocols. Wang *et al.* show that although the IEEE 802.11 DCF with RTS/CTS is not affected by the initial CW size significantly, the effect is considerable without RTS/CTS [71]. To decrease the probability of collisions under congested traffic in IEEE 802.11 networks, Ksentini *et al.* propose a new CW size adjustment method which defines a backoff lower bound in combination with doubling the CW size [72] that is referred as *backoff range*.

A method to tune the CW size by observing the network traffic is proposed in [73]. The proposed algorithm computes an estimate of the collision cost and an estimate of the number of active stations assuming that all contending stations continuously have packets ready for transmission. These estimates are obtained by observing the three events that occur on the channel: idle slots, collisions, and successful transmissions. Similarly, the algorithm proposed in [74] aims to approximate the number of contending nodes from the number of idle slots observed before packet transmissions and dynamically adjust the CW size till a designated optimum number of consecutive idle slots is reached. However, these methods require a closed system with continuous traffic load to converge. Although, Xia *et al.* defines a feedback control system in [75] that makes the former proposed method adaptive to changes in the number of contending nodes, it still requires stable and continuous traffic loads to approximate the number of nodes successfully. The effect of different network conditions related to the CW adjustment method is also investigated. For instance, Jin *et al.* investigate the stability of IEEE

802.11 where selfish users exist in the network that dynamically change their CW sizes overriding the standard window size update procedure [76].

IEEE 802.11e introduces the enhanced distributed coordination function (EDCF) which defines different CW size settings for different traffic classes to achieve QoS requirements. Several techniques have been proposed to enhance the performance of EDCF such as the Sliding Contention Window method [77] which adjusts the backoff ranges of the traffic classes according to the QoS requirements and dynamic network behavior. In [78], another adaptive technique is proposed for IEEE 802.11e which takes into account the congestion level of the network before resetting the CW size. The congestion level of the network is decided by previous CW size values.

The unslotted CSMA-CA in IEEE 802.15.4 for nonbeacon-enabled mode has no power saving mechanism, hence the slotted version for beacon-enabled mode is preferred for energy-efficient network operation [66]. Although in IEEE 802.15.4, the parameter Backoff Exponent (BE) replaces the term *contention window size*, several studies prefer to use the latter term. Pang *et al.* propose a memorized backoff scheme to dynamically adjust the CW size based on the traffic load [79]. A retransmission algorithm that uses a Synchronized, Shared Contention Window (SSCW) is proposed in [80] where an analytical approximation is presented for the optimization of the CW size as a function of the probability of collision in the contentions.

For WSN, two level contention window is proposed in SCP-MAC to improve the contention performance [69]. Similarly in Z-MAC [70], two different CW sizes are proposed for prioritization. However, since the CW sizes in both methods are constant, the size settings are still critical. Although the uniformly random slot selection is generally used in contention-based schemes, alternative slot selection distributions are also proposed. Tay *et al.* proposed a slot selection distribution which minimizes the collision probability [27] and which is used by the Sift protocol [26]. Nevertheless, there is still possibility of collision and the total contention time or the consumed energy are not studied in the case of collisions. A default contention window size of 63 is defined in S-MAC [13] and the contention window size is advised to be in format of $2^n - 1$ most

likely for computational reasons. However, S-MAC still does not provide an efficient way to set the contention window size.

4.3. Analysis of the Contention Delay

The expected contention delay is defined as the expected duration between the beginning of the contention till a successful medium access and denoted as Ω. As shown in Figure 4.2, it can be decomposed into two phases: i) the expected time spent for collisions and retrials till the beginning of the collisionless slot selection, Λ, and ii) the expected carrier sense duration within this successful contention from the beginning of the contention window till the first occupied slot, Γ. We will derive the equations of both components in terms of the contention window size, W and the number of contending nodes, N. At each contention, N nodes select a slot independently and uniformly randomly from the slots with numbers one to W.

Let the random variable Ψ represent the first occupied slot number, whether the slot selection results in a collision or not. The probability that the first occupied slot is ψ, $Pr[\Psi = \psi]$ is defined as

$$Pr[\Psi = \psi] = Pr\left[(s_i \geq \psi, \quad \forall i \in \{1, .., N\}) \wedge (s_i = \psi, \quad \exists i \in \{1, .., N\})\right] \tag{4.1}$$

$$= Pr\left[(s_i \geq \psi, \quad \forall i \in \{1, .., N\}) \wedge \neg(s_i > \psi, \ \forall i \in \{1, .., N\})\right] \tag{4.2}$$

$$= Pr\left[s_1 \geq \psi, \ \ldots, \ s_N \geq \psi\right] - Pr\left[s_1 \geq \psi + 1, \ \ldots, \ s_N \geq \psi + 1\right], \tag{4.3}$$

where $\psi \leq W$ and s_i represents the slot chosen by node i. Consequently,

$$Pr[\Psi = \psi] = \frac{(W - \psi + 1)^N - (W - \psi)^N}{W^N}. \tag{4.4}$$

Let $Pr[\Psi = \psi, \Upsilon = success]$ represent the probability that ψ is the first occupied slot and it is selected by only one node, hence, random variable Υ indicates whether the slot selection is successful, i.e., collisionless. There are W^N different slot assignment

possibilities among which the following assignment results in collisionless transmission: ψ is chosen by any of N nodes and the slots $\psi+1$ to W, i.e., $W-\psi$ slots, are chosen randomly by $N-1$ nodes. As a result, for a given N,

$$Pr[\Psi=\psi,\Upsilon=success]=\frac{N(W-\psi)^{N-1}}{W^N}. \tag{4.5}$$

Equivalently, this probability can be thought of as one node selecting the slot ψ, with probability $1/W$ and the remaining nodes selecting slots after ψ each with probability $\frac{W-\psi}{W}$. There are $N-1$ such independent selection probabilities and N possible selections of the successfully transmitting node, resulting in Equation 4.5.The probability that a slot assignment results in a collisionless transmission can be calculated by Equation 4.5 as

$$Pr[\Upsilon=success]=\sum_{\psi=1}^{W-1}Pr[\Psi=\psi,\Upsilon=success]=N\frac{(1^{N-1}+\ldots+(W-1)^{N-1})}{W^N}. \tag{4.6}$$

Now, we analyze the expected carrier sense duration for a collisionless slot selection, Γ. If the first occupied slot is ψ then the carrier sense duration of that contention will be $(\psi-1)t_{slot}$ where t_{slot} is one slot duration. Then,

$$\Gamma=\sum_{\psi=1}^{W}Pr[\Psi=\psi|\Upsilon=success](\psi-1)t_{slot}. \tag{4.7}$$

By the definition of the conditional probability,

$$Pr[\Psi=\psi|\Upsilon=success]=\frac{Pr[\Psi=\psi,\Upsilon=success]}{Pr[\Upsilon=success]}, \tag{4.8}$$

$$Pr[\Psi=\psi|\Upsilon=success]=\frac{\frac{(W-\psi+1)^N-(W-\psi)^N}{W^N}}{N\frac{(1^{N-1}+\ldots+(W-1)^{N-1})}{W^N}}. \tag{4.9}$$

Substituting Equation 4.9 into Equation 4.7, we obtain

$$\Gamma = \sum_{\psi=1}^{W} (\psi - 1) \frac{(W-\psi)^{N-1}}{\sum_{f=1}^{W} (W-f)^{N-1}} t_{slot}. \tag{4.10}$$

The second component of Ω is the expected time spent for the collisions and the retrials, Λ, which can be calculated as follows. Let the collision probability at the contention of N nodes be ζ, which can be found if the probability of no collision, ξ, is known. Obviously, $\zeta = 1 - \xi$, where the variable ξ is equivalent to $Pr[\Upsilon = success]$. The retrials will continue until a collisionless slot selection occurs. Therefore, the expected time spent for collisions and retrials equals the expected number of retrials, τ, times the expected time elapsed in one retrial, λ, in other words,

$$\Lambda = \tau\lambda. \tag{4.11}$$

Since each contention is an independent and random event, contentions can be represented with a Bernoulli trial with success and fail probabilities of ξ and ζ which corresponds to the contentions with no collision and with collision, respectively. The expected number of collisions and the resulting retrials are then found to be

$$\tau = \frac{1}{\xi} - 1, \tag{4.12}$$

since $\frac{1}{\xi}$ gives the expected number of trials till success for this Bernoulli trial. Therefore,

$$\Lambda = \lambda \left(\frac{1}{\xi} - 1 \right). \tag{4.13}$$

Assume that t_c is the duration passed for the packet transmission, for the collision to be understood and the new contention begins, which is referred to as the collision

timeout in this work. Then,

$$\lambda = \left(\sum_{\psi=1}^{W} Pr[\Psi = \psi | \Upsilon = fail](\psi - 1)t_{slot} \right) + t_c, \tag{4.14}$$

where,

$$Pr[\Psi = \psi | \Upsilon = fail] = \frac{Pr[\Psi = \psi, \Upsilon = fail]}{Pr[\Upsilon = fail]}, \tag{4.15}$$

and $Pr[\Psi = \psi, \Upsilon = fail]$ is the probability that ψ is the first occupied slot and it is selected by more than one node. Therefore,

$$Pr[\Psi = \psi, \Upsilon = fail] = \frac{\left(\sum_{m=2}^{N-1} \binom{N}{m} (W - \psi)^{N-m} \right) + 1}{W^N}, \tag{4.16}$$

where index m represents the number of nodes that selected the slot ψ. Incorporating Equation 4.15 and Equation 4.16 into Equation 4.14 yields

$$\lambda = t_c + \sum_{\psi=1}^{W} \frac{\frac{1 + \sum_{m=2}^{N-1} \left(\binom{N}{m} (W - \psi)^{N-m} \right)}{W^N}}{1 - N \frac{\sum_{f=1}^{N-1} (W - f)^{N-1}}{W^N}} (\psi - 1)t_{slot}. \tag{4.17}$$

The expected time spent for retrials is then found to be

$$\Lambda = \left(\frac{1}{\xi} - 1 \right) \left(t_c + \sum_{\psi=1}^{W} \frac{1 + \sum_{m=2}^{N-1} \left(\binom{N}{m} (W - \psi)^{N-m} \right)}{W^N - N \sum_{f=1}^{N-1} (W - f)^{N-1}} (\psi - 1)t_{slot} \right). \tag{4.18}$$

Hence, the expected contention delay is

$$\Omega = \Lambda + \Gamma \tag{4.19}$$

$$= \left(\frac{1}{\xi} - 1\right) \left(t_c + \sum_{\psi=1}^{W} \frac{1 + \sum_{m=2}^{N-1} \left(\binom{N}{m} (W-\psi)^{N-m} \right)}{W^N - N \sum_{f=1}^{N-1} (W-f)^{N-1}} (\psi - 1) t_{slot} \right)$$

$$+ \sum_{\psi=1}^{W} (\psi - 1) \frac{(W-\psi)^{N-1}}{\sum_{f=1}^{W} (W-f)^{N-1}} t_{slot}. \tag{4.20}$$

The derived equation of Ω has the following parameters: the contention window size, the number of contending nodes, one slot duration and the collision timeout duration. The delay optimizing CW size that minimizes the expected contention delay Ω is denoted as W_t^* which can be found easily from a look-up table generated a priori, since the slot duration and collision timeout duration are system parameters which are known before the deployment. Moreover, the analytical formula derived for Ω can be used to investigate the effects of different parameters on the expected contention delay such as the effect of the collision timeout duration. Although the number of contending nodes varies temporally and spatially throughout the network, different methods can be applied to approximate the optimum performance results. In Section 4.6, one such method is proposed for event-triggered WSNs.

4.4. Analysis of Energy Consumption for the Overall Contention Resolution

The network lifetime maximization is another crucial objective for the wireless sensor networks. A good communication protocol needs to minimize the energy consumed for the resolution of overall contentions which corresponds to the total energy consumed by all nodes till each of the contending node has access to the medium. In other words, for WSN applications in which the transmission of all data is essential, to investigate the first medium access is not sufficient. Instead, one has to consider the

energy consumption required for resolving all contentions. The energy consumed for resolution of all contentions, E_{total}, consists of two energy consumption components: i) the total energy consumed for unsuccessful slot selections which results from the communications of the colliding packets and their retrials, E_{coll}, and ii) the total energy consumed for the carrier sensing in the successful slot assignments (SSA), E_{ssa}.

For each contention, all of the contending nodes will choose a contention slot and listen to the medium till the first occupied contention slot. Using Equation 4.10, the total energy consumed till the medium access in all successful slot assignments is found to be

$$E_{ssa}(W,N) = \frac{W}{2} t_{slot} E_{rx} + \sum_{m=2}^{N} m \sum_{\psi=1}^{W} (\psi - 1) \frac{(W-\psi)^{m-1}}{\sum_{f=1}^{W} (W-f)^{m-1}} t_{slot} E_{rx}, \qquad (4.21)$$

where E_{rx} is the energy consumed for reception per unit time, and m represents the number of contending nodes at each contention. Note that, the first component in Equation 4.21 is for the case $m = 1$. No transmission energy is considered in E_{ssa}, since just the carrier sense is enough for the contention resolution in successful slot assignments.

The second energy consumption component of E_{total} is the total energy consumed for unsuccessful communication, i.e., for the collisions and the retrials which is denoted as E_{coll}. The derivation of the total energy consumed for unsuccessful communication is similar to the derivation of the collision and retrial duration, Λ, given in Section 4.3. However, the number of contending nodes has to be incorporated with the separation of the number of transmitting and the receiving nodes for the energy calculations.

Let $\theta(\psi, n, m)$ be the total energy consumed for one retrial if the first selected slot is ψ and m nodes out of n select that slot which is formulated as

$$\theta(\psi, n, m) = n(\psi - 1) t_{slot} E_{rx} + m t_c E_{tx} + (n - m) t_c E_{rx}. \qquad (4.22)$$

If $\hat{E}_{coll}$ represents the expected energy consumed at one collision till its retrial, then,

$$\hat{E}_{coll}(W,n) = \sum_{\psi=1}^{W} \sum_{m=2}^{n} Pr[\Psi = \psi | \Upsilon = fail] \theta(\psi, n, m). \tag{4.23}$$

The total energy consumed for unsuccessful communication till the contention resolution, which is denoted as $\dot{E}_{coll}$, equals to the expected number of retrials times the expected energy consumed at one collision till its retrial, i.e.,

$$\dot{E}_{coll}(W,n) = \tau \hat{E}_{coll}(W,n) = \left(\frac{1}{\xi} - 1\right) \hat{E}_{coll}(W,n). \tag{4.24}$$

Incorporating Equation 4.5, Equation 4.9 and Equation 4.23 into Equation 4.24 yields

$$\dot{E}_{coll}(W,n) = \left(\frac{1}{\xi} - 1\right) \frac{\sum_{\psi=1}^{W} \left(\theta(\psi,n,n) + \sum_{m=2}^{n-1} \binom{n}{m} (W-\psi)^{n-m} (\theta(\psi,n,m)) \right)}{(W^n - n\sum_{f=1}^{n-1}(W-f)^{n-1})}. \tag{4.25}$$

The total energy consumption till all data contentions are finished when initially there are N contending nodes is then,

$$E_{coll}(W,N) = \sum_{n=2}^{N} \dot{E}_{coll}(W,n) \tag{4.26}$$

which is found to be

$$E_{coll}(W,N) = \sum_{n=2}^{N} \left(\frac{1}{\xi} - 1\right) \frac{\sum_{\psi=1}^{W} \left(\theta(\psi,n,n) + \sum_{m=2}^{n-1} \binom{n}{m} (W-\psi)^{n-m} (\theta(\psi,n,m)) \right)}{(W^n - n\sum_{f=1}^{n-1}(W-f)^{n-1})}. \tag{4.27}$$

In Equation 4.26, index n starts from 2 since a collision requires at least two nodes.

After replacing ξ and doing simplifications, the total energy consumed for unsuccessful communications till all the contentions becomes

$$E_{coll}(W,N) = \sum_{n=2}^{N} \frac{\sum_{\psi=1}^{W} \left(\theta(\psi,n,n) + \sum_{m=2}^{n-1} \binom{n}{m} (W-\psi)^{n-m} (\theta(\psi,n,m)) \right)}{n \sum_{f=1}^{n-1} (W-f)^{n-1}}. \quad (4.28)$$

Since the total energy consumed for resolving contentions of N nodes with contention window size of W equals to the summation of expected energy consumed for the collisions and the retrials and the energy consumed for the communication in the successful slot assignment,

$$E_{total}(W,N) = E_{coll}(W,N) + E_{ssa}(W,N) \quad (4.29)$$

$$= \sum_{n=2}^{N} \frac{\sum_{\psi=1}^{W} \left(\theta(\psi,n,n) + \sum_{m=2}^{n-1} \binom{n}{m} (W-\psi)^{n-m} (\theta(\psi,n,m)) \right)}{n \sum_{f=1}^{n-1} (W-f)^{n-1}} + \frac{W}{2} t_{slot} E_{rx} + \sum_{m=2}^{N} m \sum_{\psi=1}^{W} (\psi-1) \frac{(W-\psi)^{m-1}}{\sum_{f=1}^{W} (W-f)^{m-1}} t_{slot} E_{rx}. \quad (4.30)$$

The energy optimizing CW size that minimizes the energy consumed for the overall contention resolution E_{total} is denoted as W_E^*. Note that, the minimization of the energy consumed for the overall contention resolution does not necessarily minimizes the expected contention delay which is shown numerically in Section 4.5. Hence, CW size must be optimized according to the objective of the WSN application.

4.5. Simulation Results and the Verification of the Contention Window Size Analysis

The analytical formulas derived for the minimum first medium access time and the minimum energy consumed for overall energy are verified via simulations using various contention window sizes and various number of contending nodes, i.e., for

various (W, N) tuples. At each run, the time consumed for the collisions and the retrials, the carrier sense duration of the successful slot selection that comes after all the collisions and the retrials, and the total contention duration, i.e., the time elapsed from the beginning of the first contention window till the successful medium access are logged for the objective of minimizing the contention delay. In addition, for the overall energy consumption of all contending nodes, the total energy consumed by the contending nodes during collisions and retrials are logged at each run along with the total energy consumed for the carrier sense of the successful slot assignments and the cumulative energy consumed till all the contentions are resolved.

The simulations are run for 1000 times for each parameter set. The communication speed is set to 20 Kbps which is the offered rate by Xbow Mica2 sensors [63]. Hence, in the simulations, $t_{slot} = 1$ ms. In addition, the collision timeout is set to $t_c = 15.15$ ms based on the S-MAC protocol specification where the timeout duration is defined to be the total of RTS transmission, SIFS duration and a specified processing delay which adds up to transmission duration of 303 bits.

4.5.1. The Contention Delay Results

To verify the analysis presented thoroughly; the total collision and the retrial duration, Λ, the carrier sense duration for a successful contention, Γ, and the contention delay, Ω, values are evaluated in the simulations separately. The effect of CW size on the total collision and retrial duration, Λ, and the carrier sense duration for a successful contention, Γ is shown in Figure 4.3(a) and Figure 4.3(b), respectively. As expected, a higher CW size causes longer time to be spent for carrier sensing, i.e, for the time till the first occupied slot. On the contrary, a higher CW size results in a decrease in the expected collision and retrial duration since the probability of collision decreases. The simulation results corroborate the analytical formula derived for Γ and Λ as seen in Figure 4.3.

The influence of the CW size on the contention delay, Ω, is clearly visible in Figure 4.4. Higher CW size results in larger contention delay due to the longer carrier

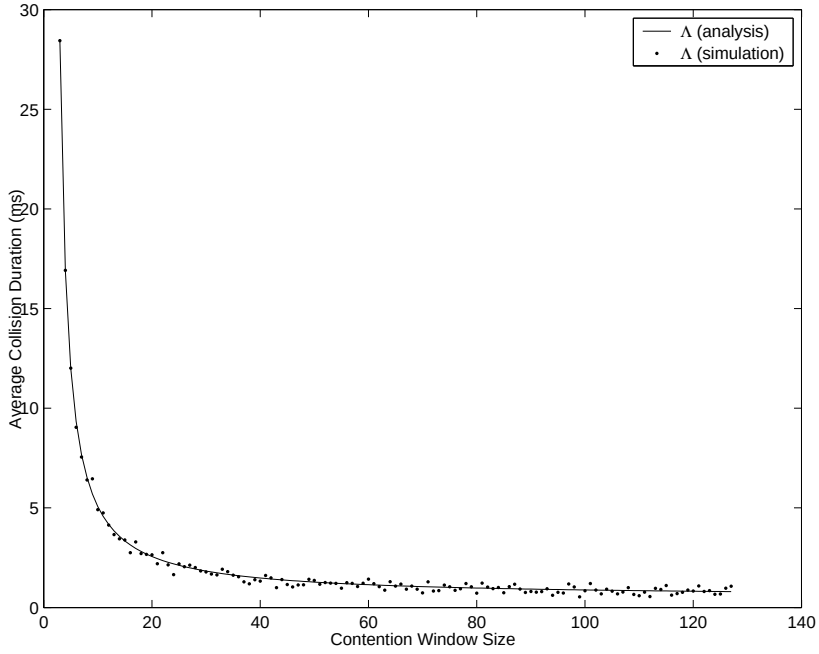

(a)

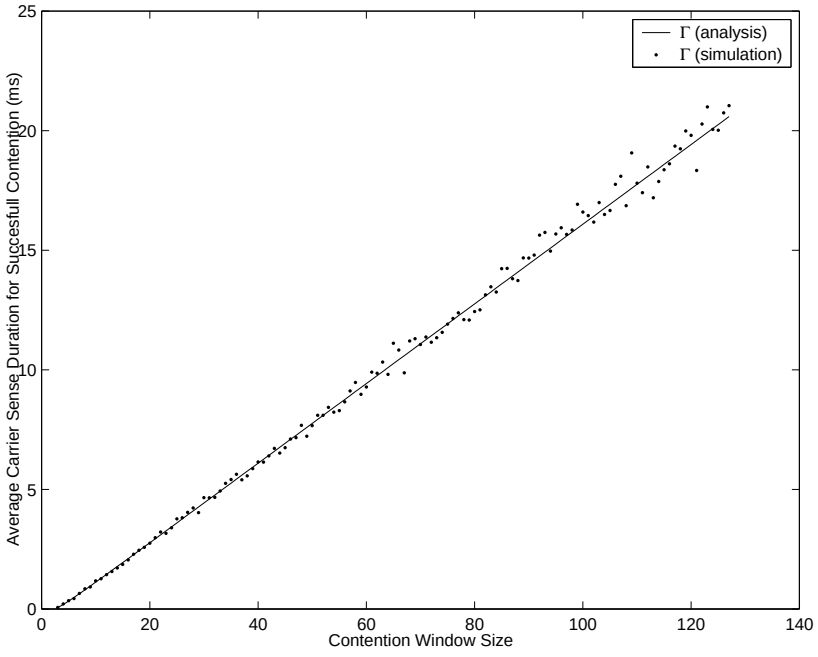

(b)

Figure 4.3. Simulation vs. analytical formula results for $N = 5$, (a) the effect of the contention window size on the expected collision duration, Λ, and (b) the effect of the contention window size on the expected carrier sense duration, Γ

sense duration, however the smaller CW sizes results in larger contention delay due to the higher collision probabilities. The delay optimizing contention window size, W_t^*,

corresponds to the global minimum of the Ω graph which can easily be calculated with Equation 4.6 and Equation 4.19. It is worth to note that the CW size defined by S-MAC leads to 2.23 times larger average contention delay compared to the W_t^* for the depicted $N = 5$ case.

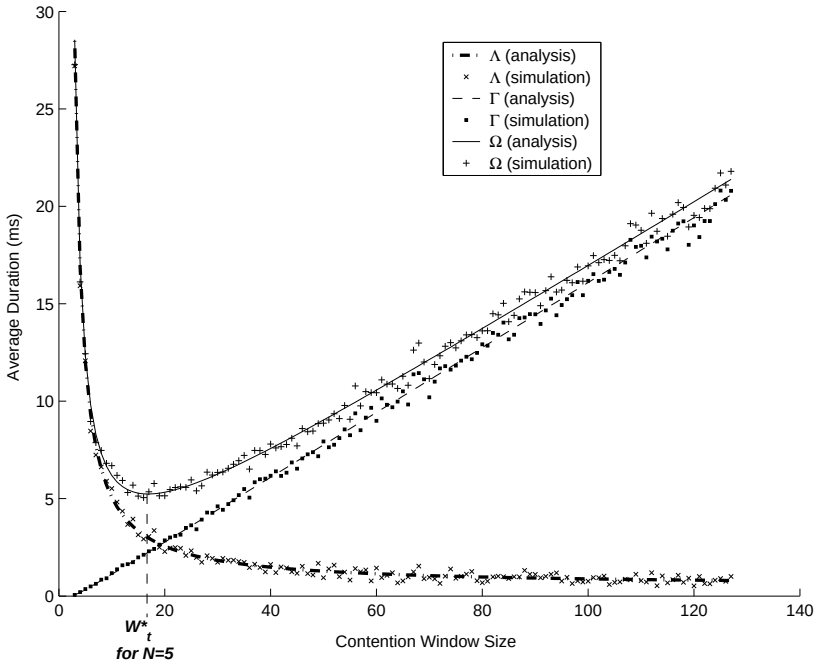

Figure 4.4. The expected collision duration, Λ, the expected carrier sense duration, Γ, and the expected contention delay, Ω, for $N = 5$

The expected contention delay caused by different CW sizes are shown in Figure 4.5 for $3 - 10$ contending nodes. Figure 4.5 indicates that for different number of contending nodes, the optimum CW size significantly varies. For instance, the optimum CW size is 32 and 17 for 10 and 5 nodes, respectively. If the window size of 32 is used for 5 contending nodes, then the average contention delay would be 25 per cent larger compared to the optimum CW size of 5 nodes. One other observation is that as the number of contending nodes increases, the *negative* effect of high CW sizes on the expected contention delay decreases. The reason is that, more contending nodes result in an earlier occupied slot which decreases the carrier sense duration. Moreover, an important observation is that small deviations from the optimal CW size do not result in large performance loss.

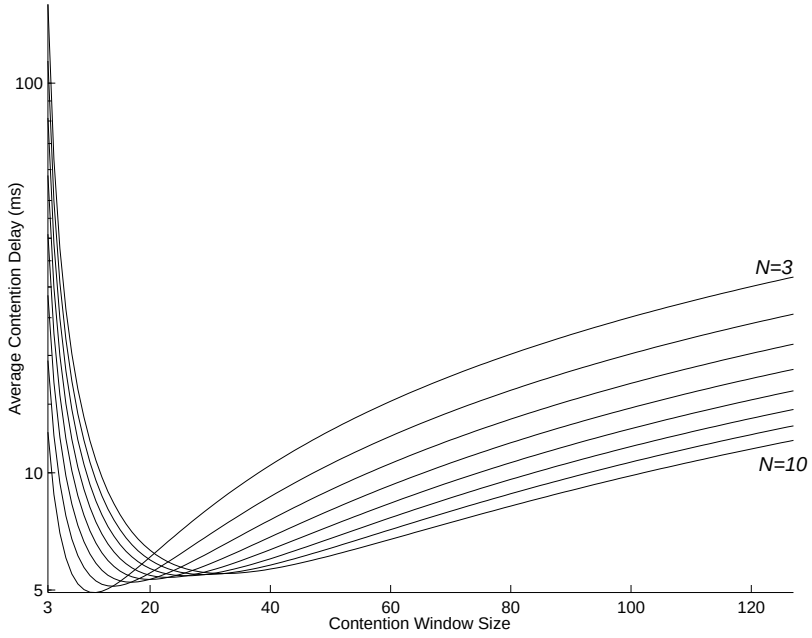

Figure 4.5. Effect of contention window size for different number of contending nodes on expected contention delay (*log*)

The SSCW method proposed in [80] defines an analytical approximation to optimize the CW size which is a function of the probability of collision in contentions. In order to compare the performance results, the probability of collision given in Equation 4.6 is incorporated into the SSCW approximation. Contention delays obtained by setting the contention window size according to SSCW approximation, W_t^* found in our study and S-MAC default value are compared. Figure 4.6(a) shows the delays obtained in the simulation runs where the corresponding CW sizes are given in Figure 4.6(b).

As seen in Figure 4.6(a), the delay optimizing window size can improve the delay significantly compared to S-MAC in which the CW size is defined to be a constant and compared to SSCW which calculates the CW size with approximate analysis. The CW sizes offered by SSCW is a step function which is the reason of the fluctuation of SSCW performance values in Figure 4.6(a). This behavior cannot be observed in [80] since the number of neighbors investigated are increased 100 nodes at a time, starting from 100 nodes. In fact, due to the limited communication range of the sensor nodes and the low deployment densities, the number of neighbors of a node is expected to be

less than 20 nodes [81]. Moreover, the number of contending nodes will be a subset of the neighbors. It is clear from Figure 4.6 that within this operational range, to use the W_t^* as the CW size is very effective considering the contention delay.

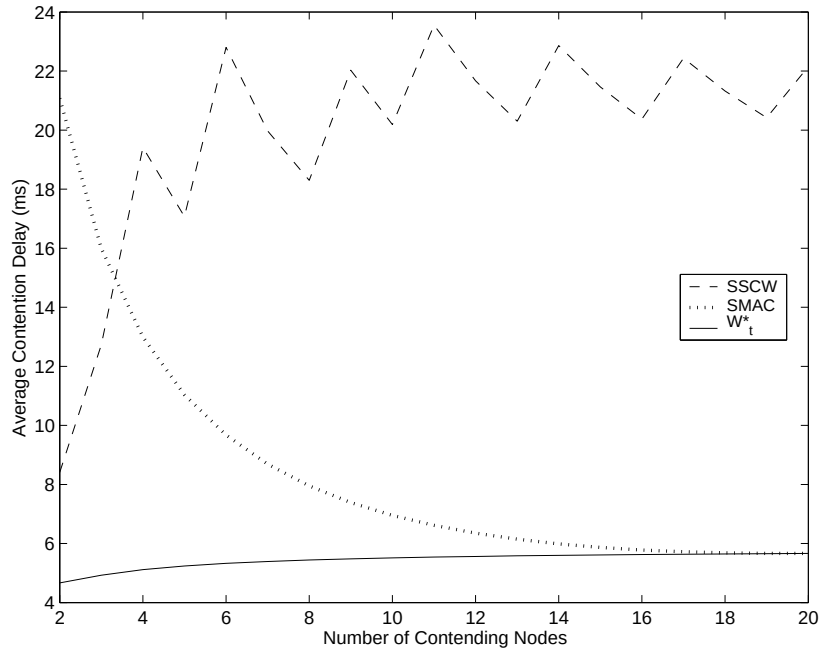

(a)

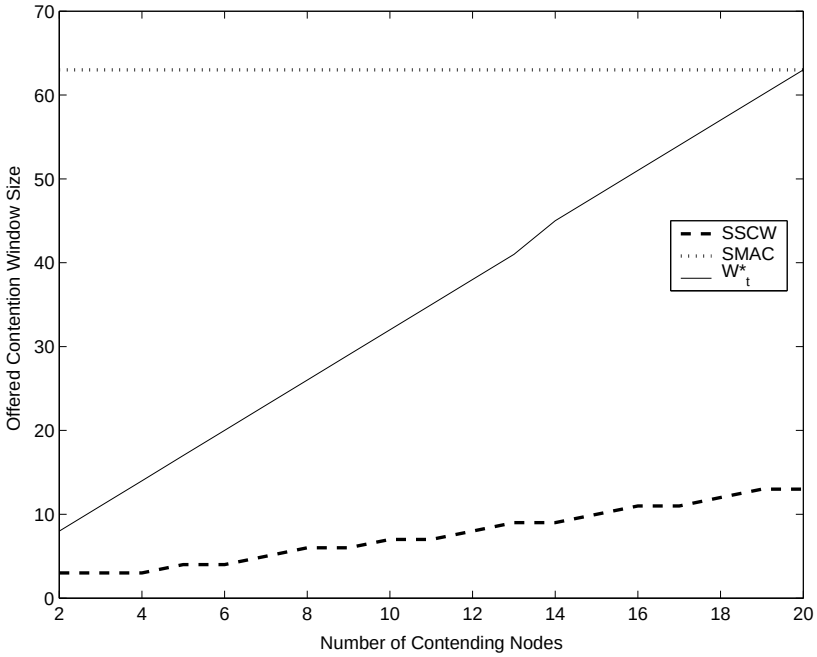

(b)

Figure 4.6. (a) The offered contention window sizes by SSCW, S-MAC, W_t^*, and (b) the resulting contention delays

4.5.2. Total Energy Consumption Results

To verify the analysis presented for the energy consumption components of the contentions, E_{coll} and E_{ssa} values are evaluated in the simulations separately. The energy consumption values for transmission and reception is 27 and 10 mJ respectively in compliance with the Xbow Mica mote products [63]. The effect of CW size on the two energy consumption components in Figure 4.7(a) and Figure 4.7(b), respectively. As expected, higher CW sizes cause higher energy to be spent for carrier sensing till the first occupied slot. On the contrary, higher CW sizes result in lower energy consumption for collisions since the probability of collision decreases.

The trade-off between energy consumed for collisions and the energy consumed for carrier sensing is clearly visible in Figure 4.8. The energy optimizing CW size, which is denoted as W_E^*, minimizes the total energy consumption caused by the contentions. An important observation is that the energy consumed for contentions is comparable to the energy consumed for data transmissions. As a numerical example, when the data packet size is 400 bits, the transmission of five data packets and their receptions result in 11.1 mJ of energy consumptions. However, the energy consumed for overall contention is 7.04 mJ which is 63 per cent of the data transmission energy requirement if the CW size is 63.

The overall energy consumption results of different CW sizes are shown in Figure 4.9 for $3-10$ contending nodes. As seen in the figure, the optimal operation point, W_E^*, gets larger as the number of contending nodes gets larger. Unlike the behavior in Figure 4.5, independent of the contention window size, the more the contending nodes the larger the average energy consumed.

The energy consumed by using W_E^* is compared to those obtained by using S-MAC default and the CW size calculated by SSCW in Figure 4.10(a) and Figure 4.10(b), respectively. The proposed CW sizes by the three methods are shown in Figure 4.11. As depicted, the energy consumption is improved significantly. The energy saving due to W_E^* is between $32-72$ per cent compared to S-MAC defaults for the range of $2-10$

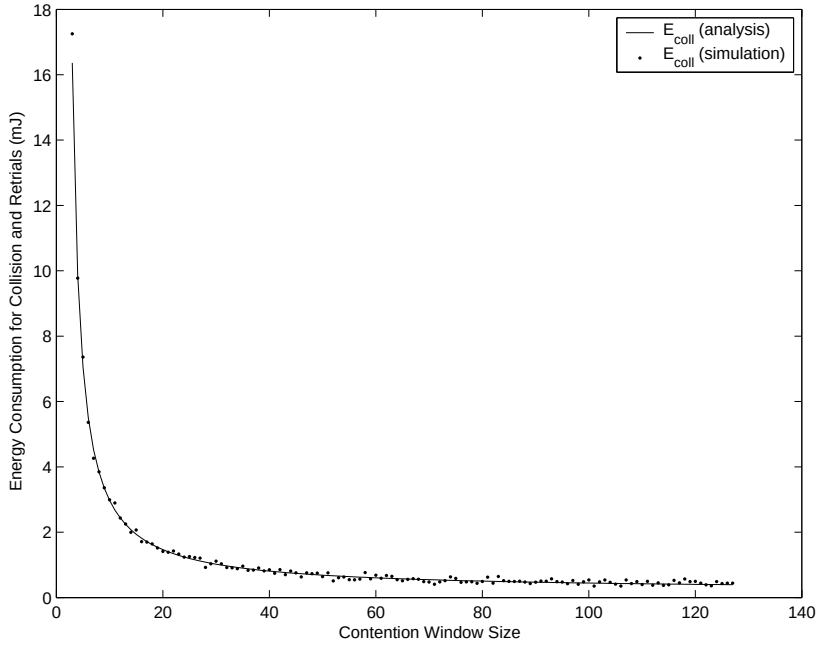

(a)

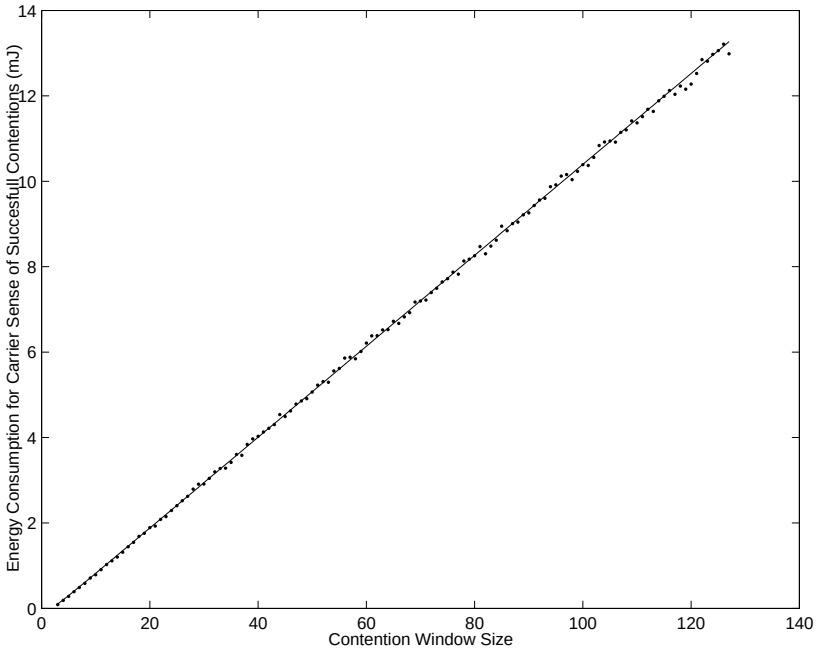

(b)

Figure 4.7. Simulation vs. analytical formula results for $N = 5$, (a) the effect of the contention window size on the total expected energy consumption via collisions, E_{coll}, and (b) the effect of the contention window size on the expected energy consumption via successful carrier sense, E_{ssa}

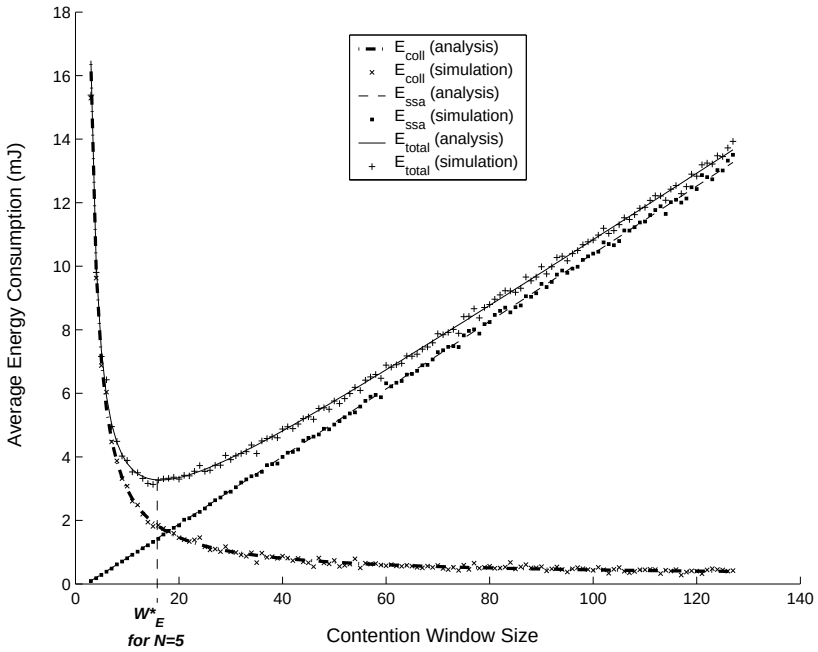

Figure 4.8. The expected energy consumption via collisions, E_{coll}, the expected energy consumption via carrier sense, E_{ssa} and the expected energy consumption of overall contention resolution, E_{total}, for $N = 5$

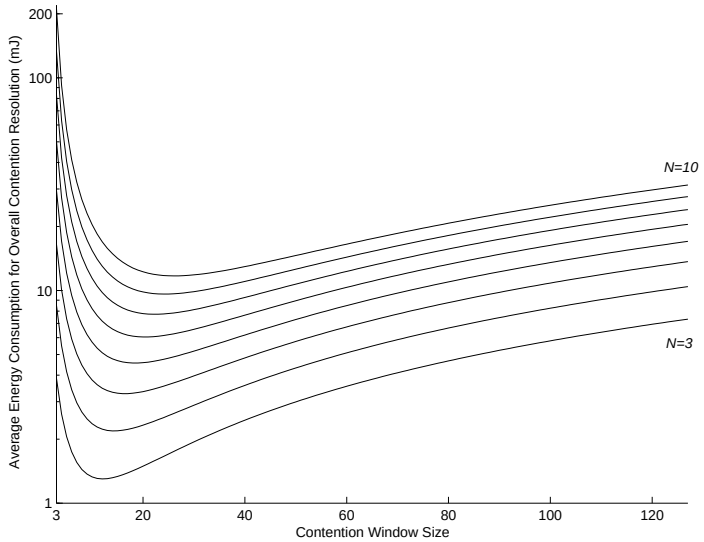

Figure 4.9. Effect of contention window size for different number of contending nodes on expected energy consumption for overall contentions (*log*)

contending nodes. The gain achieved compared to the SSCW approximation is $54-74$ per cent for the same range of contending nodes.

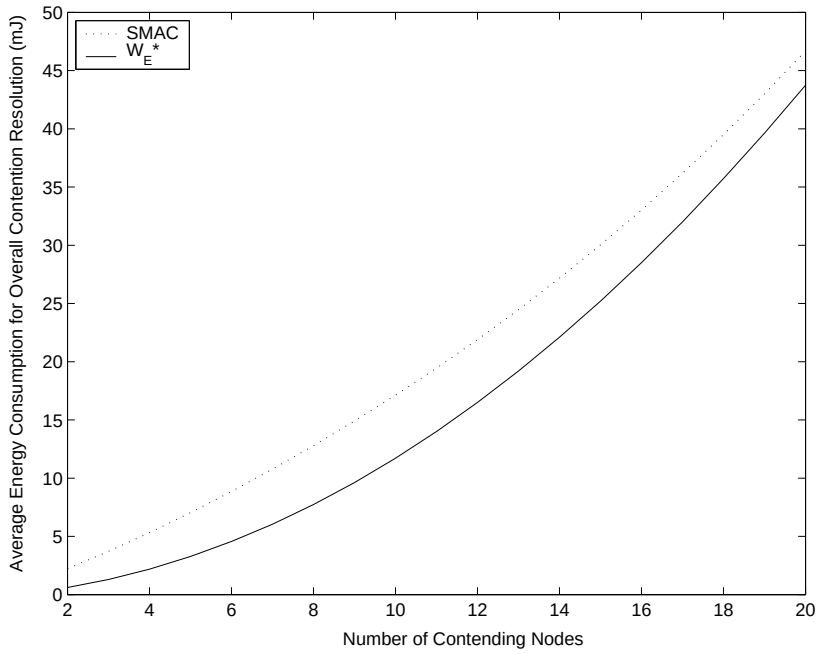

(a)

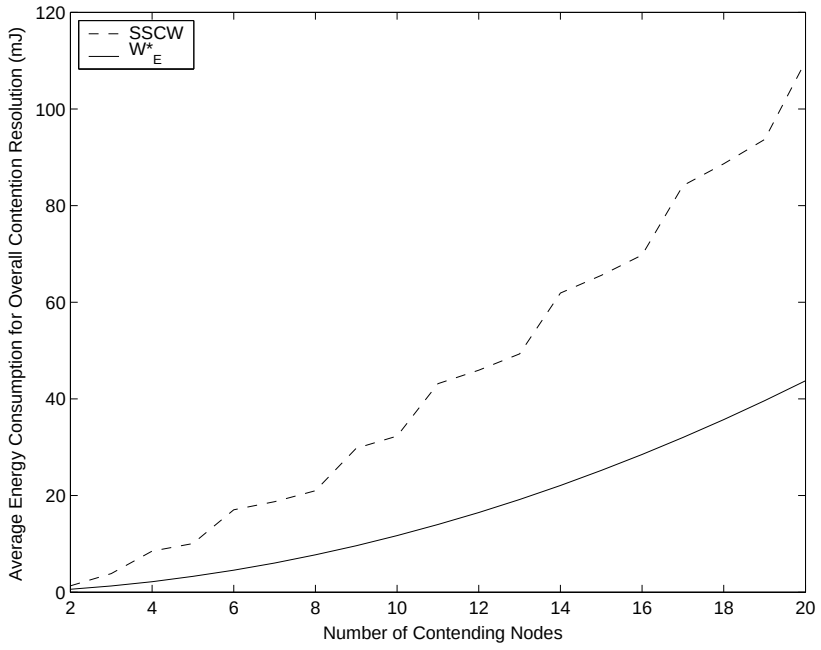

(b)

Figure 4.10. Expected energy consumptions for the offered contention window sizes of (a) S-MAC and W_E^*, and (b) SSCW and W_E^*

4.5.3. The Energy-Delay Trade-off

The energy consumption and delay are two important performance metrics for WSN protocols. However, since the minimization of one metric can introduce an in-

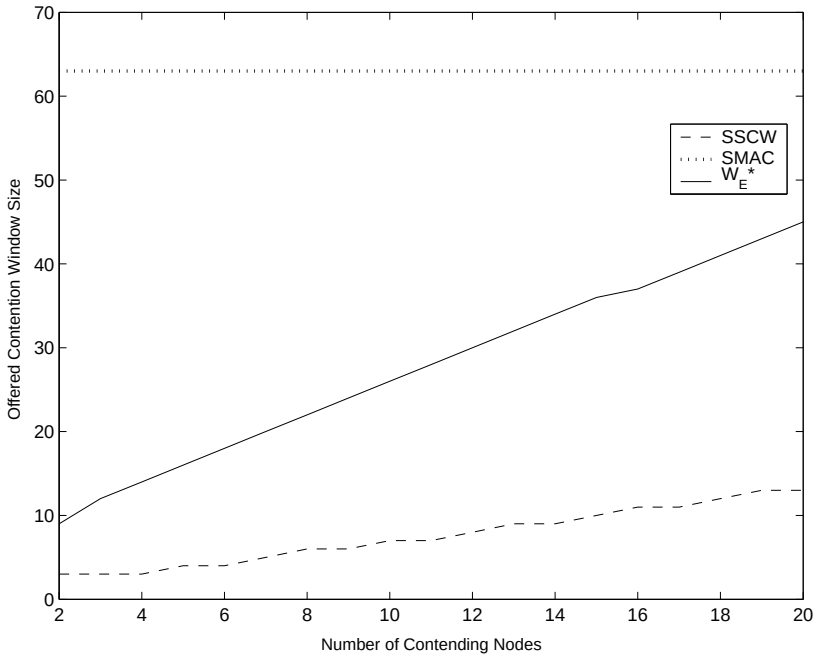

Figure 4.11. The offered contention window sizes by SSCW, S-MAC, W_E^*

crease in the value of the other, we end up with a trade-off between these two metrics which must be investigated separately. To depict this trade-off, the contention delay and energy consumption for overall contention values achieved by the the delay optimizing CW size and the energy optimizing CW size are compared in Fig. 4.12 and in Fig. 4.13, respectively. The use of energy optimizing CW size results in at most 7.5 per cent higher average delays than the minimum delay that can be achieved with a different CW size. Likewise, the energy consumption penalty of using the delay minimizing CW size instead of the energy optimizing CW size is at most 8 per cent for the given number of contenders range. Hence, we can conclude that using either delay optimizing or energy optimizing CW sizes presented in this work result in an acceptable increase in the other metric for the most of the WSN applications. As a result, although it is possible to define one of the objectives as a constraint for the optimization of the other, that kind of constrained optimization is generally not necessary.

4.6. Estimated Number of Contenders (ENCO) Method

The optimum CW size values that minimize the contention delay or the energy consumption for the overall contention, W_t^* and W_E^* respectively, are defined to be

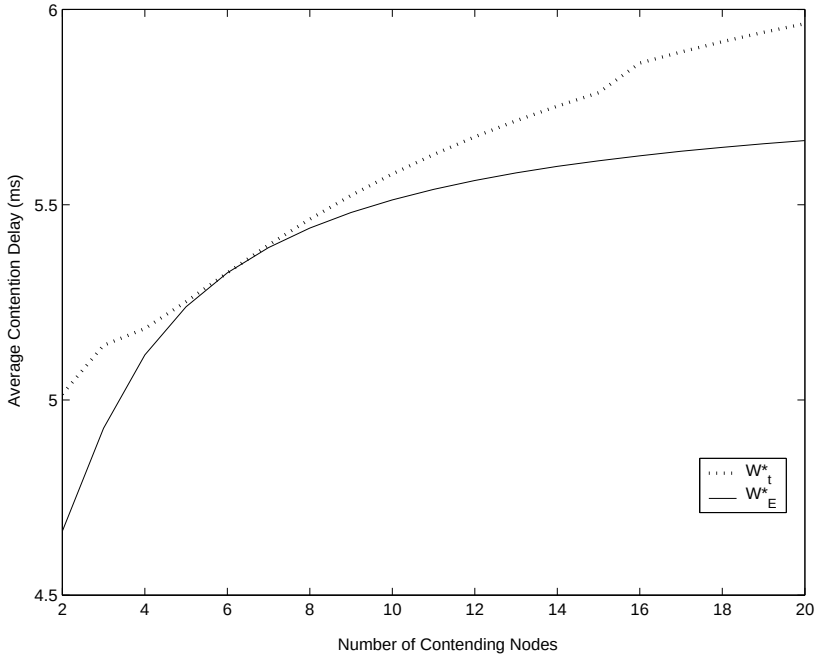

Figure 4.12. The trade-off between the energy optimizing and delay optimizing CW sizes for average contention delay

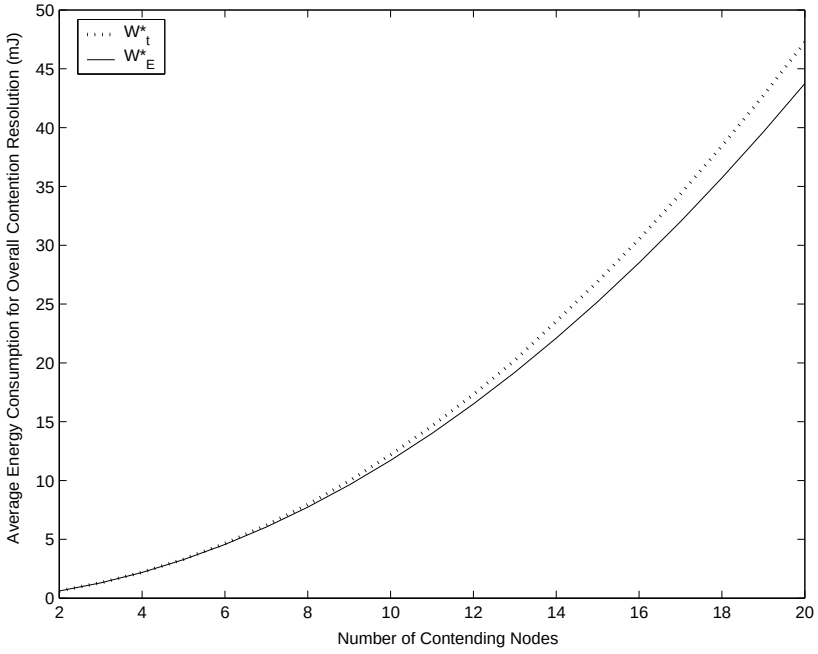

Figure 4.13. The trade-off between the energy optimizing and delay optimizing CW sizes for average energy consumed for overall contentions

a function of *the number of contending nodes*. For IEEE 802.11 networks, Ma *et al.* propose that AP (Access Point) counts the number of contending nodes and judges

whether the CW parameters should be changed or not [82]. In case a change is needed for performance issues, the AP announces it to all of its nodes. Since in contention-based WSN, the number of contending nodes are dynamic and cannot be known by individual sensors in advance, an approximation method is needed to benefit from the optimization method. We propose the Estimated Number of Contenders (ENCO) which is aimed for event-triggered WSN for such applications as surveillance, environmental monitoring, disaster monitoring and target tracking. The number of nodes that can sense the event at an area point defines the *coverage degree* of that point as described in Section 3.2.2. When an event occurs in the application area, the coverage degree of the point determines the number of contending nodes assuming that every detecting node sends this information to the sink. Hence, the mean coverage degree of a deployment area approximates the average number of contending nodes for possible events. Let the density of the deployment area be d nodes per m^2 and the sensing range of the sensors be R_s meters. Then, similarly to Equation 3.3, for the common uniformly deployment case, the mean coverage degree C is defined as

$$C = \pi R_s^2 d, \tag{4.31}$$

since the nodes that are at most R_s away can sense the event.

In the ENCO method, the mean coverage degree is used to approximate the expected number of contending nodes, which then can be used to calculate an approximate value for the optimum CW size that is set to all sensors of the network before the deployment since the required information for the mean coverage degree value is available before the deployment. Although the density that should be chosen depends on the application requirements, the method presented in [49] can be used to calculate the required density for a given breach detection probability level. To show how well the ENCO method approximates the optimum CW size results, it is tested in two different types of event-driven WSN applications: one where the event locations are independent, and the other where the event locations are correlated. Let the number of contending nodes in consecutive events be represented with $c(t)$ where t represents the event sequence. In random event location (REL) applications, the locations of

consecutive events are independent. Precision agriculture is an instance of REL applications where the earth humidity or salinity levels can trigger such events. Here, $c(t)$ is a memoryless process, i.e, consecutive number of contending nodes are not dependent on previous values. However, in correlated event location (CEL) applications, the consecutive event locations are dependent on each other such as the behavior in target tracking applications. The consecutive detection points in such applications are spatially correlated. Hence, the consecutive number of contending nodes are not independent and $c(t)$ is not memoryless [15]. The performance of the ENCO method is investigated for example CEL and REL applications via simulations for $20-200$ nodes that are deployed in a uniformly random manner to a 300x300 m^2 area. A node can detect an event, if the event occurs within 50 m distance of the node.

In REL applications, events occur in different parts of the deployment area randomly. Each parameter set is simulated 1000 times. At each run, the nodes deployed to the area uniformly randomly. Afterwards, 10 event points are selected randomly and the number of nodes that detect this event is logged. The contention of the detecting nodes are simulated under three different contention window sizes: W_E^*, W_{ENCO} and the S-MAC default where W_E^* and W_{ENCO} are the energy optimizing CW size for the number of detecting nodes and CW size for the ENCO method, respectively. As seen in Figure 4.14, using W_{ENCO} results in an energy consumption very close to that which could be obtained by using W_E^*. Hence, ENCO method enables us to set the CW size efficiently in a distributed environment according to the network properties, namely the sensor density and the sensing range.

In CEL applications where the event locations have correlation, the number of nodes that detect these events, i.e., the consecutive number of nodes that will contend for the medium are not i.i.d. The consecutive detection locations result in a dependency between consecutive number of contending nodes. This dependency is studied in [15] and a packet traffic model, i.e., a model for the number of contending nodes is presented. Here, this model is used to generate the number of contending nodes for a CEL application. The model is based on uniformly random deployment and includes the parameters of the target velocity and the sensing interval which are set to

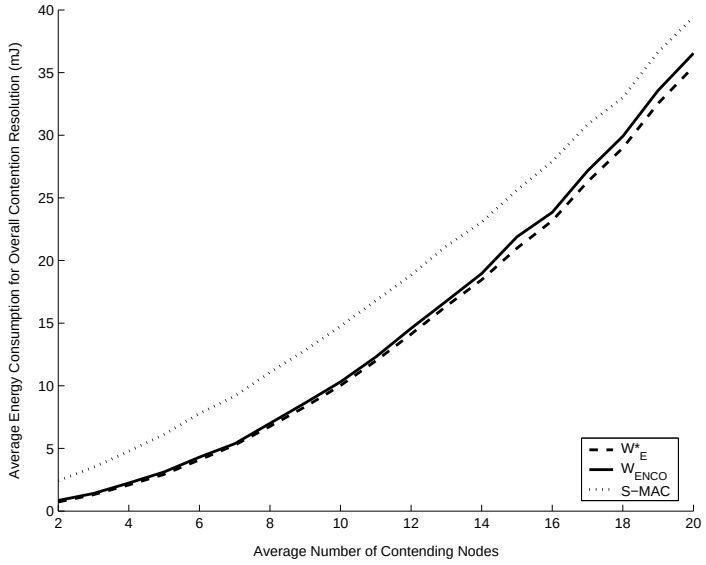

Figure 4.14. Energy consumption comparison for the overall contention resolution for a REL scenario

10 m/s and 1 sec in this work, respectively. Number of contenders for 10 consecutive sensing are generated for 1000 different sensor deployments. The resulting contentions are simulated under three different contention window sizes: W_E^*, *S-MAC default*, and W_{ENCO} where W_E^* and W_{ENCO} are the energy optimizing CW size for the number of contenders and the CW size offered by the ENCO method, respectively. As seen in Figure 4.15, the ENCO method enables the approximation of the theoretical optimum performance in a distributed manner for CEL applications as well.

4.7. An Alternative Method for Slot Selection: p^*

Most of the slotted contention based medium access mechanisms employ uniformly random slot selections such as IEEE 802.11, IEEE 802.15.4 and S-MAC. However, Tay *et al.* propose a slot selection method, namely p^*, that minimizes the probability of collision [27]. Since the p^* method use the number of contenders information, N, for practical implementation, Sift algorithm is proposed to approximate p^* performance without the knowledge of N [26]. However, instead of its proposed approximation, we concentrate on the p^* method and investigate whether minimizing the collision probability in slot assignments reveals the best performance for WSN.

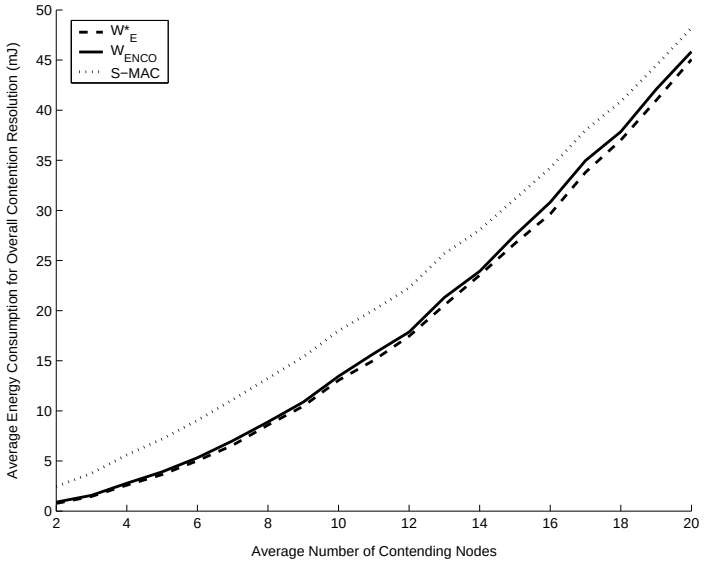

Figure 4.15. Energy consumption comparison for the overall contention resolution for a CEL scenario

The p^* method is developed by analytical derivation of the optimum slot selection probability distribution based on the N and CW size information. An example probability distribution for the contention slot selection is illustrated in Figure 4.16 for 5 contenders and 63 contention slots. The general idea of the p^* method is to have small probabilities for the slots with small indices. The success of the method is seen in Figure 4.17 where it is compared with uniformly random slot selection method by simulating 10000 random slot assignments. However, the question is: does this minimization of the collision probability result in the best performance of the medium access? To answer this question, one needs to select a crucial medium access objective and then investigate the slot selection methods under this objective. Although in [26] and [27], it is shown that p^*-based slot selection results in less collisions and less delay compared to IEEE 802.11, optimization of an overall performance metric is not investigated. In addition, although the CW size is used as a parameter for the p^* method, the best CW size for the performance of the method is not given either.

In this section, we select the contention delay as the performance metric and study the overall performances of p^* and uniformly random slot selection methods. The average contention delay results achieved vary depending on the CW size employed as

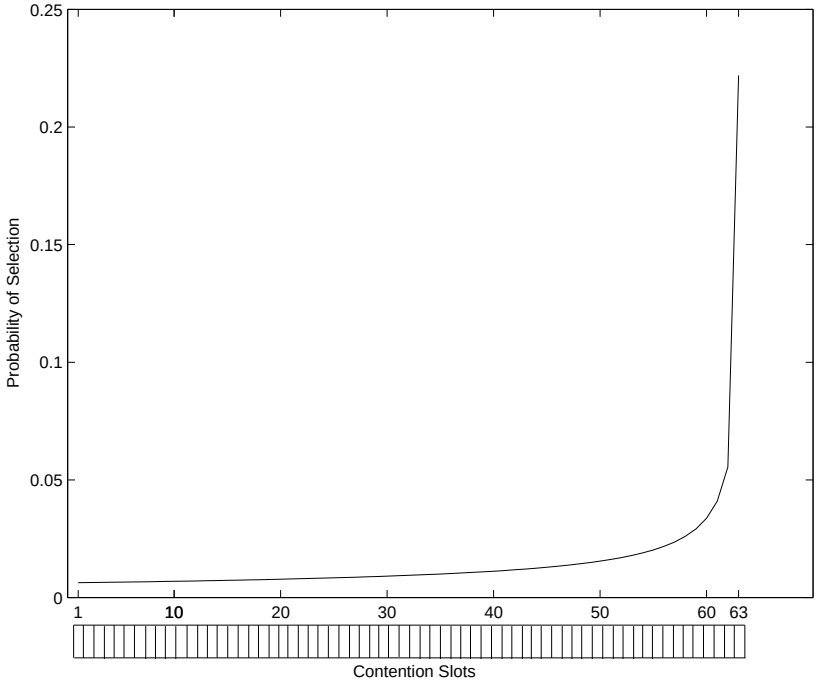

Figure 4.16. The probability mass function for slot selections where $N = 5$ and $W = 63$

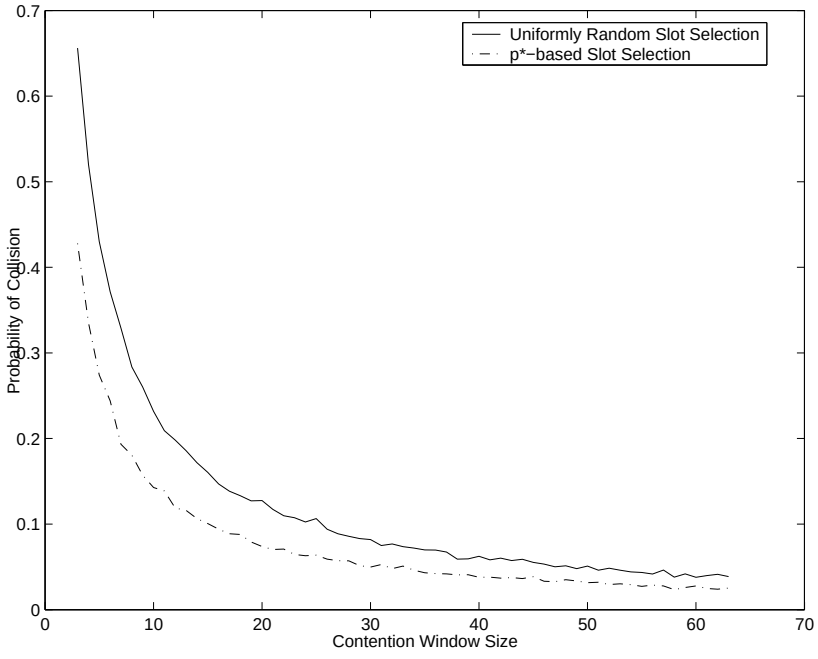

Figure 4.17. The probability of collisions for different slot selection methods for $N = 5$

shown in Figure 4.18. Hence, first, we investigate both methods under the optimal contention window size for the uniformly random slot selection, W_t^*, which can be found by the analytical formula developed in Chapter 4. Then, to achieve a more fair

comparison, the performance of the p^* method is investigated under the CW size that optimizes its performance which is found by simulations since there is no study for its optimized CW size.

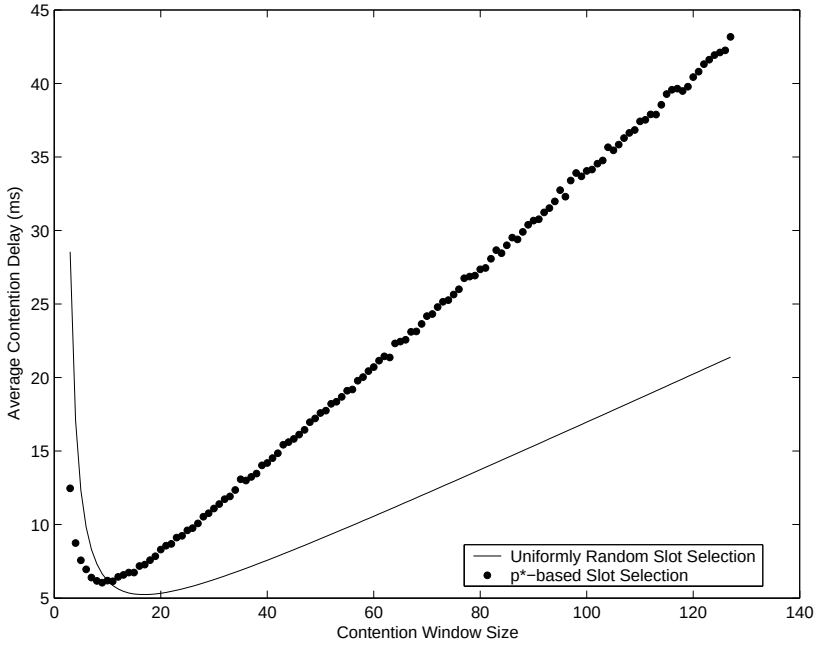

Figure 4.18. Average contention delays observed for $N = 5$

The overall comparison for the contention delay results of both methods for CW size of W_t^* are given in Figure 4.19. The worse results of the p^* method can be explained by the fact that for the expected contention delay values, the mean carrier sense duration till the first selected slot is important which is, on average, higher in p^* method compared to the uniformly random method. The contention delay results of the uniformly random slot selection method is calculated by Equation 4.19 whereas the p^* method results are calculated by averaging the results of 10000 simulations for each N value.

Comparing the performance results of both methods using the CW size optimized for one of them leads to a subjective comparison. Hence, another set of simulations are performed where the CW size used for the p^* method is the one that optimizes its average contention delay, namely $W_{p^*}^*$. Since there is no optimum CW size setting proposed in [26] or [27], a prior work is done to extract the optimum CW size values for each possible N value. This is done by simulating 10000 medium accesses for each

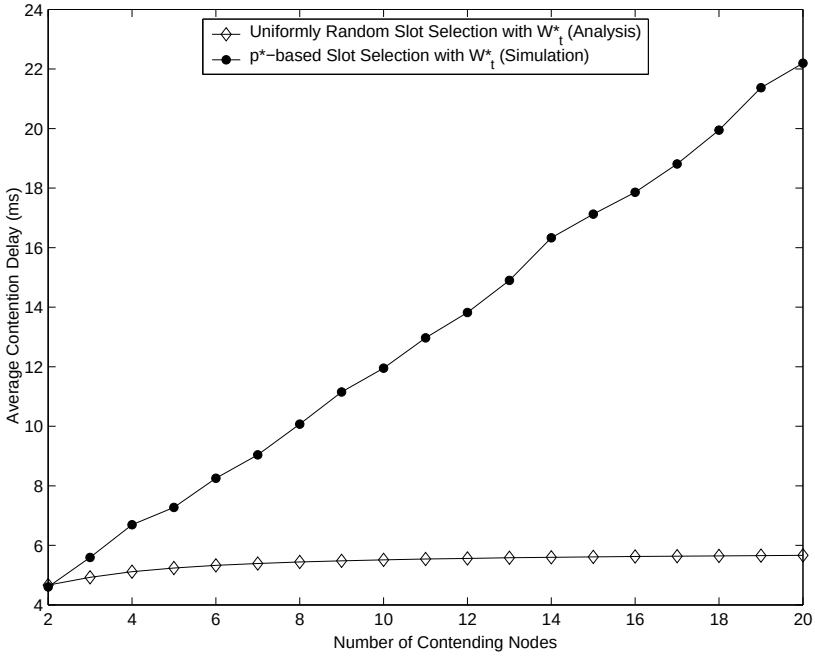

Figure 4.19. Average contention delay results for different slot selection methods for CW size of W_t^*

CW size and N pairs and averaging the results. The CW size values that result in minimum average contention delays are defined as $W_{p^*}^*$ for each N value and displayed in Figure 4.20 along with the corresponding W_t^* values.

Both slot selection methods are evaluated for their average contention delay performances with their optimum CW size values which are shown in Figure 4.21. As seen in the figure, instead of minimizing the probability of collision with a different slot assignment algorithm, optimizing the contention window size with the default uniformly random slot assignment method is advantageous for the *average contention delay* metric. The results of the p^* method is found by averaging 10000 simulation runs whereas the results for the uniformly random slot assignment method is found by Equation 4.19.

As a result, p^* method does not improve the average contention delays compared to the uniformly random slot selection method. However, it is still an open issue whether the latter is the slot selection method that optimizes the average contention delay. It is important to note that, to achieve the optimum performance results, the slot

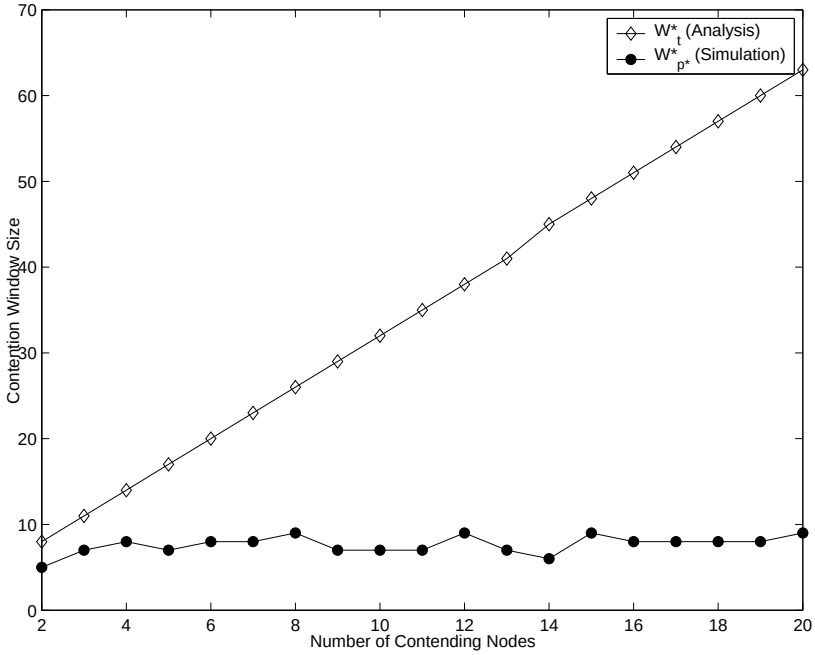

Figure 4.20. Optimum CW sizes for uniformly random slot selection (W_t^*) and p^* method ($W_{p^*}^*$)

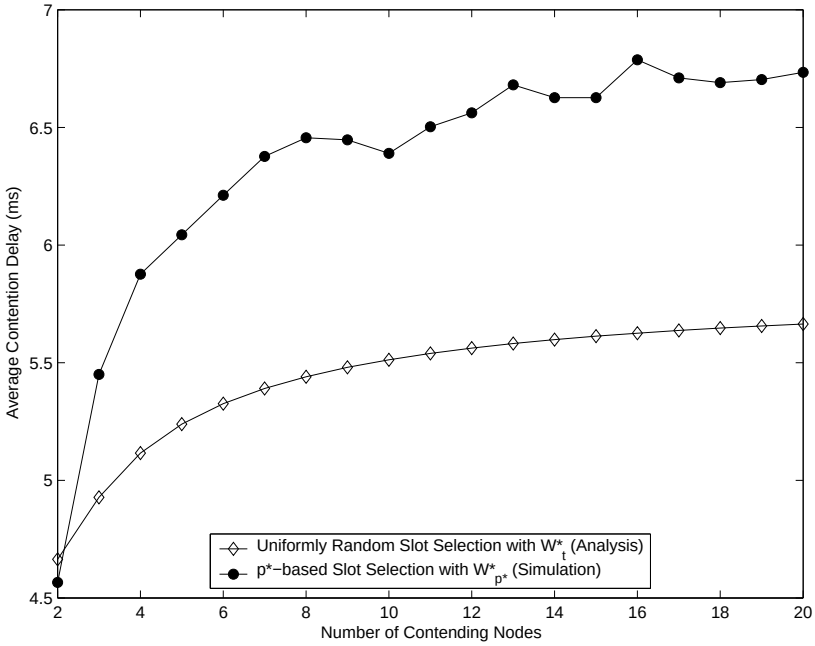

Figure 4.21. Average contention delay results for different slot selection methods using their optimum CW sizes

assignment method and the contention window size setting method should be studied together.

4.8. Conclusion and Future Work for Contention Window Size Optimization

Due to the limited battery capacities of the sensor nodes, minimizing the energy consumption is a crucial objective for all WSN studies. For the delay-sensitive applications such as disaster monitoring and target tracking applications, the minimization of the communication delay presents another critical objective. In this chapter, the contention delay and the energy consumption for the contention resolution are shown to be important factors of these objectives. The significance of the contention window size setting on the two former factors is depicted both analytically and by simulations. With the analyses presented, the energy optimizing contention window size or the delay optimizing contention window size can be calculated depending on the primary objective of the network. It is shown that the performance of contention-based MAC protocols can be significantly improved using the optimum contention window size. Although the significance of CW size optimization is shown for S-MAC, the presented analysis and optimizations are applicable to all MAC protocols proposed for WSN or for other wireless networks that define a fixed contention window size and uniformly random contention.

Moreover, the Estimated Number of Contenders (ENCO) method is proposed for event-triggered WSN where the optimum contention window size can be approximated by individual sensor nodes in a distributed manner. The main idea of the ENCO method is using the mean coverage degree of the network which is a function of the network properties *sensor density* and the *sensing range*. The simulations show that this method achieves close performance results to the optimum contention window size results. As a future work, local information such as the number of neighbors can be embedded into the contention window size setting mechanism to improve the performance of the ENCO method. In addition, if clustering is used, the information of number of nodes within a cluster can be retrieved from the cluster head which can, then, be used to select the CW size.

Another contribution of this work is the evaluation of the collision minimizing slot selection method for an overall MAC performance metric. It is shown that minimizing the collision probability does not improve the overall contention delay compared to the uniformly random slot assignment with its optimum CW size. As a future work, the combinations of slot assignment methods and the CW size optimization based on each slot assignment method can be investigated for optimizing the specified performance metrics.

5. IMPROVING THE CAPABILITIES OF VIDEO SENSOR NETWORKS WITH THE CONTENTION WINDOW SIZE OPTIMIZATION

5.1. Introduction and Motivation

In Chapter 4, it is shown that the contentions can be optimized for the energy consumed or the delay incurred by contentions. However, WSN performances are depicted by the performance values for the end-to-end packet transmissions, i.e., for the transmissions of packets from the source nodes to the sink node. Therefore, to investigate the overall effect of the contention optimization, we evaluate *video sensor networks* for the end-to-end network performances. Video sensor networks (VSNs) are a special type of WSNs where sensor nodes equipped with video cameras send the captured video according to the requirements of the VSN application implemented. By doing simulations of VSN with the default CW size setting and the optimized one, we show that the optimization of contentions provides a significant improvement on the overall network performances as well.

5.2. Video Sensor Networks

Video sensor networks (VSNs) are the new members of the WSN family in which multirate streaming data traffic and related Quality of Service (QoS) requirements result in new problems that require novel solutions. Traditional wireless sensor networks are generally tuned for scalar data that is being relayed through multihop routes towards the data sink. Therefore, previously proposed WSN protocols may be insufficient for VSNs as the video streams require very large bandwidth compared to scalar data such as temperature readings. Additionally, due to the nature of the video, the streams have always realtime requirements. Moreover, since the logical unit of the communicated data becomes video frames, either successful delivery of all or a large percentage of packets of a video frame are required to be delivered to the sink node.

Majority of the available video coding schemes such as MPEG are designed to have computationally intensive video processing at the sender and less computational effort at the receiving side. However, the requirements in WSNs are exactly the opposite. Sensor nodes have less computational power and energy capacities, on the other hand, the data sink is usually assumed to be computationally more powerful and has unlimited source of energy. This makes the complicated inter-frame coding based video processing techniques infeasible for the VSNs [83]. For that reason, a very low frame rate video is assumed which is basically a sequence of images to be transferred to the sink. However, in order for individual images to be useful for tracking or identification purposes, a certain percentage of the packets are required to be delivered to the sink.

Introducing a sleep schedule is required to increase the energy efficiency of a WSN. For traditional scalar type of data traffic, lowering the duty cycle results in a higher energy efficiency at the expense of increased delay [13]. However, in the context of video traffic, changing the duty cycle not only affects the delay but also the throughput of the system, which in turn affects the object identification or tracking quality. In general, due to the congestion in the network and the limited buffers of the sensor nodes, not all of the packets will be delivered to the data sink. For that reason, increasing the sensor video quality generated at individual nodes does not necessarily entail an increase in the received video quality at the data sink. In this work, first, we explore the limitations on VSNs in terms of the carried traffic rate and application level requirements with a default contention mechanism. We run simulations with realistic parameter values to explore the effect of the duty cycle and the frame rate on the performance of VSNs. Then, we investigate the improvement in certain performance metrics using the ENCO method for the contention window size setting. Although improvements are required at each networking layer for VSN, the effect of MAC layer improvements are significant alone on the overall network performance.

5.3. System Model and Simulation Parameters

To asses the performance behavior of VSNs, simulations are run under OPNET simulation environment [61] with realistic parameter values reflecting the hardware and

software capabilities that are currently available. The deployment is done with single sink node located in the geometric center of the surveillance area. Nodes are equipped with image modules composed of cameras capable of producing and compressing video images [84, 85]. Raw image format is software adjustable and in our simulations SQ-CIF (128 x 96) format is assumed. The image module employs intra-frame encoding which results in compressed images of size 10 Kbits. Predictive encoding alternatives such as ISO MPEG or H.26x cannot practically be used in VSNs due to the high complexity involved [86]. Distributed source coding techniques are promising alternatives for encoding video in VSNs as they exploit the inter-frame redundancy with affordable complexity in the sensor nodes [83]. However, due to the lack of practical implementations yet available, we resort to the JPEG compression available on the image module. Software controlled frame rate feature allows video streams with rates between $1 - 12$ fps to be introduced to the network by each individual sensor node. Event triggered data generation is simulated where the triggering event is the visual detection of the target. Since the cameras employed support the background subtraction feature, they only produce an image when the scenery changes significantly. Triggering occurs when the target is within the camera detection range of 30 m and is within the Field of View (FOV) of 52 degrees. The target is assumed to move within the surveillance area according to the Random Waypoint Mobility model where the target velocity is set to 10 m/s and pause time is set to zero seconds. Crucial simulation parameters are tabulated in Table 5.1. Data transfer at the frame level to the sink is assumed to be done in the application layer whereas packet level communications at the MAC and network layers are handled with S-MAC [13] and GPSR [87], respectively. Both protocols are implemented in OPNET simulator based on their specifications.

5.4. The Capabilities of Video Sensor Networks with Default Contention Window Size

5.4.1. Effect of Sleep Schedule and Frame Rate in Video Sensor Networks

Several simulation runs are performed with different duty cycles and the sensor camera frame rates where the default CW size setting of S-MAC is used. At each run,

Table 5.1. Simulation parameters for VSN performance evaluation

Parameter	**Value**
Surveillance Area	400 x 400 m^2
Network Size	60 Nodes
Deployment Type	Uniform random
Video Frame Size	10 Kbits
Packet Size	1 KBits
Camera Frame Rate	1 to 12 fps
Field of View	52 deg.
Camera Detection Range	30 m
Bandwidth	250 Kbps
Buffer size	20 Kbits
Target Mobility Model	Random Waypoint

the total number of frames created is recorded along with the number of received video frames at the sink.

5.4.1.1. Effective Traffic Carried in the Network. Generally, higher *video quality* is required for better VSN application performance. Video quality can be adjusted in the system by varying the image resolution and the camera frame rate. In our case, we fix the image resolution since a lower resolution may not be tolerated by the identification application, whereas a higher resolution results in frame sizes that cannot effectively be carried in the network. Therefore, in the simulations the frame rate of the cameras on the sensors is varied to alter the video quality throughout the network. As depicted in Figure 5.1, increasing the video quality in the sensors only pays-off up to a saturation point, after which the throughput drops, hence the average frame rate received at the sink decreases. To show the limiting factors on the throughput, the experiments are repeated for three different duty cycle values. Figure 5.1 exhibits that the saturation point is dependent on the duty cycle of the system. A higher duty cycle value enables higher network service rate by handling more packet transmission per unit time.

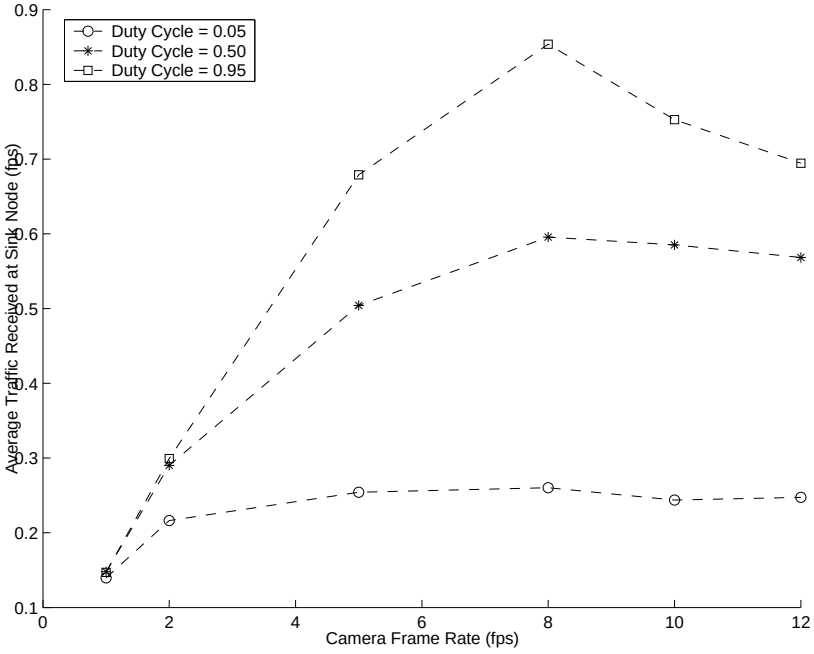

Figure 5.1. Effect of sensor video quality (frame rate) on the received frame rate at the sink

5.4.1.2. Delivery Ratio. As the compressed video includes dense information, a frame can be defined as lost after a certain drop percentage for the packets that belong to that frame. In our simulations, we set that threshold to 10 per cent, i.e., if more than 10 per cent of packets that belong to a frame are dropped, then that frame could not be recovered and is labeled as a lost frame. Figure 5.2 shows the successful frame delivery ratio for different sensor frame rates under different duty cycles.

Depending on the QoS requirements of the application, the maximum allowed sensor frame rate can be extracted from this figure. For instance, if the application requirement is 90 per cent successful frame delivery ratio, then for 50 per cent duty cycled network operation, the sensor frame rate must be 2.5 fps or less to achieve that QoS requirement.

To further understand how the duty cycle introduced by the sleep schedule affects the application level performance, we need to examine the main cause of the packet drops experienced in the network. Figure 5.3 depicts that as the duty cycle is lowered, considerable amount of video traffic is dropped at the source nodes. A sensor node

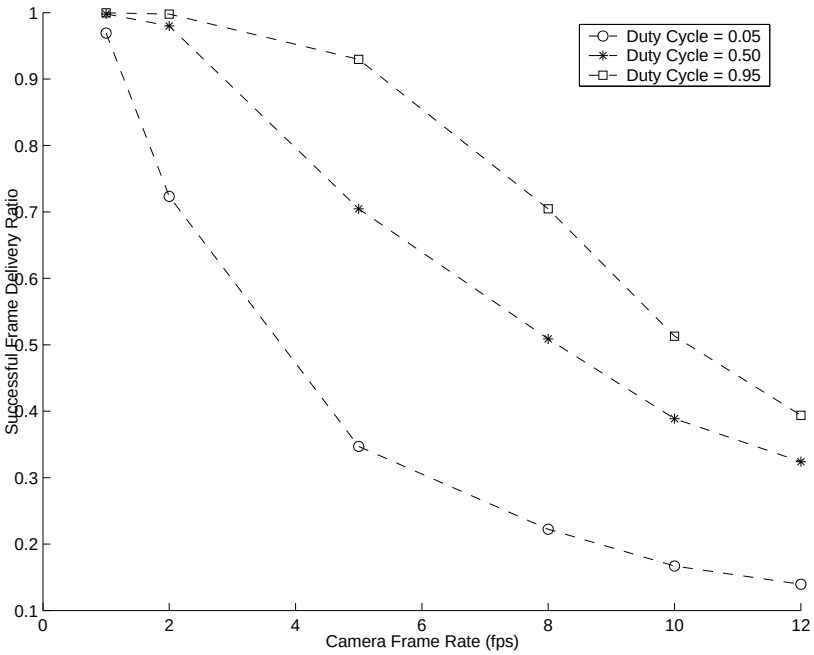

Figure 5.2. Successful frame delivery ratio

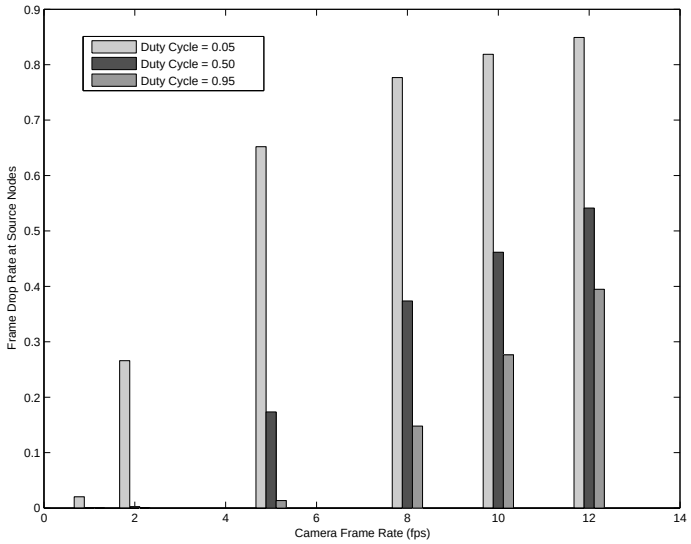

Figure 5.3. Ratio of aggregate dropped traffic at source nodes to aggregate created traffic

operating at a low duty cycle, upon detecting the target begins to accumulate video frames as the probability to have an awake neighbor gets lower and buffer overflow occurs.

5.4.1.3. Effect of Buffer Size. Current sensor nodes generally have around 60 Kbits of RAM available [63]. Our choice of 20 Kbits buffer size is based on the assumption that available RAM area that is not used by the communications stack and the application code can be allocated as a buffer to handle the images conveyed from the camera module. However, it is possible to increase the physical RAM size to create more buffer for image handling at the expense of increased costs. Here, we explore the effect of increasing buffer size to alleviate the overflow problem. The previous simulation runs are repeated for the buffer size value of 250 Kbits.

As shown in Figure 5.4, the successful delivery ratio is considerably higher for the new buffer size. The major reason for this behavior is that high drop rates at source nodes are now eliminated, i.e., the video traffic is now being let into the network with a much less loss rate. How the increased buffer affects the average delay in the system is shown in Figure 5.5 and Figure 5.6. Here the delay experienced by the packets as they travel from the source to the sink is measured. As expected, increased delay is observed which is also heavily affected by the duty cycle. For the duty cycle values of 50 per cent and 95 per cent, the delay is observed to be bounded by three seconds with frame loss ratio bounded by two per cent, which can be considered as acceptable for many applications.

The delay observed for the lowest duty cycle value is depicted in Figure 5.5. Here, it is clearly seen that increasing the buffer size puts the system in a non-functional state, as the camera frame rate goes above 1 fps. Although, successful delivery ratio depicted in Figure 5.4 indicates that, more than 75 per cent of the frames are received at the sink even for 12 fps with high buffering capacity, due to the limited communication capacity and the low duty cycle, packets are received at sink with unacceptable delays.

5.5. Improving VSN Network Performance with ENCO Method

In the former section, the capabilities of VSNs are studied which are constrained by the current hardware properties and the available video encoding methods. The default contention mechanism of S-MAC method is the slotted CSMA where the con-

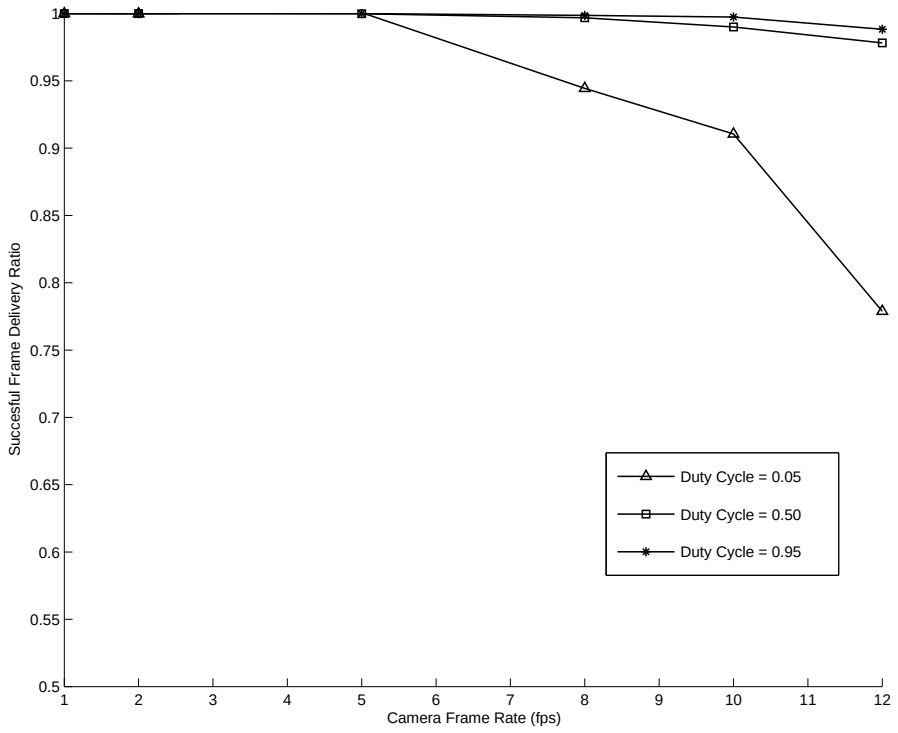

Figure 5.4. Successful frame delivery ratio obtained when buffer size is increased to 250 Kbits

tention window size is set to 63. In this section, we use the ENCO method presented in Section 4.6 to set the contention window size and investigate the effect of the ENCO method on the overall network performance. The same simulation setup and parameter values are employed as of Section 5.4 except the CW size setting.

As shown in Section 5.4, increasing the quality of video captured, i.e., increasing the camera frame rate can improve the quality of video received at the sink until a certain value. By employing the ENCO method, the quality of video received is higher as seen in Figure 5.7. With the ENCO method, the throughput of the network is increased. As a numerical example, the system throughput is increased between $10 - 28$ per cent for the camera rate of eight fps for all investigated duty cycle values.

An important application level requirement of VSNs is the successful frame delivery ratio whose results are depicted in Figure 5.8. For almost all camera frame rate

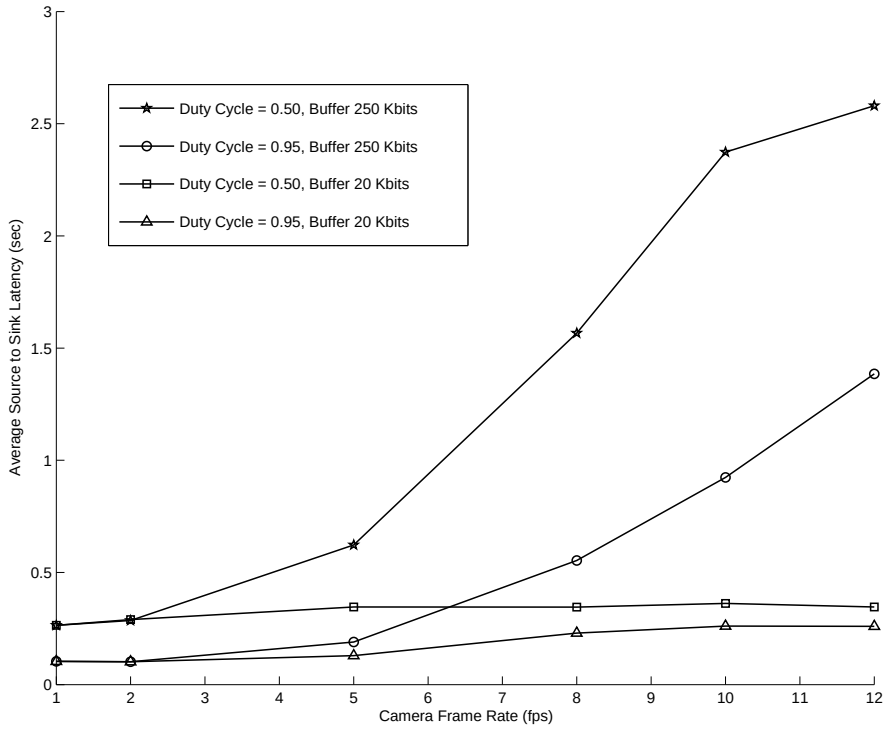

Figure 5.5. Effect of increased buffer size for duty cycle values of 50 per cent and 95 per cent

and duty cycle values, the ENCO method increases the successful frame delivery ratio. Note that, these improvements are achieved without incurring any overhead, but with just setting the default CW size wisely.

Another crucial performance metric for VSN is the latency, i.e., the end-to-end delay observed. Although the analysis and the simulations presented in Chapter 4 had the medium access delay (contention delay) as a performance metric, its effect on the application level performance is via the end-to-end delay. Figure 5.9 shows the effect of the ENCO method on the latency values achieved. As seen in the figure, for all camera frame rates and duty cycle values, latencies are decreased when the ENCO method is applied. The effect is higher for the lowest duty cycle investigated, where the latency is improved between $20 - 35$ per cent for different camera frame rate values. Hence, an important observation is that, the ENCO method improves the latency and the network throughput simultaneously.

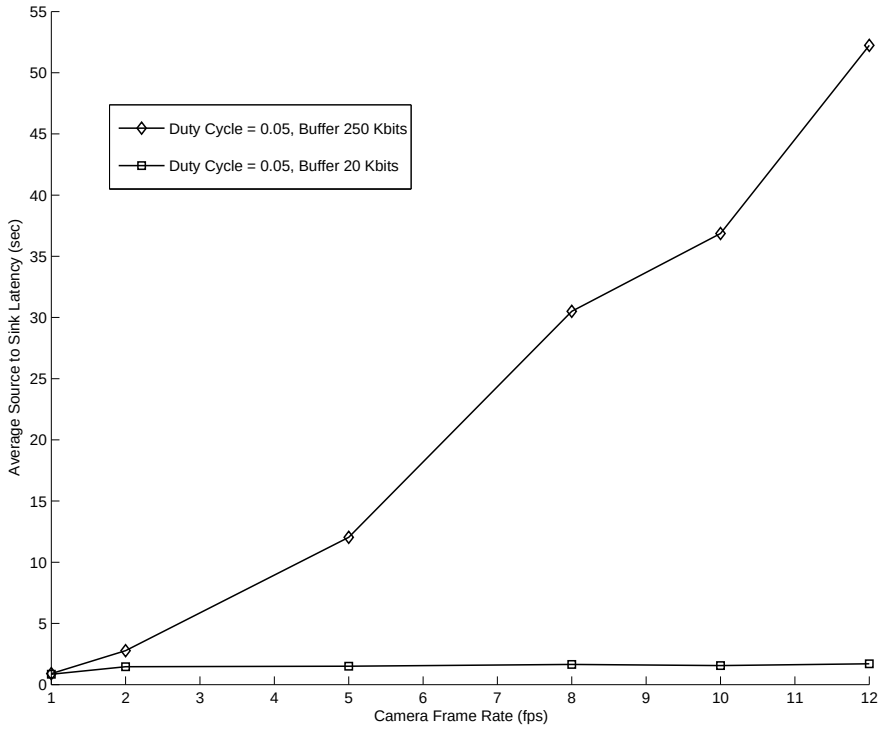

Figure 5.6. Effect of increased buffer size for duty cycle value of 5 per cent

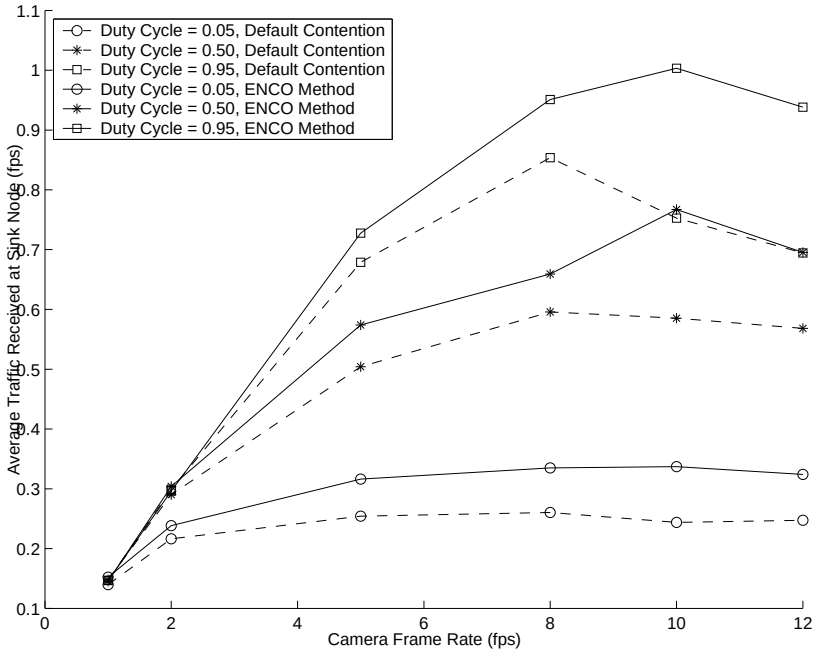

Figure 5.7. Effect of ENCO method on received frame rate at sink

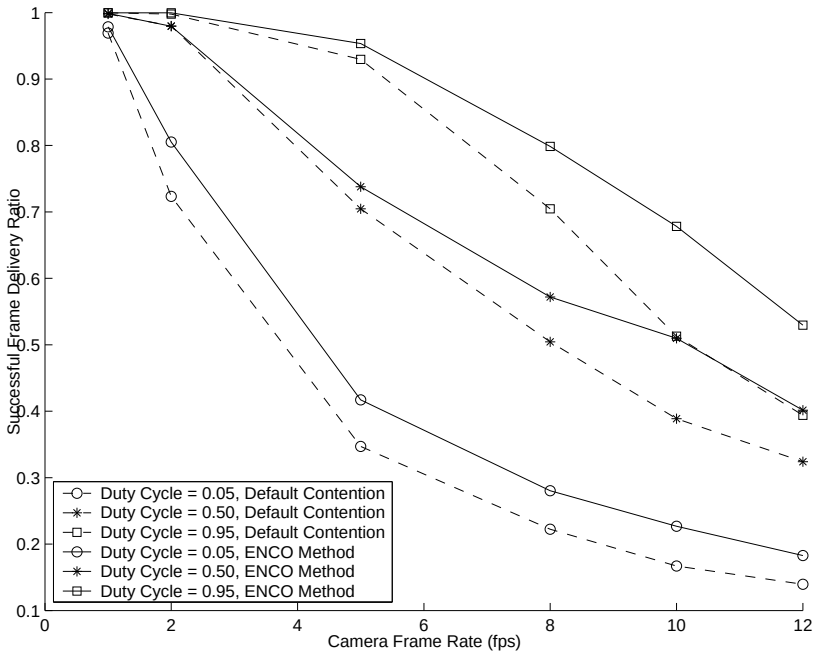

Figure 5.8. Effect of ENCO method on successful frame delivery ratio

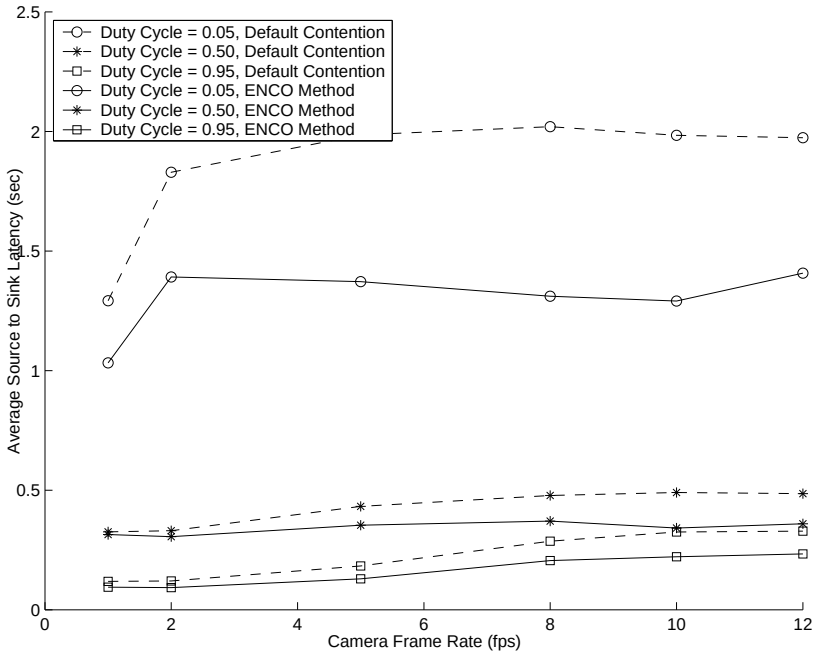

Figure 5.9. Effect of ENCO method on end-to-end latency

5.6. Conclusion and Future Work for Improving VSN Capabilities with CW Size Optimization

In this chapter, first, the capabilities and the limitations of VSNs which are implemented with the currently available technology are explored. It is observed that

sending images with higher frame rates from individual nodes can achieve better application level quality only within a bounded operational region. This region is determined by the available constraints on the sensor node hardware (communication bandwidth, buffer size) and also by the sleep schedule introduced. Simulation runs with realistic parameter values are conducted to show the limits of the carried video traffic in relation to the application level requirements.

Then, the effect of the ENCO method is investigated on the observed limitations and capabilities of VSNs. It is shown that the ENCO method can improve both latency and throughput values of the network without incurring any overhead. Since the ENCO method is not specific to a certain MAC protocol, it can be applied to any MAC protocol that employs slotted-CSMA. Although the ENCO method defines a static and network-wide CW size setting, as shown in this work, it improves the network performance considerably. This improvement can be increased by spatial settings such as by a method that considers the *number of neighbors*. Alternatively, a spatio-temporal method can result in better performance, for instance, one that considers the history of the number of contending nodes. All of these methods can utilize the contention window size optimizations presented in Chapter 4. The impact of ENCO method in the presence of transmission errors can be investigated as another future work. The transmission errors are important for VSN, since the successful delivery of a frame requires a high portion of its packets are delivered without any errors.

6. CONCLUSIONS

Wireless sensor networks present a promising technology for many application areas such as environmental monitoring, surveillance systems and tactical systems. Although there is no standardization of the communication protocols yet, there are numerous studies that propose protocols for different networking layers. In this thesis, we investigated MAC layer properties of WSNs by first presenting a brief survey of MAC protocols proposed and discussing the advantages and disadvantages of different medium access schemes.

An important observation about the MAC protocols proposed is that the performance studies are performed with either periodic or Poisson data traffic. However, in reality, the data traffic generated in WSNs depends on the application. For instance, event-driven applications such as habitat monitoring or surveillance systems yields bursty data traffic which cannot be modeled by Poisson or periodic data traffic. By doing detailed simulations, we show that the performance results of a communication protocol depend on the packet traffic model employed. Moreover, we developed an analytical packet traffic model for surveillance wireless sensor networks which utilize a parametric and probabilistic sensor detection model. The packet traffic model uses the following parameters: the number of sensors deployed, the area size of the border, the detection distance thresholds, the target velocity, the sampling interval and the detection model parameters. This model can be used to generate the time-based packet traffic load generated by an intrusion to a target area.

Another work presented in this thesis is the energy and delay optimization of contentions for contention-window based MAC protocols. Various MAC protocols such as S-MAC, IEEE 802.11, IEEE 802.15.4 utilize contention windows which consist of a specified number of contention slots. However, the contention window size setting is shown to be crucial for the performance of the MAC protocol used. Although exists in other type of wireless networks, there is no study for contention window size optimization in WSN which needs further work since the WSN MAC protocols

generally employ a different back-off mechanism and are optimized not only for the delay but also for the energy consumed.

The importance of the contention window size setting on the energy consumption and the delay incurred is depicted both analytically and by simulations. Separate optimum contention window size setting methods are presented for the energy consumption and the incurred contention delay. It is shown that the performance of contention-based MAC protocols can be significantly improved using the optimum contention window sizes. The presented analysis and optimizations are also applicable to other wireless networks that define a fixed contention window size and uniformly random contention. For practical implementation of the CW size optimization in event-triggered WSN, the ENCO method is proposed. The simulations show that the ENCO method achieves close performance results to the optimum contention window size results. The performance of the ENCO method can be increased with spatio-temporal information such as the history of number of contending nodes.

The CW size studies presented in this thesis base on the uniformly random slot selection method which is the most widely used slot selection method. However, an alternative method is proposed which minimizes the collision probability. This method is compared to the uniformly random method for the contention delay metric. It is shown that the uniformly random slot assignment performs better when used with the optimized CW size.

Another contribution of this thesis is the improvements of the capabilities and the limitations of VSNs based on currently available hardware and encoding technology with the contention optimization methods proposed. Video Sensor Networks (VSNs) are a special type of WSNs where sensor nodes equipped with video cameras send the captured videos according to the requirements of the VSN application implemented. In this work, it is shown that increasing the quality of video capture frame rates results in a drop in the video quality received at the sink even for low rates. Along with the proposed contention window size optimization work, ENCO method is employed to improve the overall VSN performance. The network performance results of VSN with

the ENCO method show that this method can extend the capabilities of VSN by both decreasing the end-to-end delay and increasing the average number of frames received at the sink, i.e., the system throughput at the same time.

REFERENCES

1. Saffo, P., "Sensors: The Next Wave of Infotech Innovation", *Institute for the Future: 1997 Ten-Year Forecast*, pp. 115–122, 1997.

2. Aylward, R. and J. A. Paradiso, "A compact, high-speed, wearable sensor network for biomotion capture and interactive media", *IPSN '07: Proceedings of the 6th International Conference on Information Processing in Sensor Networks*, pp. 380–389, ACM, New York, NY, USA, 2007.

3. Farella, E., A. Pieracci, L. Benini, and A. Acquaviva, "A Wireless Body Area Sensor Network for Posture Detection", *ISCC '06: Proceedings of the 11th IEEE Symposium on Computers and Communications*, pp. 454–459, IEEE Computer Society, Washington, DC, USA, 2006.

4. Li, H. and J. Tan, "Heartbeat driven medium access control for body sensor networks", *HealthNet '07: Proceedings of the 1st ACM SIGMOBILE International Workshop on Systems and Networking Support for Healthcare and Assisted Living Environments*, pp. 25–30, ACM, New York, NY, USA, 2007.

5. Poon, C., Y.-T. Zhang, and S.-D. Bao, "A novel biometrics method to secure wireless body area sensor networks for telemedicine and m-health", *Communications Magazine, IEEE*, Vol. 44, pp. 73–81, 2006.

6. Timmons, N. and W. Scanlon, "Analysis of the performance of IEEE 802.15.4 for medical sensor body area networking", *Sensor and Ad Hoc Communications and Networks, 2004. IEEE SECON 2004. 2004 First Annual IEEE Communications Society Conference on*, pp. 16–24, 2004.

7. Cho, J., Y. Shim, T. Kwon, and Y. Choi, "SARIF: A novel framework for integrating wireless sensor and RFID networks", *IEEE Wireless Communications*, Vol. 14, No. 6, pp. 50–56, December 2007.

8. Sample, A., D. Yeager, P. Powledge, and J. Smith, "Design of a Passively-Powered, Programmable Sensing Platform for UHF RFID Systems", *RFID, 2007. IEEE International Conference on*, pp. 149–156, 2007.

9. Boumerdassi, S., P. K. Diop, E. Renault, and A. Wei, "T2MAP: A Two-Message Mutual Authentication Protocol for Low-Cost RFID Sensor Networks", *Vehicular Technology Conference, 2006. VTC-2006 Fall. 2006 IEEE 64th*, pp. 1–5, 2006.

10. Boone, G., "Reality Mining: Browsing Reality With Sensor Networks", *Sensors*, Vol. 21, No. 9, p. 14, September 2004.

11. Uusitalo, M. A., "Global Vision for the Future Wireless World from the WWRF", *Vehicular Technology Magazine, IEEE*, Vol. 1, No. 2, pp. 4–8, 2006.

12. Kulkarni, S., "TDMA service for sensor networks", *Proceedings of 24th International Conference on Distributed Computing Systems Workshops*, pp. 604–609, 2004.

13. Ye, W., J. Heidemann, and D. Estrin, "Medium access control with coordinated adaptive sleeping for wireless sensor networks", *IEEE/ACM Trans. Netw.*, Vol. 12, No. 3, pp. 493–506, 2004.

14. Demirkol, I., C. Ersoy, and F. Alagoz, "MAC protocols for wireless sensor networks: a survey", *IEEE Communications Magazine*, Vol. 44, No. 4, pp. 115–121, April 2006.

15. Demirkol, I., F. Alagöz, H. Deliç, and C. Ersoy, "Wireless sensor networks for intrusion detection: packet traffic modeling", *IEEE Commununications Letters*, Vol. 10, No. 1, pp. 22–24, January 2006.

16. Demirkol, I., F. Alagoz, H. Delic, and C. Ersoy, "The Impact of a Realistic Packet Traffic Model on the Performance of Surveillance Wireless Sensor Networks", *Elsevier Computer Networks (under review)*, 2008.

17. Demirkol, I. and C. Ersoy, "Energy and Delay Optimized Contention for Wireless Sensor Networks", *Elsevier Computer Networks (under review)*, 2008.

18. Demirkol, I. and C. Ersoy, "Does Minimizing the Collision Probability Reveal the Best Performance?", *In preparation*, 2008.

19. Ozgovde, A., I. Demirkol, and C. Ersoy, "Effect of Sleep Schedule and Frame Rate on the Capabilities of Video Sensor Networks", *International Symposium on Wireless Pervasive Computing*, 2008.

20. Durmus, Y., A. Ozgovde, I. Demirkol, and C. Ersoy, "Exploring the Effect of the Network Parameters of Video Sensor Networks", *International Symposium on Computer Networks*, 2008.

21. Demirkol, I., A. Ozgovde, and C. Ersoy, "Improving Latency and Throughput by Intelligent Contention Window Size Adjustment for Video Sensor Networks", *In preparation*, 2008.

22. El-Hoiydi, A., "Spatial TDMA and CSMA with preamble sampling for low power ad hoc wireless sensor networks", *Computers and Communications, 2002. Proceedings. ISCC 2002. Seventh International Symposium on*, pp. 685–692, 2002.

23. Enz, C., A. El-Hoiydi, J.-D. Decotignie, and V. Peiris, "WiseNET: an ultralow-power wireless sensor network solution", *Computer*, Vol. 37, No. 8, pp. 62–70, Aug. 2004.

24. Rajendran, V., K. Obraczka, and J. J. Garcia-Luna-Aceves, "Energy-efficient collision-free medium access control for wireless sensor networks", *SenSys '03: Proceedings of the 1st International Conference on Embedded Networked Sensor Systems*, pp. 181–192, ACM, New York, NY, USA, 2003.

25. Bao, L. and J. J. Garcia-Luna-Aceves, "A new approach to channel access scheduling for Ad Hoc networks", *MobiCom '01: Proceedings of the 7th Annual Interna-*

tional Conference on Mobile Computing and Networking, pp. 210–221, ACM, New York, NY, USA, 2001.

26. Jamieson, K., H. Balakrishnan, and Y. Tay, "Sift: A MAC Protocol for Event-Driven Wireless Sensor Networks", *Third European Workshop on Wireless Sensor Networks (EWSN)*, Zurich, Switzerland, February 2006.

27. Tay, Y. C., K.Jamieson, and H. Balakrishnan, "Collision-minimizing CSMA and Its Applications to Wireless Sensor Networks", *IEEE Journal on Selected Areas in Communications*, Vol. 22, No. 6, pp. 1048–1057, August 2004.

28. Lu, G., B. Krishnamachari, and C. S. Raghavendra, "An adaptive energy-efficient and low-latency MAC for tree-based data gathering in sensor networks", *Wirel. Commun. Mob. Comput.*, Vol. 7, No. 7, pp. 863–875, 2007.

29. Dam, T. V. and K. Langendoen, "An adaptive energy-efficient MAC protocol for wireless sensor networks", *Proc. ACM SenSys*, pp. 171–180, Los Angeles, USA, November 2003.

30. Halkes, G. P., T. van Dam, and K. G. Langendoen, "Comparing energy-saving MAC protocols for wireless sensor networks", *Mob. Netw. Appl.*, Vol. 10, No. 5, pp. 783–791, 2005.

31. Lin, P., C. Qiao, and X. Wang, "Medium access control with a dynamic duty cycle for sensor networks", *Proc. IEEE WCNC*, Vol. 3, pp. 1534–1539, Atlanta, USA, March 2004.

32. Safwat, A., H. Hassanein, and H. Mouftah, "ECPS and E2LA: new paradigms for energy efficiency in wireless ad hoc and sensor networks", *Global Telecommunications Conference, 2003. GLOBECOM '03. IEEE*, Vol. 6, pp. 3547–3552, 2003.

33. Cui, S., R. Madan, A. Goldsmith, and S. Lall, "Joint routing, MAC, and link layer optimization in sensor networks with energy constraints", *IEEE International Conference on Communications, ICC*, Vol. 2, pp. 725–729, 2005.

34. Ding, J., K. Sivalingam, R. Kashyapa, and L. J. Chuan, "A multi-layered architecture and protocols for large-scale wireless sensor networks", *Vehicular Technology Conference, 2003. VTC 2003-Fall. 2003 IEEE 58th*, Vol. 3, pp. 1443–1447, 2003.

35. Zorzi, M. and R. Rao, "Geographic random forwarding (GeRaF) for ad hoc and sensor networks: energy and latency performance", *Mobile Computing, IEEE Transactions on*, Vol. 2, No. 4, pp. 349–365, Oct.-Dec. 2003.

36. Rugin, R. and G. Mazzini, "A simple and efficient MAC-routing integrated algorithm for sensor network", *Communications, 2004 IEEE International Conference on*, Vol. 6, pp. 3499–3503, 2004.

37. Zorzi, M., "A new contention-based MAC protocol for geographic forwarding in ad hoc and sensor networks", *Communications, 2004 IEEE International Conference on*, Vol. 6, pp. 3481–3485, 2004.

38. Gedik, B., L. Liu, and P. S. Yu, "ASAP: An Adaptive Sampling Approach to Data Collection in Sensor Networks", *IEEE Transactions on Parallel and Distributed Systems*, Vol. 18, No. 12, pp. 1766–1783, December 2007.

39. Kashihara, S., N. Wakamiya, and M. Murata, "Implementation and evaluation of a synchronization-based data gathering scheme for sensor networks", *Proc. IEEE ICC*, Vol. 5, pp. 3037–3043, Korea, May 2005.

40. Gandham, S., M. Dawande, and R. Prakash, "An integral flow-based energy-efficient routing algorithm for wireless sensor networks", *Proc. IEEE WCNC*, Vol. 4, pp. 2341–2346, Atlanta, USA, March 2004.

41. Ma, Y. and J. H. Aylor, "System lifetime optimization for heterogeneous sensor networks with a hub-spoke topology", *IEEE Transactions on Mobile Computing*, Vol. 3, No. 3, pp. 286–294, July/September 2004.

42. Manjeshwar, A., Q. Zeng, and D. Agrawal, "An analytical model for information retrieval in wireless sensor networks using enhanced APTEEN protocol", *IEEE Transactions on Parallel and Distributed Systems*, Vol. 13, No. 12, pp. 1290–1302, December 2002.

43. Shi, X. and G. Stromberg, "SyncWUF: An Ultra Low-Power MAC Protocol for Wireless Sensor Networks", *IEEE Transactions on Mobile Computing*, Vol. 6, No. 1, pp. 115–125, January 2007.

44. Muruganathan, S. D. and A. O. Fapojuwo, "A Hybrid Routing Protocol for Wireless Sensor Networks Based on a Two-Level Clustering Hierarchy with Enhanced Energy Efficiency", *Wireless Communications and Networking Conference, 2008. WCNC 2008. IEEE*, pp. 2051–2056, 2008.

45. Crossbow Technology Inc., *MPR-MIB Users Manual*, June 2006.

46. Zou, Y. and K. Chakrabarty, "Sensor deployment and target localization based on virtual forces", *Proc. IEEE INFOCOM'03*, Vol. 2, pp. 1293–1303, San Francisco, USA, March 2003.

47. Zou, Y. and K. Chakrabarty, "Uncertainty-aware and coverage-oriented deployment for sensor networks", *Journal of Parallel and Distributed Computing*, Vol. 64, No. 7, pp. 788–798, July 2004.

48. Elfes, A., "Occupancy grids: a stochastic spatial representation for active robot perception", Iyengar, S. S. and A. Elfes (editors), *Autonomous Mobile Robots: Perception, Mapping and Navigation*, Vol. 1, pp. 60–70, IEEE Computer Society Press, 1991.

49. Onur, E., C. Ersoy, and H. Deliç, "How many sensors for an acceptable breach detection probability?", *Computer Communications*, Vol. 29, pp. 173–182, 2006.

50. Onur, E., C. Ersoy, H. Deliç, and L. Akarun, "Surveillance Wireless Sensor Networks: Deployment Quality Analysis", *IEEE Network*, Vol. 21, No. 6, pp. 48–53, November-December 2007.

51. Peng-Jun, W. and Y. Chih-Wei, "Coverage by randomly deployed wireless sensor networks", *IEEE Transactions on Information Theory*, Vol. 52, No. 6, pp. 2658–2669, June 2006.

52. Ren, S., Q. Li, H. Wang, X. Chen, and X. Zhang, "Design and Analysis of Sensing Scheduling Algorithms under Partial Coverage for Object Detection in Sensor Networks", *IEEE Transactions on Parallel and Distributed Systems*, Vol. 18, No. 3, pp. 334–350, March 2007.

53. Wang, G., G. Cao, T. L. Porta, and W. Zhang, "Sensor relocation in mobile sensor networks", *Proc. IEEE INFOCOM*, Vol. 4, pp. 2302–2312, Miami, USA, March 2005.

54. Pandana, C. and K. J. R. Liu, "Maximum connectivity and maximum lifetime energy-aware routing for wireless sensor networks", *Proc. IEEE GLOBECOM'05*, Vol. 2, pp. 1034–1038, St. Louis, USA, November/December 2005.

55. Zhu, J., S. Papavassiliou, and J. Yang, "Adaptive Localized QoS-Constrained Data Aggregation and Processing in Distributed Sensor Networks", *IEEE Transactions on Parallel and Distributed Systems*, Vol. 17, No. 9, pp. 923–933, September 2006.

56. Ergen, S. C. and P. Varaiya, "PEDAMACS: Power Efficient and Delay Aware Medium Access Protocol for Sensor Networks", *IEEE Transactions on Mobile Computing*, Vol. 5, No. 7, pp. 920–930, July 2006.

57. Karmokar, A. K., D. V. Djonin, and V. K. Bhargava, "Optimal and suboptimal packet scheduling over correlated time varying flat fading channels", *IEEE Transactions on Wireless Communications*, Vol. 5, No. 2, pp. 446–456, February 2006.

58. Zhenghua, F., L. Haiyun, P. Zerfos, S. Lu, L. Zhang, and M. Gerla, "The impact of multihop wireless channel on TCP performance", *IEEE/ACM Transactions on Networking*, Vol. 4, No. 2, pp. 209–221, March/April 2006.

59. Bettstetter, C., G. Resta, and P. Santi, "The Node Distribution of the Random Waypoint Mobility Model for Wireless Ad Hoc Networks", *IEEE Transactions on Mobile Computing*, Vol. 2, No. 3, pp. 257–269, 2003.

60. Hu, L. and D. Evans, "Localization for mobile sensor networks", *Proc. ACM MobiCom*, pp. 45–57, Philadelphia, USA, 2004.

61. Opnet Modeler, `http://www.opnet.com/products/modeler/home.html`, 2008.

62. The Network Simulator - ns-2, `http://www.isi.edu/nsnam/ns/`, 2008.

63. Crossbow Technology, `http://www.xbow.com`, 2008.

64. Yang, Y., J. Wang, and R. Kravets, "Distributed Optimal Contention Window Control for Elastic Traffic in Single-Cell Wireless LANs", *IEEE/ACM Transactions on Networking*, Vol. 15, No. 6, pp. 1373–1386, Dec. 2007.

65. Joshi, T., A. Mukherjee, Y. Yoo, and D. P. Agrawal, "Airtime Fairness for IEEE 802.11 Multirate Networks", *IEEE Transactions on Mobile Computing*, Vol. 7, No. 4, pp. 513–527, April 2008.

66. Kim, T. H. and S. Choi, "Priority-based delay mitigation for event-monitoring IEEE 802.15.4 LR-WPANs", *IEEE Communications Letters*, Vol. 10, No. 3, pp. 213–215, Mar 2006.

67. Anastasi, G., E. Borgia, M. Conti, E. Gregori, and A. Passarella, "Understanding the real behavior of Mote and 802.11 ad hoc networks: an experimental approach", *Pervasive and Mobile Computing*, Vol. 1, No. 2, pp. 237–256, July 2005.

68. Woo, A. and D. E. Culler, "A transmission control scheme for media access in sensor networks", *MobiCom '01: Proceedings of the 7th annual international conference on Mobile computing and networking*, pp. 221–235, 2001.

69. Ye, W., F. Silva, and J. Heidemann, "Ultra-low duty cycle MAC with scheduled channel polling", *SenSys '06: Proceedings of the 4th international conference on Embedded networked sensor systems*, pp. 321–334, 2006.

70. Rhee, I., A. Warrier, M. Aia, and J. Min, "Z-MAC: A hybrid MAC for wireless sensor networks", *SenSys '05: Proceedings of the 3rd International Conference on Embedded Networked Sensor Systems*, pp. 90–101, 2005.

71. Wang, X., J. Yin, and D. P. Agrawal, "Effects of contention window and packet size on the energy efficiency of wireless local area network", *Proc. of IEEE WCNC*, Vol. 1, pp. 94–99, March 2005.

72. Ksentini, A., A. Nafaa, A. Gueroui, and M. Naimi, "Determinist contention window algorithm for IEEE 802.11", *IEEE 16th International Symposium on Personal, Indoor and Mobile Radio Communications, PIMRC 2005*, Vol. 4, pp. 2712–2716, Sept 2005.

73. Cali, F., M. Conti, and E. Gregori, "IEEE 802.11 protocol: design and performance evaluation of an adaptive backoff mechanism", *IEEE Journal on Selected Areas in Communications*, Vol. 18, No. 9, pp. 1774–1786, Sep 2000.

74. Heusse, M., F. Rousseau, R. Guillier, and A. Duda, "Idle sense: an optimal access method for high throughput and fairness in rate diverse wireless LANs", *SIGCOMM Comput. Commun. Rev.*, Vol. 35, No. 4, pp. 121–132, October 2005.

75. Xia, Q. and M. Hamdi, "Contention Window Adjustment for IEEE 802.11 WLANs: A Control-Theoretic Approach", *Proc. of IEEE International Conference on Communications, ICC '06*, Vol. 9, pp. 3923–3928, June 2006.

76. Jin, Y. and G. Kesidis, "Distributed Contention Window Control for Selfish Users in IEEE 802.11 Wireless LANs", *IEEE Journal on Selected Areas in Communications*, Vol. 25, No. 6, pp. 1113–1123, August 2007.

77. Nafaa, A., A. Ksentini, A. Mehaoua, B. lshibashi, Y. Iraqi, and R. Boutaba, "Sliding contention window (SCW): towards backoff range-based service differentiation over IEEE 802.11 wireless LAN networks", *IEEE Network*, Vol. 19, No. 4, pp. 45–51, July-Aug. 2005.

78. Artail, H., H. Safa, J. Naoum-Sawaya, B. Ghaddar, and S. Khawam, "A simple recursive scheme for adjusting the contention window size in IEEE 802.11e wireless ad hoc networks", *Comput. Commun.*, Vol. 29, No. 18, pp. 3789–3803, 2006.

79. Pang, A.-C. and H.-W. Tseng, "Dynamic backoff for wireless personal networks", *IEEE Global Telecommunications Conference, GLOBECOM '04*, Vol. 3, pp. 1580–1584, Dec 2004.

80. Tian, Q. and E. Coyle, "A MAC-Layer Retransmission Algorithm Designed for the Physical-Layer Characteristics of Clustered Sensor Networks", *IEEE T Wirel Commun*, Vol. 5, No. 11, pp. 3153–3164, November 2006.

81. Bapat, S., V. Kulathumani, and A. Arora, "Analyzing the Yield of ExScal, a Large-Scale Wireless Sensor Network Experiment", *Proceedings of the 13th IEEE International Conference on Network Protocols ICNP '05*, pp. 53–62, Washington, DC, November 2005.

82. Ma, H., X. Li, H. Li, P. Zhang, S. Luo, and C. Yuan, "Dynamic optimization of IEEE 802.11 CSMA/CA based on the number of competing stations", *IEEE Int. Conference on Communications, ICC'04*, Vol. 1, pp. 191–195, June 2004.

83. Xiong, Z., A. Liveris, and S. Cheng, "Distributed source coding for sensor networks", *Signal Processing Magazine, IEEE*, Vol. 21, No. 5, pp. 80–94, 2004.

84. Downes, I., L. Rad, and H. Aghajan, "Development of a mote for wireless image sensor networks", *Proc. of COGnitive systems with Interactive Sensors (COGIS), Paris, France, March*, 2006.

85. Kulkarni, P., D. Ganesan, P. J. Shenoy, and Q. Lu, "*SensEye*: a multi-tier camera sensor network.", *Proceedings of the 13th ACM International Conference on Multimedia, November 6-11, 2005, Singapore*, pp. 229–238, ACM, 2005.

86. Akyildiz, I., T. Melodia, and K. Chowdhury, "A survey on wireless multimedia sensor networks", *Computer Networks*, Vol. 51, No. 4, pp. 921–960, 2007.

87. Karp, B. and H. T. Kung, "GPSR: greedy perimeter stateless routing for wireless networks", *MOBICOM*, pp. 243–254, 2000.